INFRARED STUDIES OF GAS ADSORPTION ON SEMICONDUCTOR SURFACES

A thesis presented for the
degree of Doctor of Philosophy in Chemistry,
in the University of Canterbury,
Christchurch, New Zealand

by

S. Ude Shankar

1979

ACKNOWLEDGEMENTS

I am most grateful to my supervisor, Dr Alan Metcalfe, for his help and encouragement during the last 4 years.

Thanks are also due to the technical staff of the Chemistry Department, particularly Mr Kevin Gillard for the construction of the infrared-evaporation apparatus. I also acknowledge the help given by the operator of the electron microscope at the Department of Mechanical Engineering, and Dr A. Wilkinson at the Computer Centre.

I am especially grateful to my wife and my parents for their patience and support during the course of this work.

The granting of a Teaching Fellowship during 1976-78 by the Chemistry Department is gratefully acknowledged.

PUBLICATIONS

1. Infrared spectra of Ethanol Adsorbed on Porous Glass, A. Metcalfe and S. Ude Shankar, J.C.S. Faraday 1, 1978, 74, 1945.

2. Adsorption of Water Vapour on Evaporated Germanium Films - An Infrared Study, A. Metcalfe and S. Ude Shankar, J.C.S. Faraday 1, accepted for publication 1979.

Three other papers are in preparation for publication in J.C.S. Faraday 1.

ABSTRACT

The interaction of various gases on evaporated germanium and silicon surfaces has been studied at room temperature ($27^{o}C$) by means of infrared spectroscopy.

Water vapour has been found to dissociate on germanium surfaces as a result of which bands have been observed at 1980-60, 770 and 675, and at 730 and 875-825cm^{-1}. These are attributed to three adsorbed species; the first to Ge-H, the second pair to Ge-OH groups and the third pair to $Ge-O^{-}$ and oxygen incorporated in the lattice respectively. From the observed changes in the Ge-H band intensity (in the presence of water vapour) a mechanism is proposed for H_2 formation over the surface, as a result of the reaction:

$$H_{ads} + H_2O_{ads} \longrightarrow OH_{ads} + H_2$$

The adsorption of ammonia on germanium gave rise to a number of bands which are attributed to three different surface species. These are physically adsorbed ammonia, co-ordinated ammonia, and a primary amine group. On oxidised germanium the interaction is found to be much weaker, although some dissociation is thought to occur since in addition to the bands corresponding to a primary amine a sharp hydroxyl band has also been observed.

A different mode of adsorption to that proposed by Bennett and Tompkins is suggested for carbon dioxide adsorption on germanium. The interaction is thought to occur between the oxygen atoms of carbon dioxide and

surface germanium atoms. Some evidence for dissociation of carbon dioxide is suggested by the appearance of a band near the gas-phase frequency of carbon monoxide.

The interaction of oxygen on silicon surfaces has been found to give rise to a number of bands during different stages of exposure to oxygen. At very low exposures a peroxide-like silicon-oxygen surface structure is proposed by comparison with data obtained by other workers. At high exposures a bulk oxide species is thought to be responsible for two strong bands which show logarithmic growth.

CONTENTS

LIST OF FIGURES

LIST OF TABLES

CHAPTER ONE

INTRODUCTION

1.1 General Introduction

The work described in this thesis is a continuation of a general study of gas adsorption on semiconductor surfaces which received some attention from Howe, [1] in this laboratory, several years ago. The technique used, which was developed by Howe, enables the detection and identification of adsorbed species on germanium and silicon surfaces by means of infrared spectroscopy.

The application of infrared spectroscopy to the study of gas adsorption on semiconductor surfaces was first suggested by Eischens, [2] and since then several studies have been reported in the literature.[3-6] The technique is particularly successful with surfaces prepared by evaporation of elemental semiconductors in an inert gas atmosphere, because these surfaces satisfy the two most important conditions necessary for observing the spectra of adsorbed species, viz. transparency in the infrared, and a high surface area necessary for obtaining a detectable concentration of the adsorbed species. The technique is discussed in some detail in Section 1.2.

The study of the adsorption of gases and vapours on semiconductor surfaces has been pursued with much vigour in the last ten years, especially since the advent of micro-electronics technology. As the electronic devices manufactured today have a high surface-to-volume ratio the electronic properties, and thus the performance of these

devices, can be greatly affected by the adsorption of ambient gases.[7,8] The catalytic properties of semiconductors have also attracted wide attention, mainly because of the possibility of varying the bulk properties of such materials by adding trace amounts of impurities.[9-11]

The experimental technique used in this work was essentially the same as that employed by Howe.[1] The germanium and silicon surfaces were generated in an argon atmosphere by deposition onto potassium bromide plates. A new infrared-evaporation apparatus was built of metal, and after a considerable time spent in leak checking it was possible to achieve a good vacuum, bordering on the ultra-high vacuum region. This is described in detail in Chapter Two.

In Chapter Three the structure, properties and the electronic description of the evaporated films prepared in this work are discussed.

The adsorption of water vapour, ammonia and carbon dioxide on germanium, and oxygen on silicon were studied with a view to obtaining information about the adsorption processes. Some of these have been investigated before by other workers,[12-19] using different techniques, but results are lacking or conflicting in many instances.

Water vapour has been found to oxidise surfaces of germanium single crystals or powders, with the release of molecular hydrogen.[12-15] However, no technique has yet been able to directly establish the nature of the reaction intermediates. While the formation of surface hydroxyls and surface hydrides during the interaction has been inferred,[21,22]

their role in the oxidation of the surface, and the production of H_2, has not been clearly determined. In Chapter Four a study of the interaction of water vapour with evaporated germanium surfaces is described, and the reaction intermediates identified by their infrared absorption.

Chapter Five describes the interaction of ammonia on evaporated germanium films. No such study has been reported in the literature previously, although some work on germanium dioxide has shown that degradation of ammonia occurs on these surfaces.[16]

Bennett and Tompkins[17] found a small irreversible uptake of carbon dioxide by evaporated germanium films, with the eventual oxidation of the surface. However, no infrared study of this interaction has been conducted previously. In Chapter Six such a study is described, and the observed infrared spectra discussed.

The nature of the adsorbed species during the interaction of oxygen on silicon surfaces, obtained by cleavage of single crystals in vacuum, has been a subject of some controversy. Two different models have been proposed recently [18,19] for the structure of the adsorbed species at monolayer level. Both models seem to be consistent with their respective experimental data. Therefore, further study was needed in order to make an unambiguous choice between the structure models. Such a study is described in Chapter Seven where the infrared spectra of the interaction of oxygen on evaporated silicon films is discussed.

1.2 Infrared Spectroscopy applied to Surface Studies

1.21 Prerequisites for Observing Adsorbate Bands

For an optically homogeneous solution, the absorbance (D) of a particular band at νcm^{-1} can be obtained from the Beer-Lambert Law[20] given in 1a below.

$$D = -\log (T/T_0) = cel \qquad (1a)$$

where T/T_0 is the fraction of incident radiation transmitted at νcm^{-1}, e the molar extinction coefficient, c the molar concentration of the adsorbing species, and l the pathlength. It is apparent from equation 1a that for a reasonably transparent solvent there is a wide range of concentrations and pathlengths available to ensure the appearance of a band with a given e maximum. However, this favourable situation rarely exists in an adsorbent-adsorbate system because the incident radiation is attenuated by reflection and scattering losses. Even if these were kept to a minimum, it is essential to have a large enough surface area and coverage to attain the required magnitude of the c term, in 1a. For example, if n molecules of gas are adsorbed onto an adsorbent of thickness 1 cm and cross sectioned area A cm^2, then cl in equation 1a becomes

$$cl = \frac{n}{A} \text{ molecules } cm^{-2} \qquad (1b)$$

Under normal conditions the smallest detectable band, for example, using the PE 421 infrared spectrometer (Chapter 2, Section 2.2), will have an absorbance of about 0.01. Inserting a value for e of 8.3×10^{-19} cm^2 $molecule^{-1}$ (a typical value for an intense band)[21] in 1a, and combining 1b, gives

$$\left(\frac{n}{A}\right)_{min} = 1.2 \times 10^{16} \text{ molecules } cm^{-2} \qquad (1c)$$

as the minimum number of adsorbed molecules necessary to give a measurable band.

Germanium films prepared in an inert gas atmosphere, at pressures around 1.3×10^{-1} (10^{-3} Torr), have been reported to have surface areas 20 times greater than their geometric area.[1,3,4] Assuming that the number of adsorption sites at monolayer coverage is about 7×10^{14} cm^{-2},[22] then the concentration of the adsorbed molecules can be up to 1.4×10^{16} molecules cm^{-2}. This value compares favourably with that obtained previously through equations 1a and 1b for the minimum number of adsorbed molecules necessary to give a detectable absorption. Thus the necessity for preparing films of high surface area.

Generally to obtain well-defined spectra the following conditions should be satisfied:

a) a high area to give a detectable concentration of the adsorbed species;

b) scattering and reflection losses kept to a minimum so that sufficient radiation reaches the detector of the spectrometer;

c) the adsorbent is transparent in the infrared regions that are of interest, so that absorption bands are not superposed on background bands.

1.22 Spectra of Adsorbed Species

Information about the structure of an adsorbed species can often be obtained by comparing its infrared spectrum with the spectra of bulk compounds of known structure.[23] If this is not possible, identification may be made by

reference to tabulations of known group frequencies.[24-26] This kind of identification of surface species is, however, subjected to some limitations. For example, because of absorption or scattering of radiation by the adsorbent material in some regions of the spectrum, it is not always possible to observe all the bands associated with a particular species. Furthermore, the asymmetric environment at a gas-solid interface may drastically perturb an infrared spectrum in a manner which cannot always be predicted beforehand. In some cases, the asymmetry of the surface force field is such that normally forbidden bands become infrared active.[27,28]

Since the exact frequency of a vibration is dependent on the environment of the vibrating bond or group, the shift in frequency accompanying the adsorption of a gas molecule onto a surface can provide information about the nature of the gas-surface interaction. In physically adsorbed gases, frequency shifts are generally small[29,30] (about 2% - the same order of magnitude as the shifts accompanying the gas to liquid transition), whereas for chemisorbed molecules, which may be considerably altered in structure, the frequency shifts are much larger.[29] For example, when carbon monoxide is adsorbed on iron,[31] the gas-phase bands are shifted from 2110 and 2165 cm^{-1} (a doublet) to 1970 cm^{-1} (where a broad band is observed). This large frequency shift is attributed to the decrease in the carbon-oxygen bond order caused by the electronic rearrangement resulting from the carbon atom forming a covalent bond with a surface atom. When O_2 is chemisorbed, after carbon monoxide adsorption, the C-O stretching frequency was observed to shift to higher values.[31] Blyholder[32] interpreted this shift in terms of a molecular

orbital model of the metal-carbon-oxygen bond; oxygen adsorption is thought to increase the carbon-oxygen bond order which results in an increased stretching frequency.

Isotopic exchange of adsorbed atoms is frequently used to facilitate the assignment of observed infrared bands to particular vibrational modes. The isotopic substitution of an adsorbed atom does not significantly alter the electronic state of the molecule, and therefore the force constants are virtually unchanged. Thus the only effect on the vibrational states is that caused by the mass change. For example, if the hydrogen atom in a hydroxyl group is substituted with a deuterium atom, and if treated as a diatomic case, will produce a frequency shift given by ϑ_2/ϑ_1, where ϑ_2 is the frequency associated with the deuterium atom and ϑ_1 the frequency associated with the H atom ($\vartheta = (K/M)^{\frac{1}{2}}$, where M is the reduced mass, and K the force constant).[20] Thus $\vartheta_2/\vartheta_1 = \sqrt{\frac{1}{2}} = 0.707$. Peri and Hannan[33] investigated the isotopic exchange of H atoms on the hydroxyl groups present on alumina and observed a shift in the bands, to lower frequencies, by a ratio of 0.738, close to the calculated value of 0.707.

FIGURE 2.1 INFRARED-EVAPORATION APPARATUS

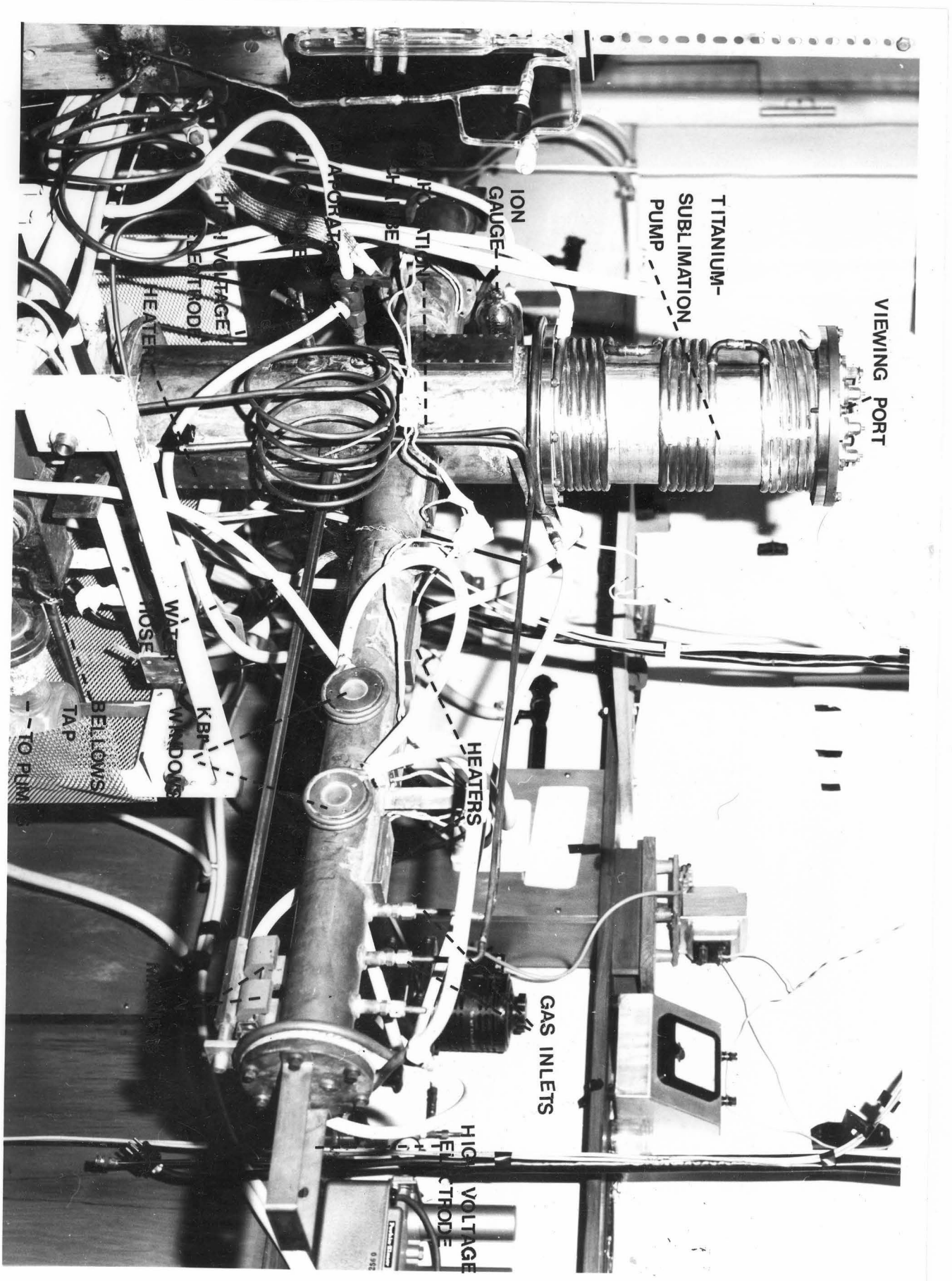

CHAPTER TWO

EXPERIMENTAL

The technique used to observe the spectra of adsorbed species in this work, has been previously developed and used successfully by Howe[1] in his adsorption studies on germanium. It was therefore decided that a similar system, with some modifications, would suit the purpose of this study. Thus a combined evaporation and infrared apparatus was constructed of copper and stainless steel (in place of the all-glass system employed by Howe) whereby thin films of germanium or silicon could be prepared in situ. Spectra were recorded digitally on magnetic tape.

The technique essentially involved the evaporation of germanium or silicon onto potassium bromide plates in an inert gas atmosphere and observing the spectral changes after adsorbing the gas or vapour to be studied, at the desired pressure. Difference spectra were then obtained and expanded on a suitable scale to clearly display the absorption bands due to the adsorbed species.

2.1 The Infrared-Evaporation Apparatus and the Gas-Handling Line.

The infrared-evaporation apparatus is shown in Figure 2.1. It consisted of a main chamber, housing a titanium-sublimation pump and the evaporation assembly, and a horizontal tube to which four infrared windows (KBr) were attached. The subtrate plates (KBr), 40 x 23 x 5 mm were fastened to a mechanical jig (Fig. 2.2) situated inside the horizontal tube. The jig, which was placed on stainless steel rails, could be moved between the

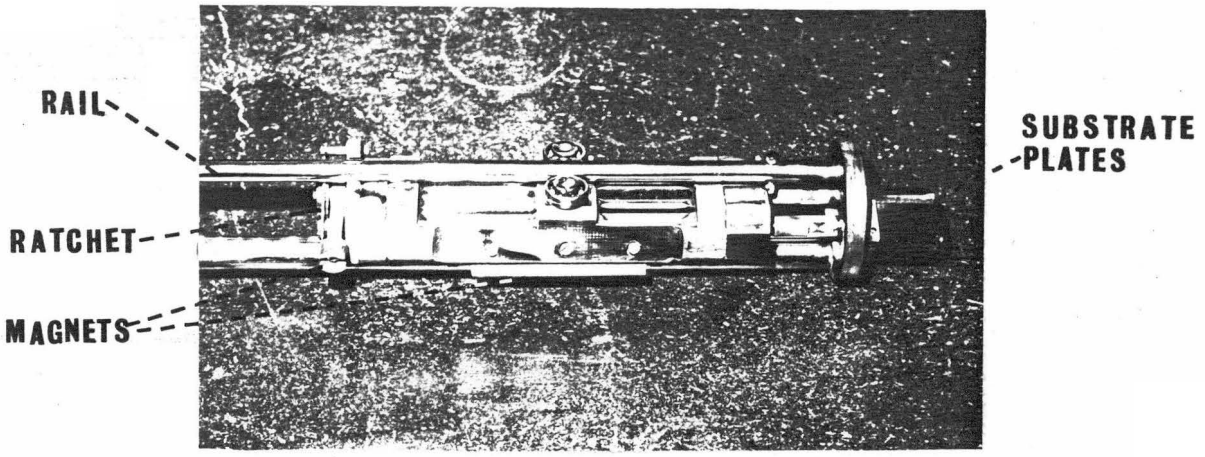

Figure 2.2 The mechanical jig for supporting substrate plates.

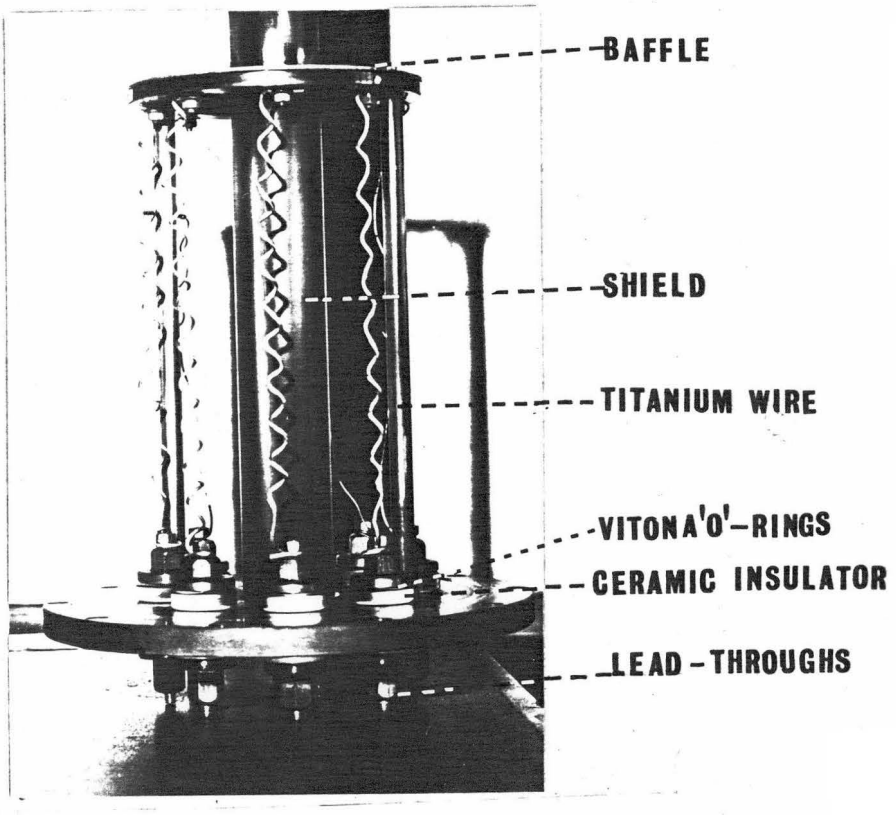

Figure 2.3 Titanium-sublimation pump.

evaporation chamber and the infrared end by means of external magnets. The substrate plates could also be manipulated magnetically to any desired orientation.

Viton-A 'O' rings were used throughout as sealing gaskets, in preference to Buna-N gaskets which were found to contaminate the apparatus through the loss of plasticiser.[34,35] All flanges and the infrared windows were water-cooled to prevent excessive heating during the outgassing of the apparatus.

Heaters, consisting of soldering iron elements, were attached at various points on the apparatus so that a nearly uniform heating could be achieved during outgassing and during studies conducted at elevated temperatures.

In an effort to reduce the pump-down time and in order to facilitate the removal of strongly adsorbed gases, on chamber walls, a gas-discharge system was incorporated in the infrared-evaporation apparatus. Aluminium electrodes, selected because of their low sputtering rate, were attached to copper rods, soldered into 'Kovar' glass-to-metal lead throughs. When a voltage of around 1.5 KV and a current of 200 mA was applied at the electrodes, in the presence of argon flowed through to the pumps, a glow-discharge, extending throughout the apparatus, was struck.

The titanium-sublimation pump (Fig. 2.3) which was situated some 30 cm. above the evaporation source consisted of eight high-current ceramic lead-throughs attached to a flange. Coils of titanium wire (1-2 mm. thick) were suspended from these and connected at the other end to a common ground,

thus completing the circuit. Although it is reported in the literature that titanium-molybdenum alloys are superior in performance[36,37] these were not available during the course of the work. By passing a current of between 10-15 amps, at 12 volt, the titanium wire could be heated sufficiently to cause the evaporation and subsequent gettering of residual gases. Eight coils used consecutively gave a total of 20 hours pumping; in practice it was found that 2-3 hours operation was sufficient to lower the pressure to the ultimate vacuum attainable. The efficiency of the pump was improved further by cooling the walls surrounding the pump with flowing water. A baffle, attached between the pump and the evaporation region, prevented evaporated titanium from condensing on the semiconductor evaporation source.

The evaporation source was a strip of molybdenum foil (6 x 0.75 x 0.1 cm.) shaped in the form of a boat. It was attached to water-cooled copper electrodes, which were soldered into 'Kovar' lead-troughs. Currents of the order of 100 amps could be passed through the foil by means of a 4 volt, 60 to 1, step-down transformer. The substrate plates could be positioned directly over the source at a distance of ~ 10 cm.

The pressure in the vacuum chamber was monitored with an ionisation gauge positioned near the evaporation assembly. Pressures between 1.3 x 10^{-1}Pa (1 x 10^{-3} torr) and 1.3 x 10^{4}Pa (100 torr) were monitored with the aid of a 'Barocel' capacitive pressure transducer.

Isolation of the cell from the pumping line was achieved with a metal bellows valve, and from the gas-handling line

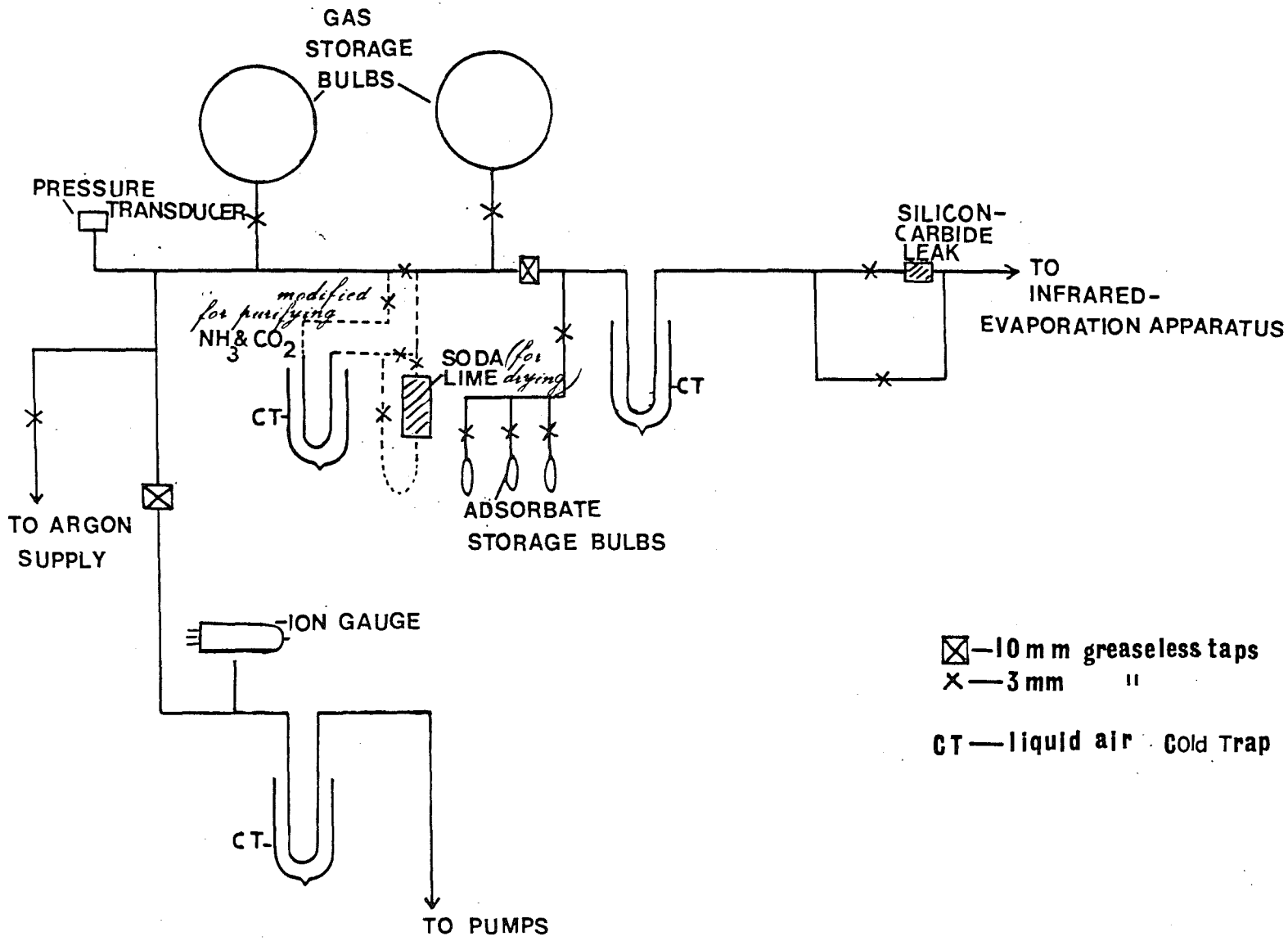
GAS
STORAGE
BULBS
PRESSURE
TRANSDUCER
SILICON-
CARBIDE
LEAK
TO
INFRARED-
EVAPORATION APPARATUS
modified
for purifying
NH3 & CO2
SODA for
LIME drying
CT
CT
CT
TO ARGON
SUPPLY
ADSORBATE
STORAGE BULBS
ION GAUGE
TO PUMPS
⊠—10 m m greaseless taps
×—3 mm "
CT—liquid air Cold Trap

with high vacuum greaseless stopcocks.

The apparatus was evacuated by a three-stage (30 litre sec^{-1}) oil-diffusion pump in series with a two-stage rotary pump. When the pressure was reduced to around 1.3×10^{-4} Pa (1×10^{-6} torr) a discharge was struck in the pressence of argon at 10^{-1} - 1.3 Pa (10^{-3} - 10^{-2} torr) for 30 minutes to 1 hour. The apparatus was re-evacuated for a further 48 hours at temperatures between 100-150°C.

The titanium-sublimation pump was finally operated for 2-3 hours, prior to film preparation. The pressure at this stage was typically around 1.3×10^{-5} Pa (1×10^{-7} - 8×10^{-8} torr). A quadrupole mass-spectrometer was attached to the apparatus at a later stage to determine the composition and partial pressures of the residual gases in the system.

Figure 2.4 shows a diagram of the gas-handling line. This system was pumped separately by a two-stage oil diffusion pump in series with a rotary pump. The pressure in the manifold was typically around 1.3×10^{-4} (1×10^{-6} torr) as measured by an ionisation gauge. A pressure transducer (L x 1603A) was attached to measure pressures between 133.3 Pa (1 torr) and 1×10^{5} Pa (760 torr). The adsorbates were stored in bulbs, isolated from the gas-handling line by means of high vacuum greaseless stopcocks; the dissolved gases in liquid adsorbates were freed by repeated freeze-pump-thaw cycles. Modifications were made to include an additional cold-trap when ammonia or carbon dioxide was used. This enabled the purification of these gases by freezing - sublimation cycles; only the middle fractions were allowed to collect in the storage bulbs.

Argon, used as an inert buffer during the evaporation procedure, was admitted into the infrared-evaporation apparatus through a silicon-carbide leak, made by sealing a short piece of silicon carbide rod in glass tubing. Pressures of the order of 1.3 - 13.3 Pa (10^{-2} - 10^{-1} torr) were maintained in the apparatus open to the pumps with an argon pressure of 1.3 x 10^{4} Pa (100 torr) on the high pressure side of the leak.

2.2 The Infrared Spectrometer

A Perkin-Elmer model 421 spectrophotometer was used in this study. It is a double beam grating instrument that operates on the optical null principle. This dual grating instrument uses two gratings, each in the first order only, with interference filters to reject unwanted orders. The frequency range of the instrument is from 4000 - 550 cm^{-1}, with a grating interchange at 2000 cm^{-1}. An absolute accuracy of ± 1 cm^{-1} is claimed, and a maximum resolution of 0.3 cm^{-1}.

The infrared end of the infrared-evaporation apparatus could be locked into position in the sample well of the spectrometer. Sample transmittance was usually below 20%; this was increased, however, by the use of an optical attenuator on the reference beam.

The operating parameters of the spectrometer were adjusted to give maximum sensitivity without significant loss of resolution. Several settings were tried before arriving at the optimum settings, given in detail below.

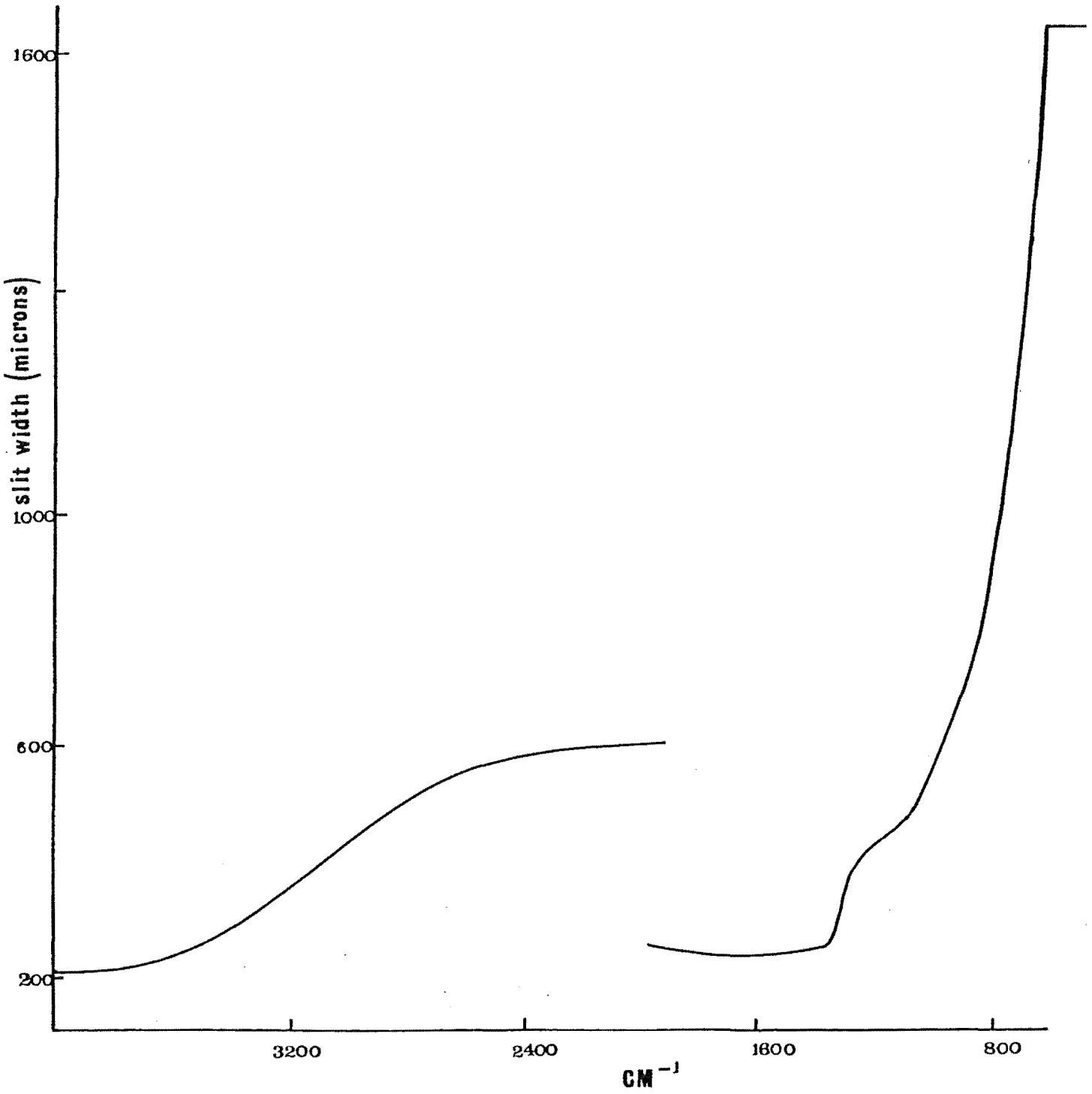

Figure 2.5 Variation of the energy of the Nernst glower with wavelength (at 2x1000 slit schedule).

A discussion of the optimization of these parameters has been given previously by Potts and Smith.[38]

The best spectra could be obtained by setting the slit schedule to twice the normal setting. This gives a continuous variation in slit width with frequency[39] to compensate for the variation of the energy of the Nernst glower with wavelength (Fig. 2.5). The amplifier gain was set just below the point where the attenuator servo loop begins to oscillate as a result of the increased noise level. The scanning speed, which is limited by two factors, viz. distortion of the spectrum at high speeds and the ability of the peripheral recording devices to cope with a fast rate of input (see Section 2.5), was set between 6-8 cm^{-1} min^{-1}.

The parameters most often used are summarised below:

Gain	4.0 to 4.5
Attenuator Speed	700-800 (normal 1100)
Scanning Speed	7 cm^{-1} min^{-1}
Source Current	0.36 amps
Slit Schedule	2 x 1000 (2 x normal)

2.3 Film Preparation

Both germanium and silicon films were prepared by evaporation in an inert gas atmosphere. The procedure for deposition of germanium films was based on the final method developed by Howe,[1] who found a two-fold increase in surface area of films prepared in argon compared to films prepared in vacuo.

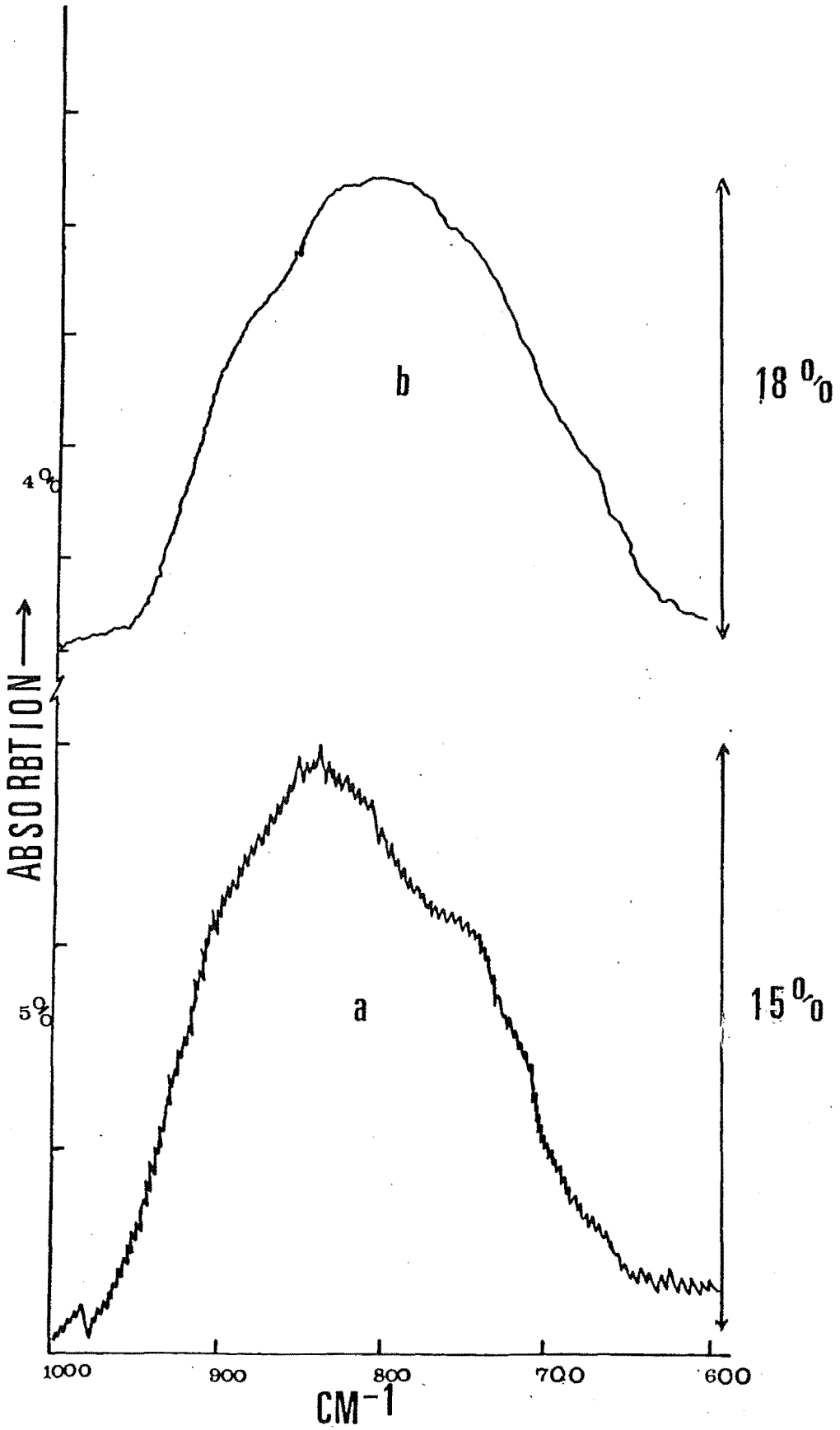

Figure 2.6 Comparison of Ge-O band heights obtained by Howe[1] (a) and that recorded on germanium films prepared in this work (b).

2.31 Germanium Films

After evacuation of the apparatus to a pressure below 1.3×10^{-5} Pa, the evaporation source (charged with approximately 0.20 gm of germanium) was outgassed at 700-800°C for 2-3 hours. The germanium was melted (at 960°C) and outgassing continued for a further 4-6 hours at 1000-1100°C. The titanium-sublimation pump was kept in operation throughout the outgassing of the source and the molten charge. As the gettering efficiency of titanium for reactive gases, such as oxygen, is very high[36] the partial pressure of these gases was reduced to a level not achieved in the previous study[1] (see Chapter 3, Section 3.2). The substrate plates (which were outgassed at 100-150°C during initial evacuation) were then positioned over the source. Argon was permitted to flow through to the pumps and when a stable pressure between 1.33 and 13.3 Pa (10^{-2} - 10^{-1} torr) was achieved the deposition started. The temperature of the source during evaporation was between 1200-1300°C as measured by an optical pyrometer.

Although the pressure of argon was higher by a factor of ten than in the previous study[1] it was not found necessary to increase the source temperature substantially to cause the evaporation. Several workers have prepared nickel[40] and germanium films[34] in the presence of inert gases at pressures exceeding 13.3 Pa (10^{-1} torr) with no detectable contamination of the films by source material. As a result of the evaporation at the higher pressure a further increase in the surface area may have occurred, judging by the intensity of the germanium-oxygen bands after exposure of the films to the atmosphere (Fig. 2.6). The reduced mean-free

path at high pressures will decrease the mobility of the vapourised atoms, thereby leading to smaller grain sizes and consequently higher surface areas.

After a pair of films were deposited, over a period of 1 hour, the plates were rotated and the procedure repeated so that a total of four films were prepared. It was not possible to measure the substrate temperature accurately during deposition but a temperature between 100-150^{o}C was measured using a chromel-alumel thermocouple (attached to two of the ceramic lead-throughs in the sublimation pump) which was allowed to make contact with one side of a substrate plate. Since the highest temperature that was employed in any of the studies was below 100^{o}C it was decided not to anneal the films any further.

Generally the films were allowed to cool for about an hour, after being positioned at the infrared end of the apparatus. Background spectra were always recorded immediately after film preparation and after the films cooled to room temperature (27^{o}C), in order to check for film contamination during the cooling period.

2.32 Silicon Films

One of the difficulties in preparing silicon films is to keep it free of silicon-monoxide contamination, which may result from reaction of silicon with oxygen adsorbed on the source material.[41]

$$Si + O_2 \longrightarrow SiO_2 \qquad (2a)$$

$$Si + SiO_2 \longrightarrow 2\ SiO \qquad (2b)$$

Thus it was necessary to thoroughly free the source of oxides by heating it to a sufficiently high temperature before melting the silicon. The source was heated to approximately 1200°C for 4-6 hours in vacuum until no significant pressure rise was observed when the apparatus was isolated from the pumps. The source temperature was then raised rapidly to melt the silicon, at temperatures around 1500°C (melting point 1410°C).[34] Although silicon begins to sublime at a temperature ~1350°C [34,42], well below the melting point, it was possible to achieve melting, without significant loss of the material, if the temperature was raised quickly. Once the silicon was melted the temperature was immediately lowered to around 1200°C and outgassing continued for a further 8-10 hours with the titanium-sublimation pump in operation. The rest of the procedure was similar to that used for preparing germanium films, although the temperature at which deposition was achieved was considerably higher (1350-1400°C).

With both germanium and silicon films deposition at high angles of incidence was tried in order to enhance the surface area of the films. As reports in the literature show[43,44] deposition at oblique angles (80° to the normal) of incidence should increase the size of the voids in the film and consequently a greater surface area should result. This is due to the self-shadowing effect of the islands growing in the direction of the vapour beam. However, no significant increase in the surface area was evident, and since it took considerably longer to deposit a film of a given thickness this technique was not used often.

2.4 Monitoring of Film Thickness

An accurate determination of the thickness of the evaporated films was not possible as equipment designed for this purpose, such as a multiple beam interferometer[45] or a quartz crystal oscillator[45,46] (which could be used directly during deposition), was not available. Howe[1] found that an approximate thickness could be obtained by monitoring the apparent absorbance of the films at 3000 cm^{-1}. A film thickness of 100 nm corresponding to a transmittance of 75% or a total transmittance for 4 films of 25%. This method is reliable if the deposition parameters, such as the rate of deposition and the source temperature, are kept constant.[45] The method derives from a relationship between the apparent 'absorption' of radiation by the films (which are transparent in the infrared), due to scattering and reflection losses, and the amount of deposited material in the infrared beam. Thus it was possible to prepare films of reproducible thickness, and thus presumably of a consistent surface area, enabling the comparison of infrared band intensities between films prepared in separate runs.

After completion of a run the film thickness (d) was routinely checked by another procedure which involved the measurement of the wavelengths at which interference maxima and minima occur. For a thin transparent film on an optically less dense substrate, transmission maxima will occur at wavelengths given by

$$\lambda(\text{max}) = \frac{2nd}{K}$$

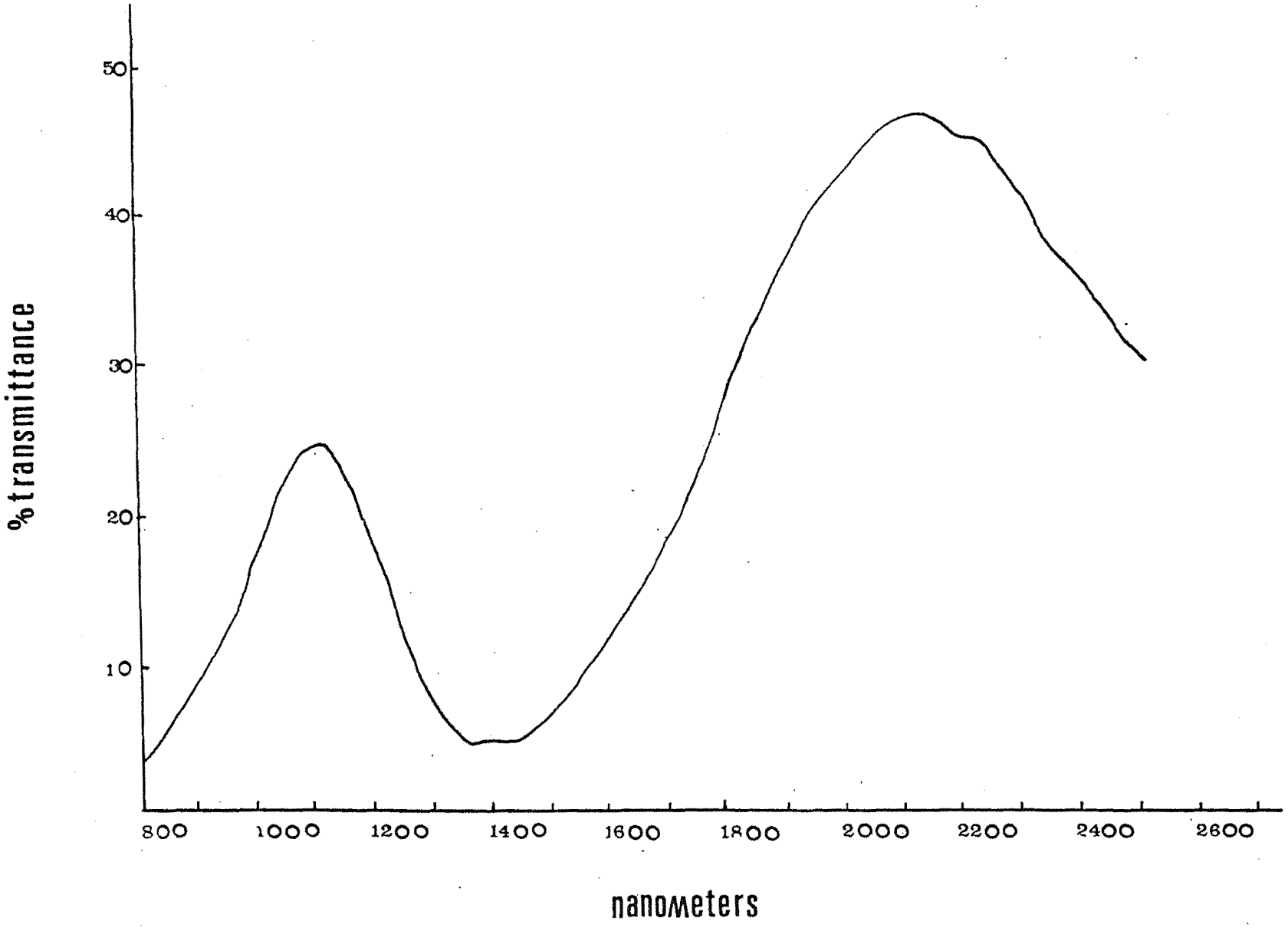
% transmittance
50
40
30
20
10
800
1000
1200
1400
1600
1800
2000
2200
2400
2600
nanometers

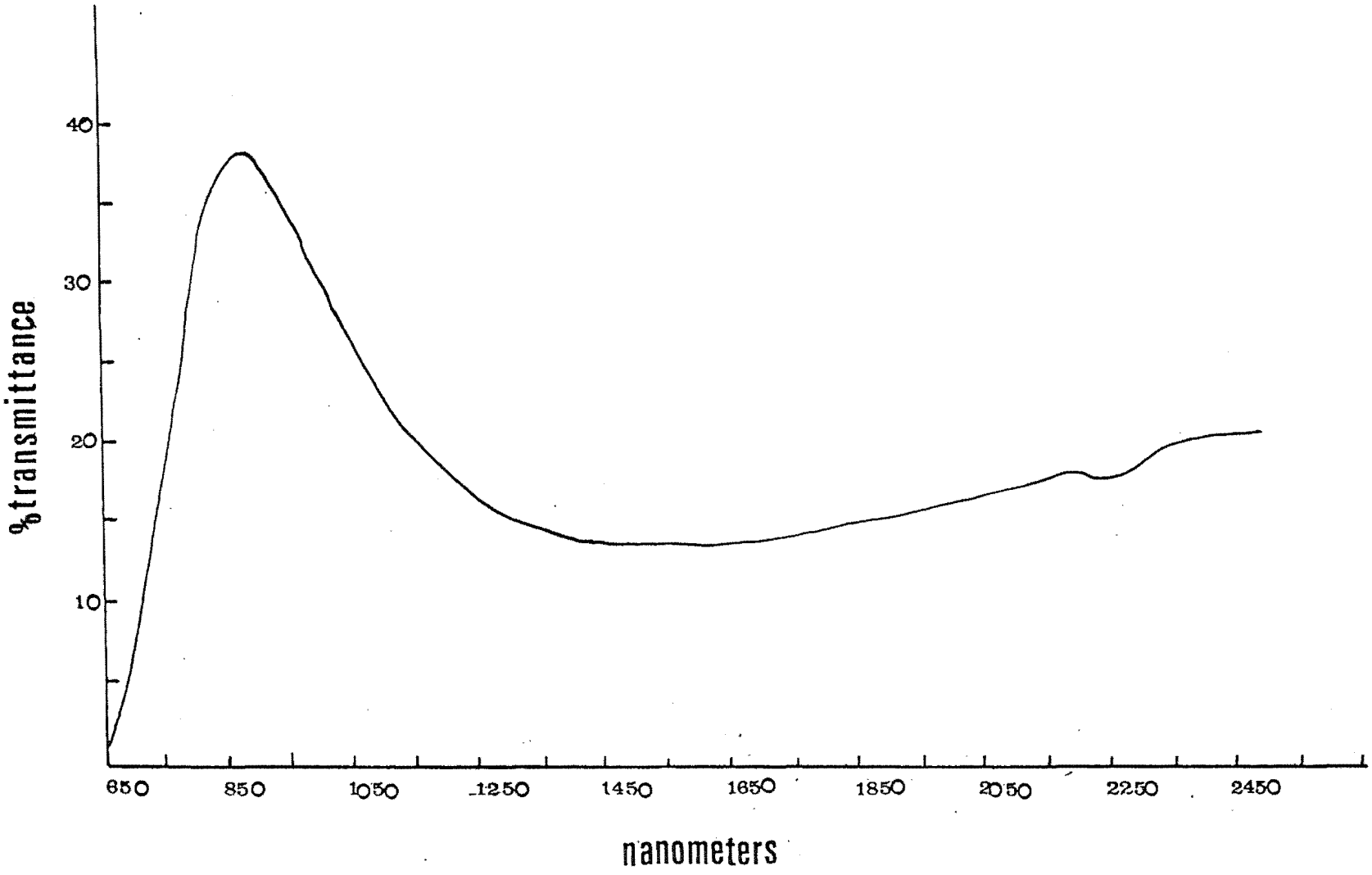

Figure 2.8 Near infrared spectrum of a silicon film prepared in this work.

and minima at

$$\lambda(\text{min}) = \frac{4nd}{2K+1}$$

where n is the refractive index of the film (assumed to be equal to the bulk value of the material), and K (the order) is an integer, 0, 1, 2 ... etc. According to Heavens[45] the method is accurate to within 10%. The interference spectrum was recorded for both germanium (Fig. 2.7) and silicon (Fig. 2.8) films on a MPS 50 spectrometer in the near-infrared region (between 600-2400 nm). The calculated thickness of the germanium films was about 100nm each, while the silicon films were 80 nm each.

2.5 Digital Recording of Spectra

Spectra were recorded digitally using a method similar to that described by Howe,[1] and previously by Bradshaw and Pritchard,[47] and Peterson et al.[48]

An output voltage which would vary in proportion to the transmittance signal was obtained by connecting a 10 volt regulated power supply across the transmittance potentiometer (linear), which is meachanically coupled to the optical wedge attenuator in the P.E. 421 (shown schemetically in Fig. 2.9). In operation the attenuator is driven across the reference beam to maintain an optical balance between the reference and sample beams. Thus any variations in the beam intensity, resulting from the absorption of radiation, will proportionately alter the position of the wiper in the transmittance potentio-

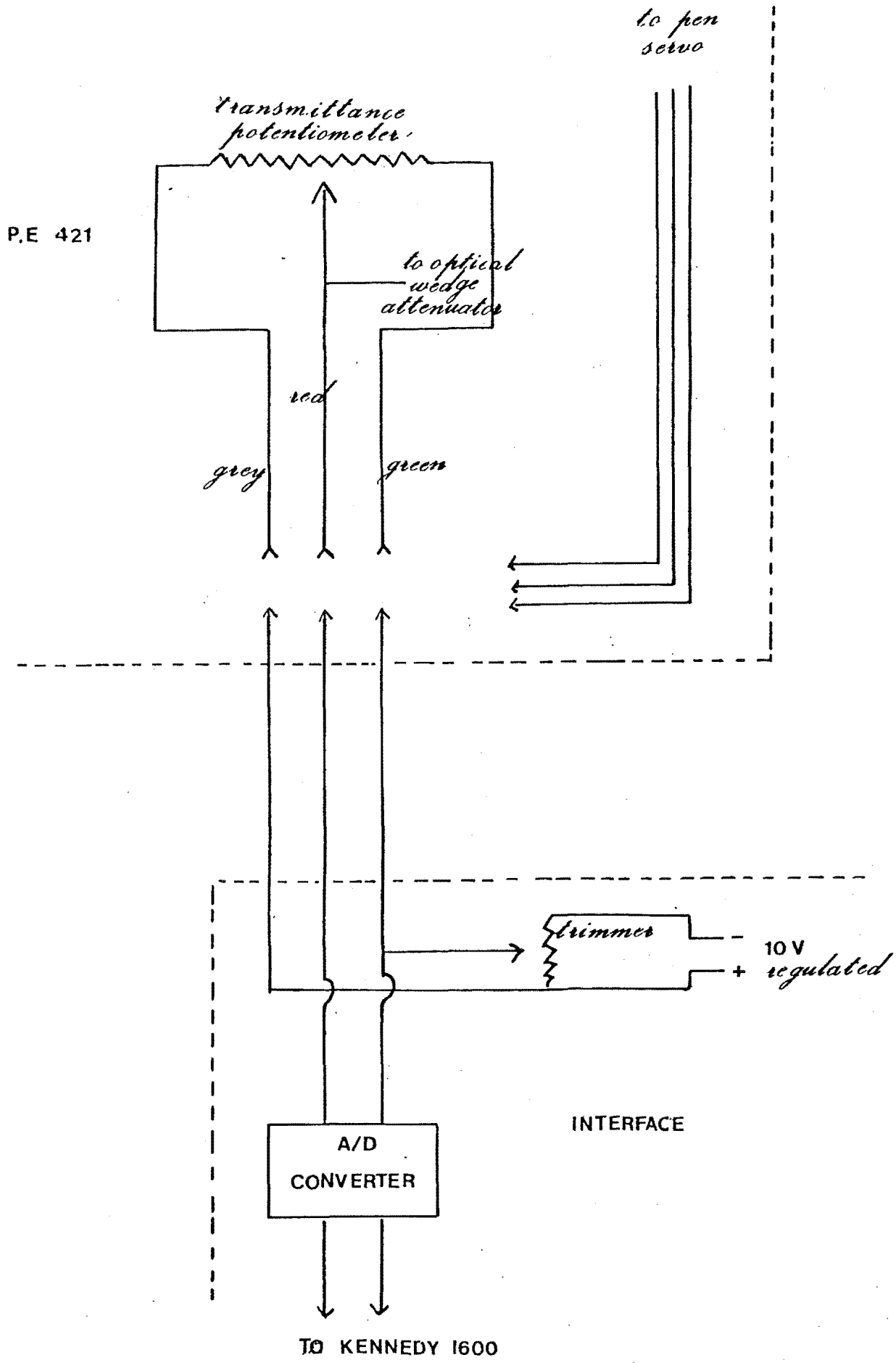

Figure 2.9 Modifications to spectrometer to read transmittance voltage.

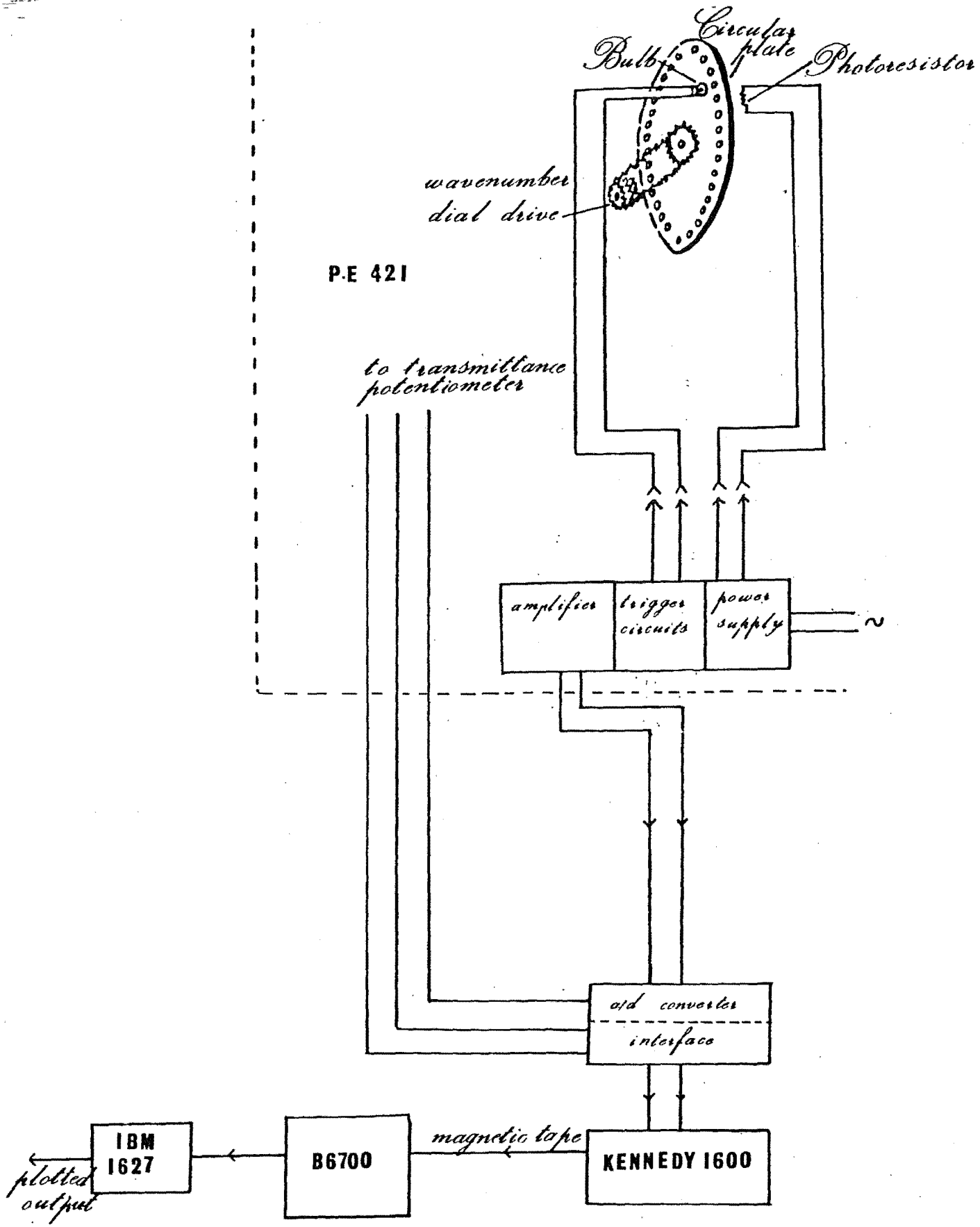

Figure 2.10 Schematic diagram of the optical switching device and the digital recording system.

meter (which is normally used to drive the chart recorder pen). By setting the spectrometer to scan in the absorbance mode, the transmittance potentiometer was freed and a voltage proportional to the percentage transmittance was taken out to an analogue-to-digital (A/D) converter.

The voltage was read at known wavenumber intervals by the use of an optical-switching device, which triggered the A/D converter at every fifth of a wavenumber. The optical switch (shown diagrametically in Fig. 2.10) consists of a circular plate with holes drilled around the periphery of the plate. This plate, which is coupled to the wavenumber dial drive by means of gears, rotates synchronously so that a beam of light directed at the holes is chopped at every fifth of a wavenumber. A photoresistor placed on the opposite side of the plate is used as the detector. A beam of light, when detected at every fifth of a wavenumber, causes a sudden change in the current passing through the photoresistor. When this change is amplified and fed into a Schmitt trigger circuit a voltage pulse is generated triggering the A/D converter to read the transmittance volatge (10.00 volts = 100.0% transmittance) at that instant. The amplifier and Schmitt trigger circuits have been described elsewhere.[1]

The digital output of the A/D converter is fed through an interface to a Kennedy Model 1600 incremental magnetic tape recorder. A 7-track tape, which advances an command when a trigger pulse arrives, records the digitised data. Data are normally recorded as 7-bit

characters (which includes one bit for vertical parity checking) on evenly spaced rows. In order to record a number corresponding to the transmittance voltage, two rows of 6-bit characters were utilised for each number; the numbers were recorded in the binary mode as 12-digit binary numbers (see Appendix I).

Since data on the tape is accessed sequentially the background was always recorded as the first file. This was followed with an end-of-file (EOF) gap which was inserted manually by a switch on the recorder. Spectra were recorded on successive files, each separated by an EOF gap.

[Note: Because of the high sensitivity of the triggering circuits in the interface (which provides the command for the tape advance mechanism) it was found necessary to always operate the tape trigger and trigger switches, on the interface panel, prior to inserting an EOF gap. This prevented the recording of noise transients on the first row of a file (which would otherwise alter the proper sequence of the recorded numbers) as a result of switching. A similar precaution was taken before the tape was initially advanced to the Load Point mark.]

In order to perform a point-by-point subtraction (section 2.6) of the spectra it is necessary to start scanning from the same wavenumber each time. A counter

was therefore connected to the triggering circuits so that it was possible to always start at exactly the same point when scanning a selected spectral region.

The maximum rated speed of the recorder is 300 characters per second, which corresponds to a maximum scanning speed of 30 wavenumbers per second. It was possible therefore to scan at the maximum speed of the spectrometer, however, in practice this was limited to around 8 wavenumbers per second in order to avoid distorting the spectra.

2.6 Processing of Digital Data

The data on tape was read into a B6700 computer with the aid of a subroutine (ALGOLSUBS) written in ALGOL (see Appendix II). This subroutine which can be accessed by the main program, written in FORTRAN, performs the desired processing of files as specified by the instructions given in the main program. As each file is accessed, the binary numbers are translated and then either added to or subtracted from an accumulating array of numbers. In order to obtain a direct correspondence with the concentration of the adsorbed species the logarithm of the numbers was obtained, and assigned as positive for background and negative for spectrum. Thus a point-by-point subtraction of the number at every fifth of a wavenumber, was achieved. The tape could be rewound on command and up to 80 spectra could be processed on any one occasion. The resulting difference spectra were then plotted directly on a Calcomp 1627 x-y plotter, linked to the B6700, by calling subroutine

PLOTS. Provisions were made in the plotting subroutine to enable a number of related spectra to be plotted on the same diagram, thus reducing the computing time and hence a faster turnaround.

It was not found necessary to smooth the final spectra, either by time averaging or by the use of convolution methods, as the quality of the spectra was sufficiently good not to warrant the use of considerable computer time called for by the smoothing procedures.

2.7 Electron Microscopy

Transmission electron diffraction photographs of germanium and silicon films were obtained by examination in a JEOL model 7A electron microscope, operated at 100KV. The films were floated free by dissolving the KBr substrate surface in distilled water, and lifted on 300 mesh copper grids.

2.8 Materials

Germanium, supplied by A.D. Mackay Inc. (USA) was 99.99999% ingot lumps.

Silicon was in the form of wafers, 0.25 mm thick (50 Ω), supplied by Adolf Heller Co. (USA).

Argon was used as supplied from a commercial cylinder (welding grade); stated purity 99.99%, with a total oxygen content less than 10 ppm.

Doubly-distilled water was freed from dissolved gases by repeated freeze-thaw-pump cycles. D_2O (99.8% D content)

was supplied by Stohler Isotope Chemicals. O^{18} water was obtained from Miles Laboratories, USA. The stated isotopic composition was O^{18} - 40.95%, O^{16} - 58.63%, and non-normalised . They were also outgassed by freeze-pumping.

Carbon dioxide and ammonia, supplied by NZIG, were purified by vacuum sublimation, the middle fractions being retained.

Oxygen was Matheson research grade, used without further purification.

CHAPTER THREE

STRUCTURE, PROPERTIES AND ELECTRONIC DESCRIPTION OF EVAPORATED GERMANIUM AND SILICON FILMS

In recent years there has been a tremendous upsurge in interest in the field of semiconductor films prepared by a variety of techniques, including evaporation, sputtering and electrolysis. Because of the vast number of practical applications, particularly in the field of microelectronics, the growth, structure and properties of these films have been the subject of many studies,[49-55] which have revealed, if anything, the difficulties encountered in obtaining a universal description of the structure and electronic properties of the films. This is largely due to the many deposition parameters (eg. deposition method,[56,57] nature of substrate,[58] substrate temperature,[59,60] rate,[61,62] quality of vacuum,[63,64] impurities in the starting material,[65] etc), and post-deposition treatments such as annealing,[66,167] which strongly influence the properties of the films.

The experimental aspects of the preparation of evaporated films have been discussed by Holland[34] and Heavens,[45] and Howe[1] has reviewed the preparation and general properties of evaporated germanium films in his thesis. Thus in the following sections, a brief discussion of the structure, properties and electronic description of evaporated germanium and silicon films will be made, together with a brief review of the current ideas in this field.

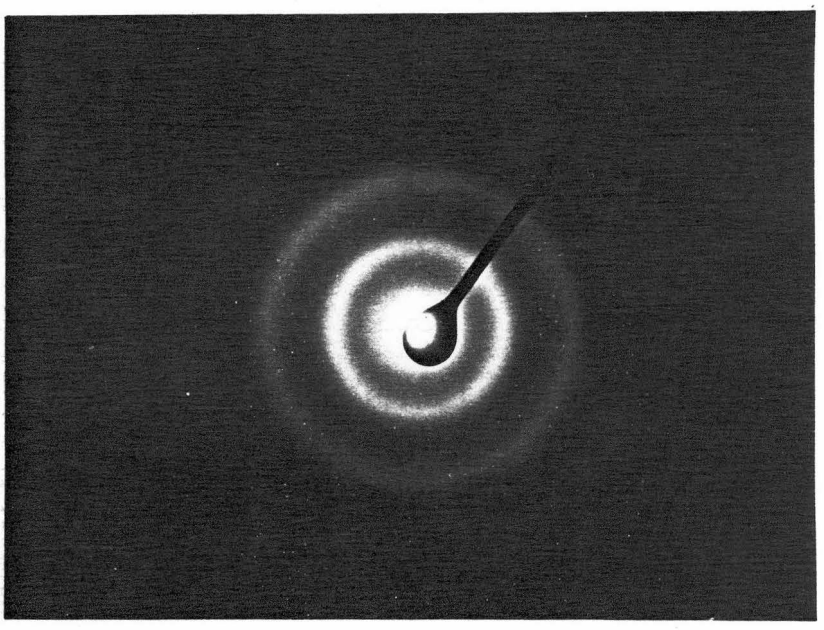

Figure 3.1 Electron diffraction pattern of an amorphous silicon film prepared in this work.

3.1 Structure

It is generally found that below a certain critical substrate temperature, which ranges between 135-375°C,[60,64,68] evaporated germanium (and silicon) films are always amorphous; the exact value of the critical temperature depends on the deposition conditions and the nature of the substrate as found in some instances.[58] The germanium films prepared by Howe,[1,5] by evaporation in an argon atmosphere, were found to be amorphous as indicated by the broad diffuse ring pattern (observed in the electron diffraction photographs) characteristic of this structure.[69] Similar patterns were obtained with the germanium and silicon films prepared in this work. It should be noted that although the source temperature was considerably higher during deposition of silicon, this did not greatly increase the substrate temperature (which depends on the source to substrate distance) to bring about crystallisation (which would result in a powder pattern)[70] of the silicon films, as a typical electron diffraction photograph of the silicon films prepared in this work shows in Figure 3.1.

No structure model has been proposed that is capable of accounting for all of the experimental data obtained for amorphous germanium and silicon films. Most models have been deduced from Radial Distribution Functions (RDFs) that have been obtained from either x-ray or electron diffraction patterns (the distribution curves are obtained from the angular distribution of the scattered intensity). The RDFs show that the first few co-ordination

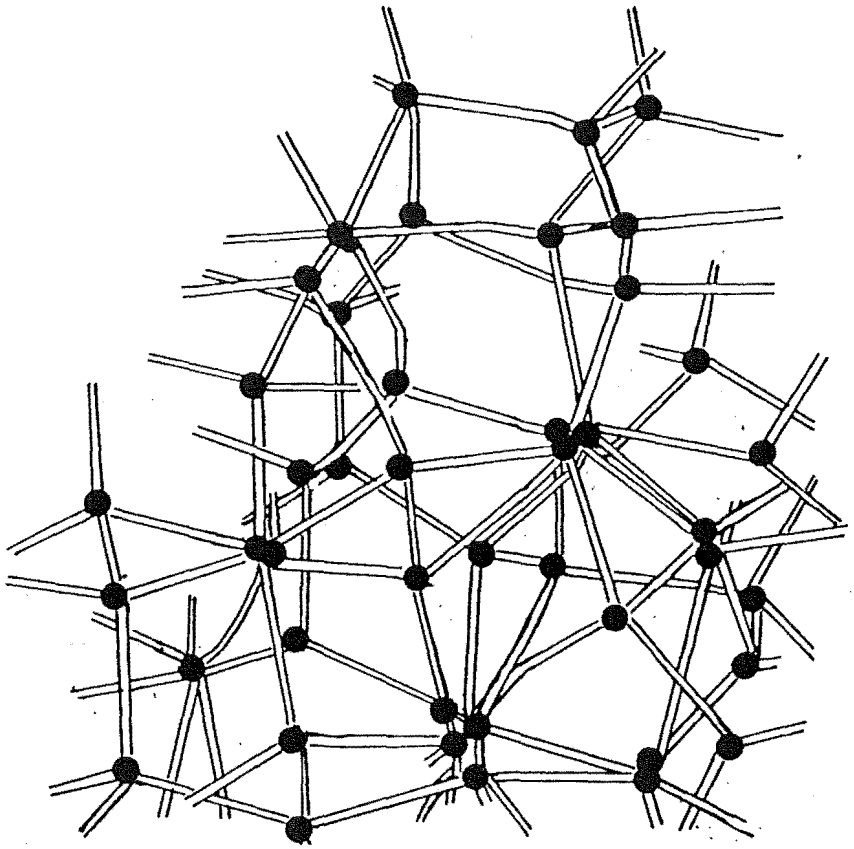

Figure 3.2 (a) Random Network Model

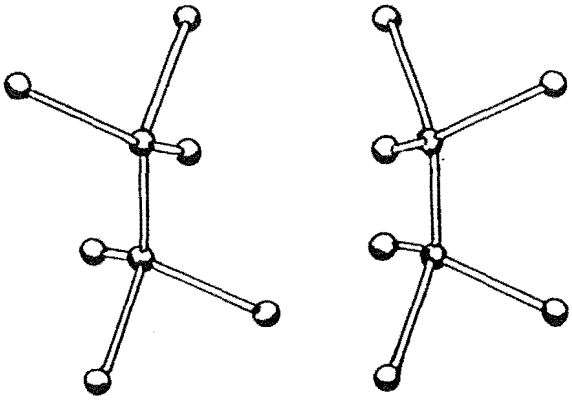

Figure 3.2b

Eight atom clusters in staggered and eclipsed configurations (Grigor0vici model).

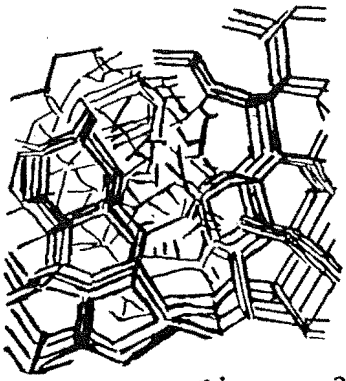

Figure 3.2 (c)

Model of boundary region between micro crystals of different orientations.

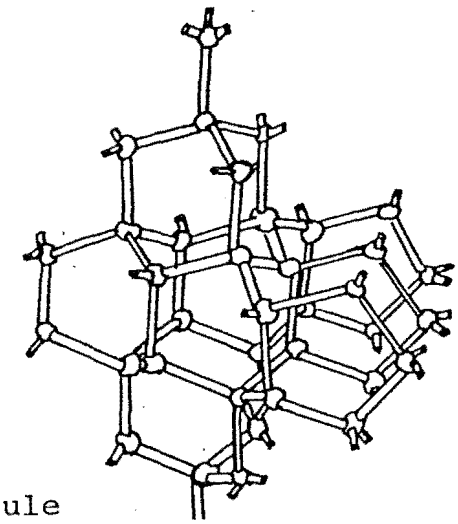

Figure 3.2d

14-atom tetrahedral module

shells are well-defined,[71-74] although there is no long-range order. The short-range order involves a tetrahedral diamond-like structure similar to the crystalline phase.

The structural models proposed can be placed in two categories: continuously random models, wherein a regular short-range order is thought to exist, and the microcrystallite models in which very small ordered domains are believed to be present.

One of the earliest models for the structure of amorphous materials, and that which is now generally accepted, is the Random Network Model,[75-80] shown in Figure 3.2a. In this model every atom has its required number of co valent bonds and a nearest neighbour environment closely resembling that in the crystalline phase. Although in the crystal structure there are only sixfold rings, in the amorphous structure odd-numbered rings, fivefold and sevenfold, are also present. Small variations in bond lengths and bond angles are permitted but with the condition that the lattice remains fully connected with no broken bonds (or 'dangling bonds'). Such a model predicts a density very close to the crystalline phase and is found to be particularly representative of annealed samples (which have a density very close to the crystalline value)[81] where as a result of annealing defects such as vacancies and voids (clusters of vacancies) are reduced to a minimum.

For non-annealed samples (such as the films prepared in this work) which show large density variations two alternative microcrystallite models have been proposed. In the first model, proposed by Grigorovici,[82,83] the structure is made up of atoms called 'amorphons' which contain only the regular staggered and eclipsed configurations of interconnecting tetrahedra, however, the 5 and 6 member rings which result are a little distorted from their ideal forms (Fig. 3.2b). A major drawback of this model, however, is that the nature of the boundary joining the 'amorphons' is not well-defined.

The second model is analogous to the Grigorovici model, only the 'amorphons' are replaced by regions of perfectly ordered phase, about 100 atoms in size, termed microcrystallites.[84-87] These microcrystallites are again connected by regions of amorphous phase, as shown in Fig. 3.2c. This model is thought to provide a realistic picture of the structure of non-annealed amorphous films which contain a large number of 'dangling bonds' (section 3.3 below), as indicated by electron paramagnetic resonance measurements.[88,89]

The various models are being continually refined in the light of more precise experimental measurements. One such model which incorporates the essential features of all three models, described above, has recently been proposed by Gaskell.[90] This model is constructed using 14-atom 'structural units' of tetrahedral shape (Tetrahedral Modules) with diamond-cubic symmetry. The structural units, shown in Figure 3.2d, are joined by planes of

eclipsed bonds (i.e. packed face-to-face). The calculated RDFs are in good agreement with experimental data for amorphous germanium and significantly improve the fit to experimental RDFs obtained for microcrystallite models, where the boundary between the crystallites is not specified.

3.2 Properties

One of the difficulties in arriving at a comprehensive structural model for evaporated amorphous semiconductors is due to the conflicting experimental data obtained from samples prepared in different laboratories employing different conditions. As mentioned previously, the deposition parameters largely determine the nature of the film that is eventually prepared, even a small difference in one of these parameters is found to affect the structure to some degree. This is indicated by the variety of values of the film density which range from 72 to 97% of the crystalline bulk value of 5.35 g/cm^3 for films deposited at 300^{o}K.[91,92]

The optical absorption edge, having an exponential decay in some cases[93,94] and an exponential decay followed by a sharp fall[60] in other cases, has been found to vary from 0.45 to 0.9eV (3630 to 7259 cm^{-1}) for amorphous germanium,[95-97] again depending on the preparatory method and deposition conditions used. The infrared refractive index of amorphous germanium, however, has been found to be close to within 7% of the crystalline bulk value of 4.0,[96,97] in contrast to the widely varying values of the

density and absorption edge. However, films prepared by different techniques show different far-infrared absorption spectra;[57] this is thought to be a result of differences in internal strains and concentration of 'dangling bonds' in the differently prepared films.

Resistivity measurements indicate that the amorphous phase is well defined in the case of germanium, since similar values for the room temperature resistivity have been found in several different laboratories (50-100 Ω cm).[61,82,98] Measurements of the rectifying properties of amorphous germanium-crystalline germanium junctions have shown that amorphous films are strongly p-type, with a hole density of 10^{18} - 10^{19} cm^{-3}.[82]

The measured parameters of evaporated silicon films have, however, been found to be very sensitive to the deposition conditions, particularly the residual pressure. The absorption edge is found to be between 1.2-1.5 eV [99] (9679 - 12100cm^{-1}) and the infrared refractive index varies between 3.9 and 4.1.[99,100] The hole density of these films is found to be in the range 10^{19} - 10^{20} cm^{-3},[99] while the resistivity for films of 420nm thickness varies from 10^{3} - 10^{5} Ω cm.[99]

Although some studies on germanium[101] have shown no significant changes in the electrical properties on improving the vacuum condition during deposition from 1.3×10^{-4} to 1.3×10^{-7} Pa, a recent investigation of evaporated silicon films showed marked differences in the surface conductivity, like density and the optical

absorption of films prepared at 4×10^{-4} Pa and 7×10^{-5} Pa.[99] It is therefore imperative that this source of contamination is reduced to a level that would permit the film surface to remain free of adsorbed species, at least for the duration of the experimental measurements. In this work the total residual pressure prior to evaporation was below 1.3×10^{-5} Pa. A typical mass spectrum, recorded with the aid of a quadrupole mass spectrometer, indicated the following residual gas composition:

Gas	Mass Peak	Estimated Pressure (Pa)
O_2	32	1.3×10^{-6}
H_2O	18	4×10^{-6}
CO, N_2	28	4×10^{-6}
CO_2	44	1×10^{-6}
H_2	2	1.3×10^{-6}
		$\simeq 1 \times 10^{-5}$ Pa

The extent of contamination by oxygen, which is the most reactive of the gases present, can be estimated from equations 3a and 3b, given below.[42]

$$t_m = N_m/(\beta\nu) \qquad (3a)$$

where N_m is the number of sites per monolayer (approximately 7×10^{14} cm^{-2}),[22] β is the sticking coefficient (for oxygen on germanium surfaces it is around 10^{-3}),[102,103] t_m is the time it would take for a monolayer to form, and ν is the number of oxygen molecules striking a square centimeter of surface per second. ν can be calculated from equation 3b, below.[104]

$$\nu = 2.6 \times 10^{20} \frac{P}{\sqrt{MT}} \beta \quad cm^{-2} \; sec^{-1} \qquad (3b)$$

where P is the gas pressure in Pa, M the molecular weight of the gas (oxygen in this example) and T the absolute temperature.

A calculation shows that t_m is of the order of 50 hours at a residual oxygen pressure of 1.3×10^{-6} Pa, although contamination by water vapour may reduce this value somewhat. The other gases (CO, N_2, H_2) do not chemisorb on germanium[17,105] (and presumably silicon), with the exception of carbon dioxide which has been found to chemisorb on germanium.[17] However, the small partial pressure, and a sticking coefficient which is likely to be less than that for oxygen, suggests that this would not be a significant source of contamination.

3.3 Electronic Description

Before the current ideas on the electronic structure of amorphous silicon and germanium are discussed it would be pertinent to consider the electronic structure of the crystalline form, since, although the long-range order is different in many ways, the short-range order of amorphous materials is reminiscent of their crystalline counterparts.

The bulk properties of crystalline semiconductors like germanium and silicon can be explained in terms of the simple band theory whereby the energy states of the free electrons can be separated into bands which may

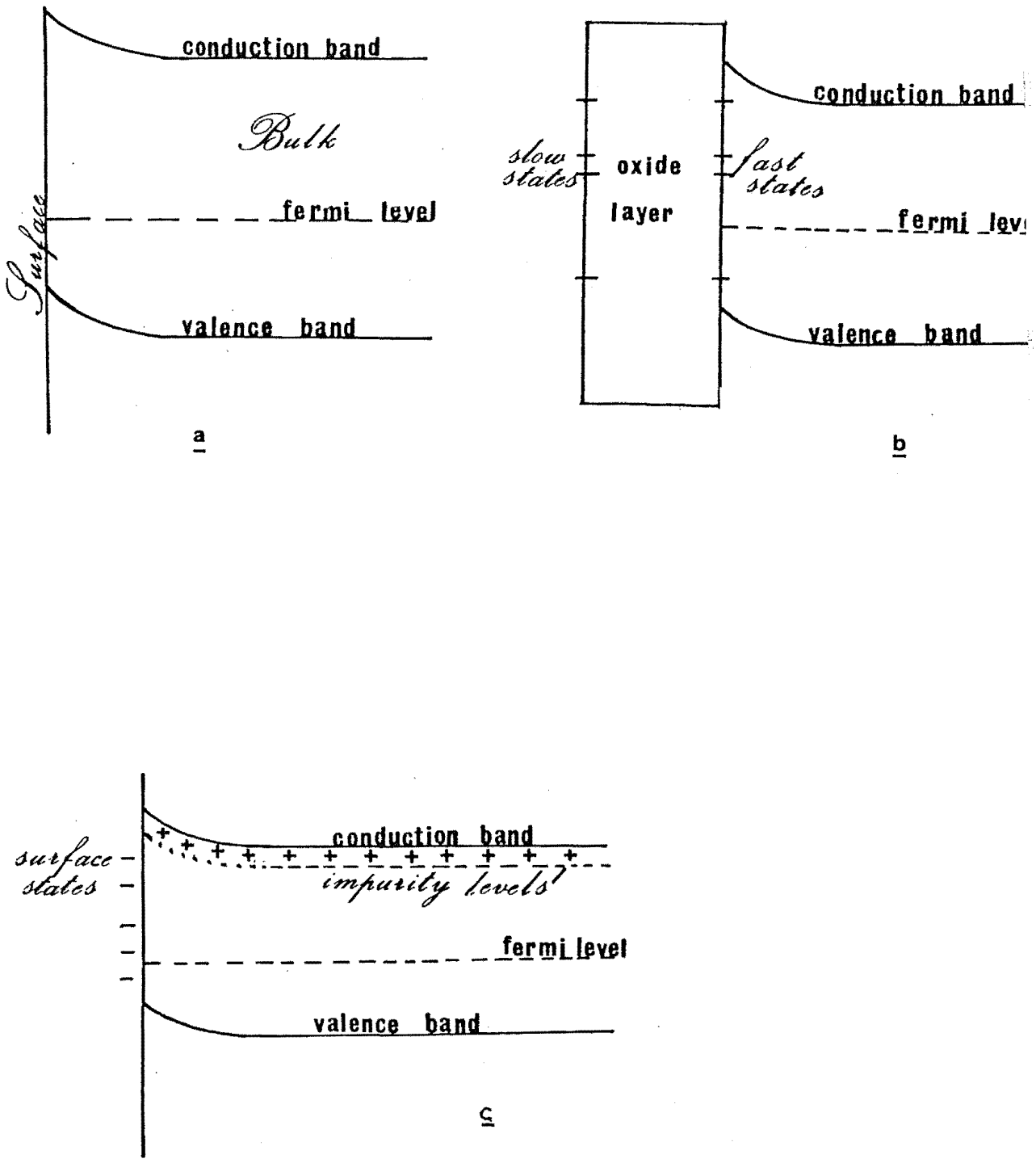

Figure 3.3 Semiconductor band diagram.

(a) Clean surface

(b) Oxide covered surface

(c) Ionisation of donor impurities in an n-type semiconductor results in electron being trapped in surface states.

overlap or be separated by gaps of forbidden energy. In intrinsic semiconductors there is a filled band of electrons (valence band) at absolute zero, which is separated by an energy gap from the conduction band, which is empty at absolute zero, but able to accommodate electrons of suitable energy at other temperatures (Fig. 3.3a). Imperfections in the crystal lattice and impurity atoms have the effect of introducing energy levels in the gap between the valence band and the conduction band. However, these are not the only energy levels that appear in the forbidden gap. The discontinuity in a perfect lattice at its surface can give rise to additional localised energy levels in the band gap. These energy levels, known as the surface states, were predicted to form a half-filled energy band at the surface, and to be equal in number to the number of surface atoms (approximately 10^{15} cm^{-2}).[106] The surface states can be regarded as 'dangling bonds' (see below) resulting from the one unsatisfied valency of each surface atom.

The existence of surface states was first suggested by Bardeen[107] in 1947, when working on metal-semiconductor rectifying contacts. Two types of surface states have been distinguished, the fast states that have relaxation times of the order of a fraction of a second,[108 & 110] and the slow states which have relaxation times that may be minutes long.[111] The fast states (approximately 10^{11} cm^{-2})[109] are associated with the acceptor levels due to surface defects at the semiconductor-oxide or semiconductor-vacuum interface, while the slow states are present

in the oxide layer (Fig. 3.3b). The time constants associated with electron exchange between the bulk and the slow states have been found to increase with increasing oxide thickness,[111] suggesting that the slow states lie mostly on the outer surface of the oxide layer. Thus they are readily removed by pumping at less than 1.3×10^{-4} Pa and are not present on initially clean surfaces oxidised by prolonged exposure to dry oxygen; it seems that they are associated with atoms or ions adsorbed from the surrounding ambient.[8]

The acceptor levels introduced by surface states can trap mobile charge carriers, either electrons or holes, and if the surface state density is large (i.e. $> 10^{12}$ cm^{-2}) then an appreciable space charge exists on the semiconductor surface. For example, on an n-type semiconductor electrons will be trapped on the surface; and a compensating layer of positive charges will be built up in the region immediately below the surface (Fig. 3.3c). Experiments of Shockley and Pearson[112] have shown that the trapped carriers lead to a much lower conductivity in the surface region. The 'double layer' that is formed as a result of positive charges aligning themselves below the surface (which now has an excess of electrons) will have the effect of bending the valence and conduction bands upwards, as is indicated in the figures. Consequently, the conduction band edge is located further above the fermi-level than in the bulk, and a potential barrier exists to electron transfer from the bulk to the exterior. If surface states are intro-

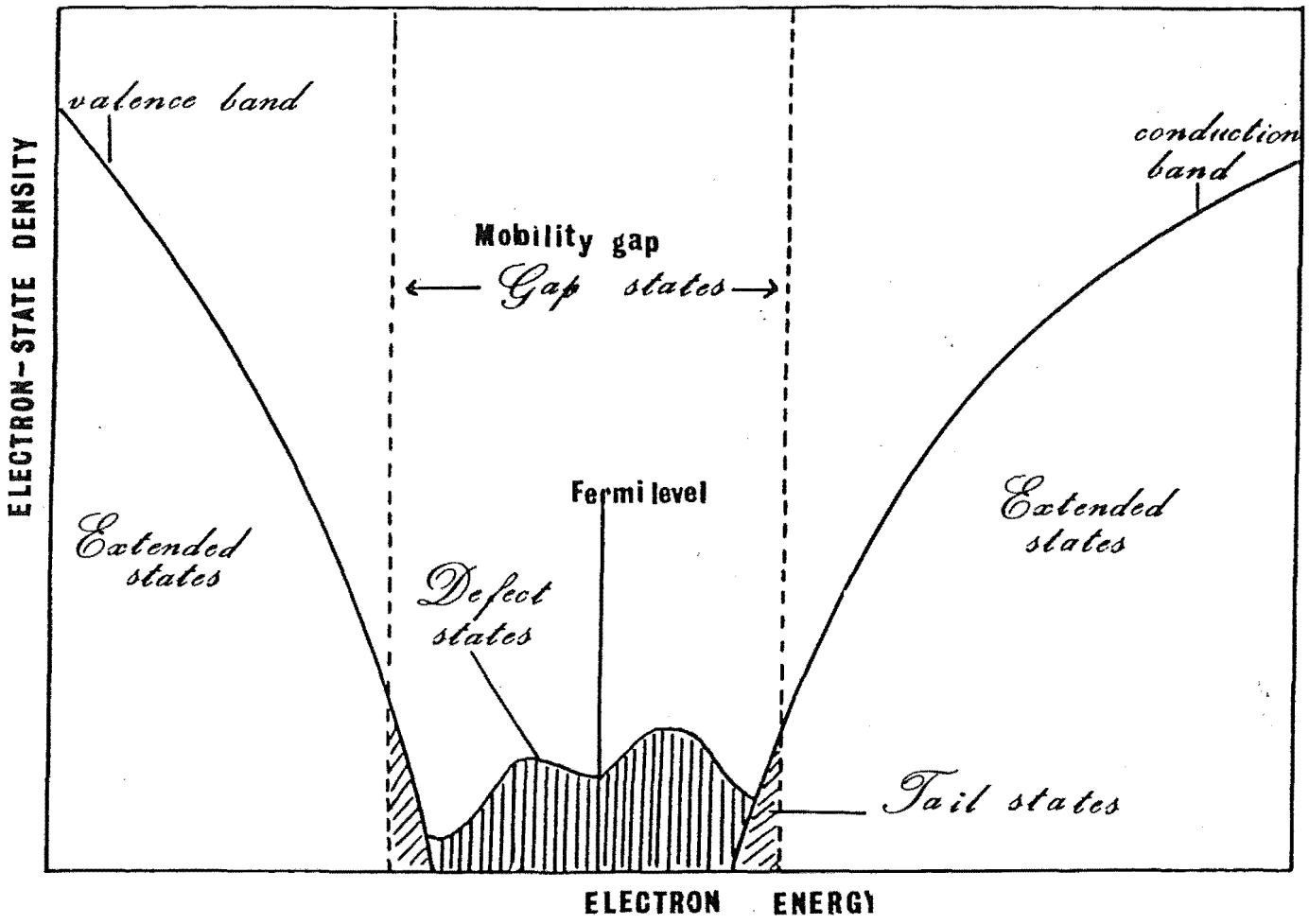

Figure 3.4 Band diagram for amorphous semiconductors.

duced by adsorbed ions a similar situation will arise. For example, oxygen adsorbed on the surface will trap electrons in the surface states and the compensating positive charges are the ionised donor levels, which are localised.

While the above described model would explain the sharp cut-off in the optical absorption edge of crystalline materials, the absorption edge of evaporated amorphous films often show an exponential decay,[93,94] sometimes accompanied with a sharp fall.[60] This has been attributed to absorption by localised states that extend into the so-called mobility gap of the band structure of amorphous materials, shown in Figure 3.4[113-116] This model is currently used as a framework for discussing the electronic states in amorphous non-mettalic solids. Much of the theoretical background to the model has been provided by Anderson,[117] Mott[118] and others.[115,119]

The energy spectrum, shown in Figure 3.4, is divided according to the electronic character of the states into extended states, the band-tail states, and the gap-states. The occurrence of the localised band-tail states is a direct consequence of the lack of long-range order, and the extent of the distribution of these states into the mobility gap is thought to approximate the disorder inherent in the structure. The deeper lying gap-states are thought to be the result of structural defects, such as 'dangling bonds' and vacancies.

The 'dangling bonds' in evaporated films would be found not only on exposed surfaces, but also on internal surfaces of voids and other defects. A dangling bond results from atoms not being able to share the electrons in a structural configuration, and the result is a broken bond. When a dangling bond is occupied by a single electron it would produce electron paramagnetic resonance (epr). Alternatively if it attracts an electron, and becomes negatively charged, or attract a hole, and become positively charged, the epr disappears. In view of the high surface-to-volume ratio of evaporated semiconductor films the dangling bonds can be expected to play in important role in gas adsorption on these films.

The band-tail states do not form a broad distribution deep into the mobility gap and are restricted to energy intervals very close to the band edges. Spear[113] reports that the tail ends 0.2 ev below the conduction-band mobility edge in his amorphous silicon films, prepared by sputtering. Their distribution is reduced even further when the films are annealed, since the microcrystallites coalesce to some extent during annealing.[101] Consequently, the optical absorption edge of annealed films becomes sharper and moves closer to that of the crystalline value.[120]

The localised tail and gap-states largely determine the electronic conductivity of amorphous semiconductors, since the mobility of the electrons falls sharply, by several orders of magnitude, in the mobility gap compared to the extended states. Electronic transport in the gap is thought to occur through thermally activated hopping.[121]

CHAPTER FOUR

INTERACTION OF WATER VAPOUR WITH EVAPORATED GERMANIUM FILMS

4.1 Review of Studies of the Adsorption of Water Vapour on Germanium Surfaces

A number of techniques have been employed in the past to study the interaction of water vapour with both oxide-covered and clean surfaces. There is very little agreement on the nature of the adsorption as various models have been proposed, mainly to account for the observed changes in the electrical properties of the surfaces.

On oxide-covered surfaces, water is thought[122] to adsorb donor fashion, the extent of adsorption increasing with the bulk resistivity, in the case of n-type samples. With p-type samples, however, an increase in the amount adsorbed occurs with decreasing resistivity,[123] suggesting that adsorption is favoured by a high hole concentration in the bulk. But such a model is not feasible on clean surfaces, because a monolayer of the fully-ionised, singly-charged, adsorbed species will give rise to too high an electrostatic repulsion energy. Green and Maxwell[105] have calculated, on the basis of dipolar interactions, that maximum binding energy is achieved in the so-called 'pirouette' configuration. Here one proton of the water molecule is between the oxygen atom and the surface, the other proton being directed upwards making the angle subtended at the centre of the oxygen atom 107°. The

calculated[105] adsorption energy is about 46 kJ mol^{-1}. However, as the experimentally determined heat of adsorption is considerably higher (between 71-84 kJ mol^{-1}) [15,124] hydrogen-bonding between the adsorbed species must also contribute significantly to the measured heat.

Water vapour shows roughly the same effect as oxygen upon the surface conductivity; giving rise initially to an increase in the p-type conductivity at exposures up to 1.3×10^{-3} Pa-min., after which there is a gradual decrease to the intrinsic value.[125] On pumping some of the water desorbs, as indicated by a small reversal in the surface conductivity. This suggests that there may be two different modes of adsorption, corresponding to the two different trends shown by the surface condictivity changes during exposure.

Volumetric studies by Boonstra[13,126] indicate that at monolayer coverage between 3 to 4 surface germanium atoms per molecule of water are precluded from further adsorption. This suggests that the molecule dissociates with the result that Ge-H, Ge-OH and Ge-O bonds are formed. This observation is in accord with the ellipsometric data of Meyer.[127] The extent of adsorption is, however, found to be plane-specific.[127] On (111) surfaces, monolayer coverage is complete when 0.3 molecules of water are adsorbed per surface germanium atom, whereas on (100) surfaces this figure is doubled. These results have been interpreted in terms of dissociative chemisorption, producing the following species:

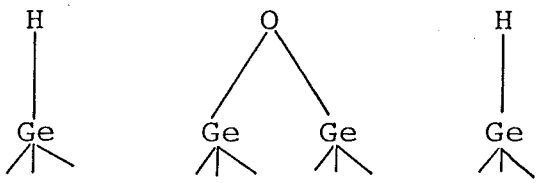

(4a)

(111) surfaces

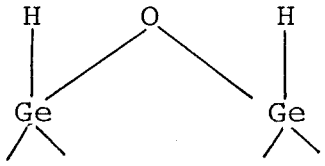

(4b)

(100) surfaces

Other studies have shown that hydrogen is liberated from the surface at temperatures above 150°C.[12-15] Although this may be a consequence of decomposition of water at high temperatures, experiments by Sparnaay[14] have suggested that the rate of hydrogen production is dependent on the thickness of the physisorbed layer above the surface. Thus any hydrogen released has to first diffuse through this layer, the rate being enhanced at higher temperatures because the layer thickness is reduced.

Ertl and Giovanelli[12] have also measured the rate of hydrogen production, but at pressures low enough to prevent any significant build up of physically adsorbed layers. They found that hydrogen production occurred through a first order process with the rate being independent of the partial pressure of water vapour. Thus

dissociation of water is suggested; however, the nature of the reaction intermediates is not known with any certainty.

A recent study using a combination of techniques has shown that there are three binding states of water, depending on the pretreatment of the surface.[15] Thermal desorption spectra show that H_2 and Ge-O are desorbed from the surface at temperature above 160^{o}C, from annealed surfaces. The broadness of the Ge-O peak after exposure to water, in contrast to the sharp peak observed when oxygen is adsorbed, suggests that surface oxidation by water is not exactly the same as by molecular oxygen. In the case of water vapour a reaction intermediate, namely Ge-OH has been suggested[12] as a possible precusor to the Ge-O species; no direct evidence for this has, however, been reported in the literature.

The concept of dissociative adsorption should therefore be considered in any explanation of the observed conductivity changes. It is possible that the dissociated species act as acceptors causing the p-type conductivity to increase during the initial stages. The decrease in conductivity, which is partially reversed on pumping, may be accounted for by the physical adsorption of undissociated water molecules.

4.2 Previous Infrared Studies of Water Adsorbed on Germanium Dioxide Surfaces

Apart from some studies on oxidised germanium, such as germania-gel, there is no mention in the literature of any infrared studies of water vapour adsorption on clean

germanium surfaces. Spectra of water adsorbed on germania-gel published by Low et al.[128] show a strong band appearing at 3673 cm^{-1} attributed to the O-H stretching fundamental of 'free' Ge-OH groups. At high exposures a broad band which is observed between 3700-2700 cm^{-1}, has been attributed to the overlapping of two absorptions due to molecular water and hydrogen-bonded surface hydroxyls.

Rzhanov and Sinyukov[129] observed a band, in the spectra of germanium dioxide, near 3700 CM^{-1} after heating the surface at 500°C in a vacuum of 1.3×10^{-4} Pa. They assigned this band to strongly adsorbed water molecules as it showed no tendency for exchange with D_2O.

A band at 1620 cm^{-1} has been assigned by Low et al.[128] and Beckmann[130] to the deformation mode of physically adsorbed water.

Some support for dissociative adsorption is shown by the appearance of a weak band at 2180 cm^{-1} in the spectra of germania-gel[128] exposed to water vapour and at 2010 cm^{-1}, in the spectra of chemically etched germanium.[130] These have been attributed to Ge-H groups.

4.3 Infrared Spectra of Water Vapour Adsorbed on Evaporated Germanium Films

Studies have been made in the usual spectral regions where infrared absorption by water molecules occurs, i.e. the 4000-3000 cm^{-1} region, where fundamental vibrations due to the -OH group occur and a region between 1700-1600 cm^{-1} where a deformation band is observed.[23] In addition the region between 1000-600 cm^{-1}, where absorption by germanium-oxygen bond stretching modes occurs,[5] and a region between 2200-1800 cm^{-1}, where germanium hydride absorbs,[23,128] have also been investigated. Labelled water, such as D_2O^{16} and D_2O^{18} has been used in order to further elucidate the nature of the interaction. For these adsorbates the regions were extended to include the absorptions that arise from the fundamental stretching modes of -OD groups, and absorptions due to $Ge\text{-}O^{18}$. A region between 1560-1300 cm^{-1} has also been monitored for likely absorptions due to Ge-D vibrations.[23]

4.31 Adsorption of H_2O^{16} on Germanium

A set of four films were prepared, allowed to cool to about 27°C, and then a background spectrum recorded. Contamination of the films due to residual gases, particularly oxygen, was not evident during the cooling period. This was determined by recording a background immediately after film preparation and one after the cooling period. The apparatus was then isolated from

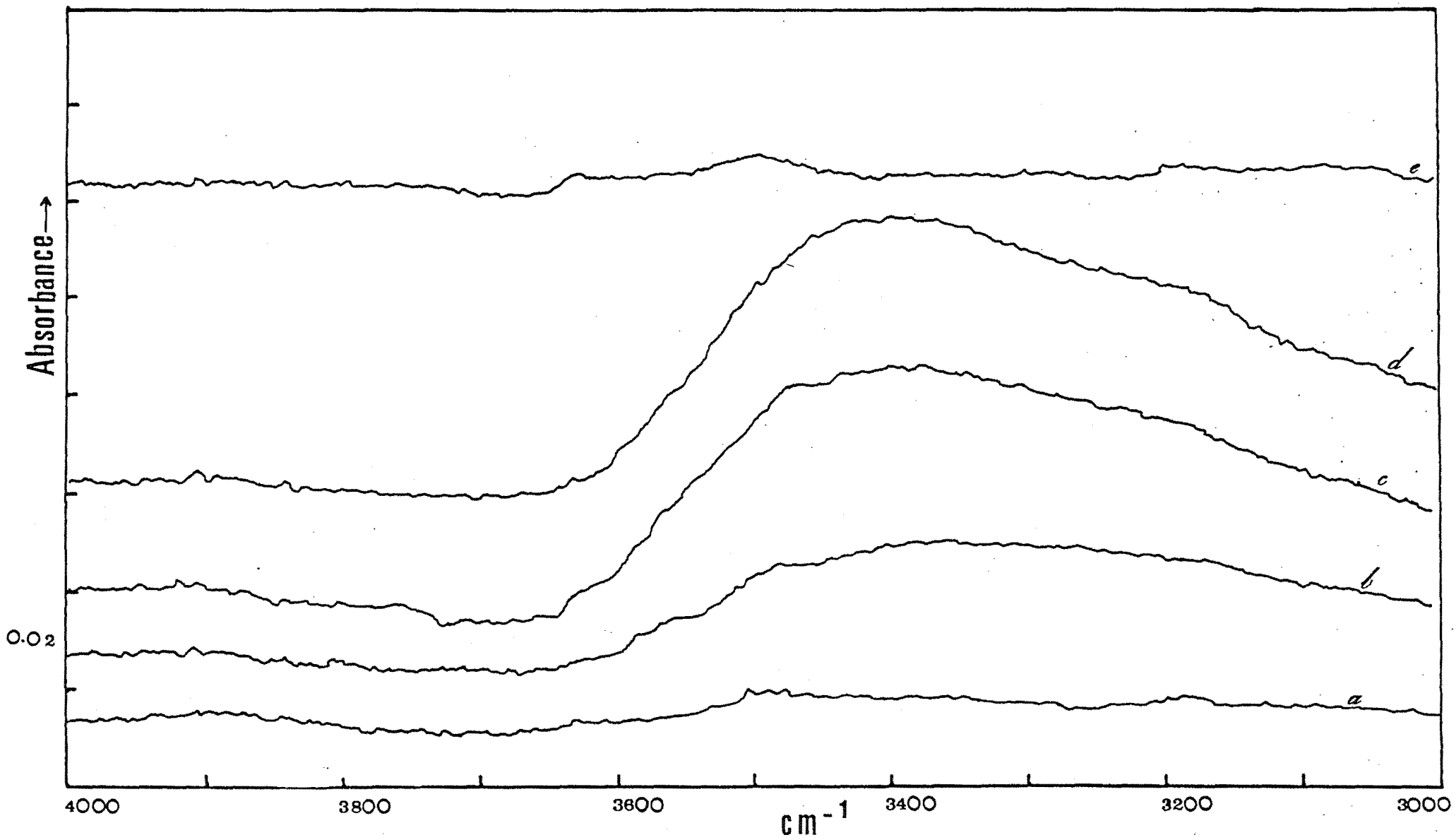
Absorbance→
0.02
e
d
c
b
a
4000
3800
3600
3400
3200
3000
cm⁻¹

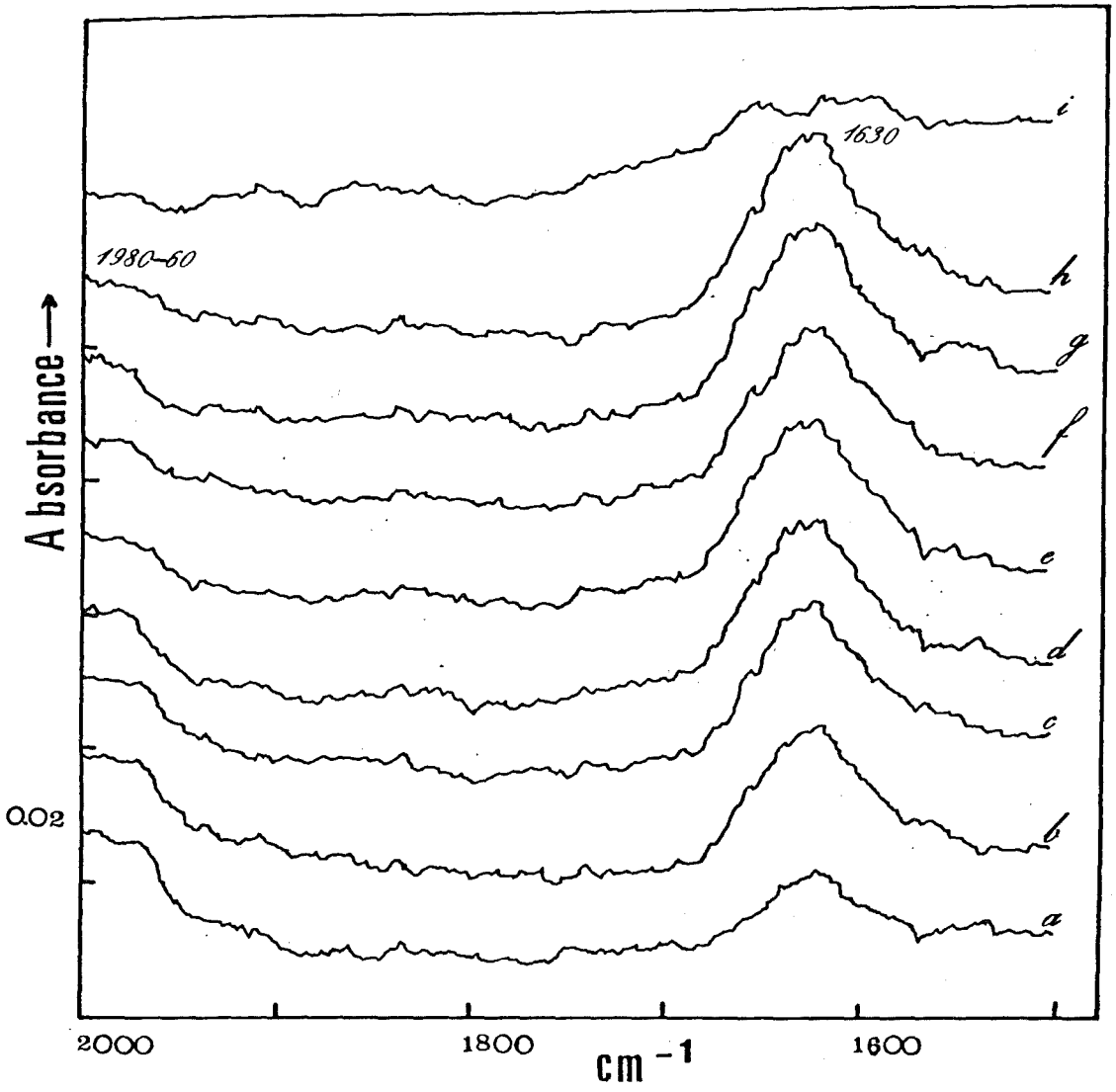

Figure 4.2 Spectra of water vapour adsorbed on germanium films, at 27°C. (a) and (b) at 1.3 Pa, (c) to (h) 773 Pa. (a) 10 min; (b) 30 min; (c) 1h 13 min; (d) 4h 13 min; (e) 20h; (f) 28h; (g) 44h; (h) 92h; (i) pumped 30 mins. Ordinates displaced.

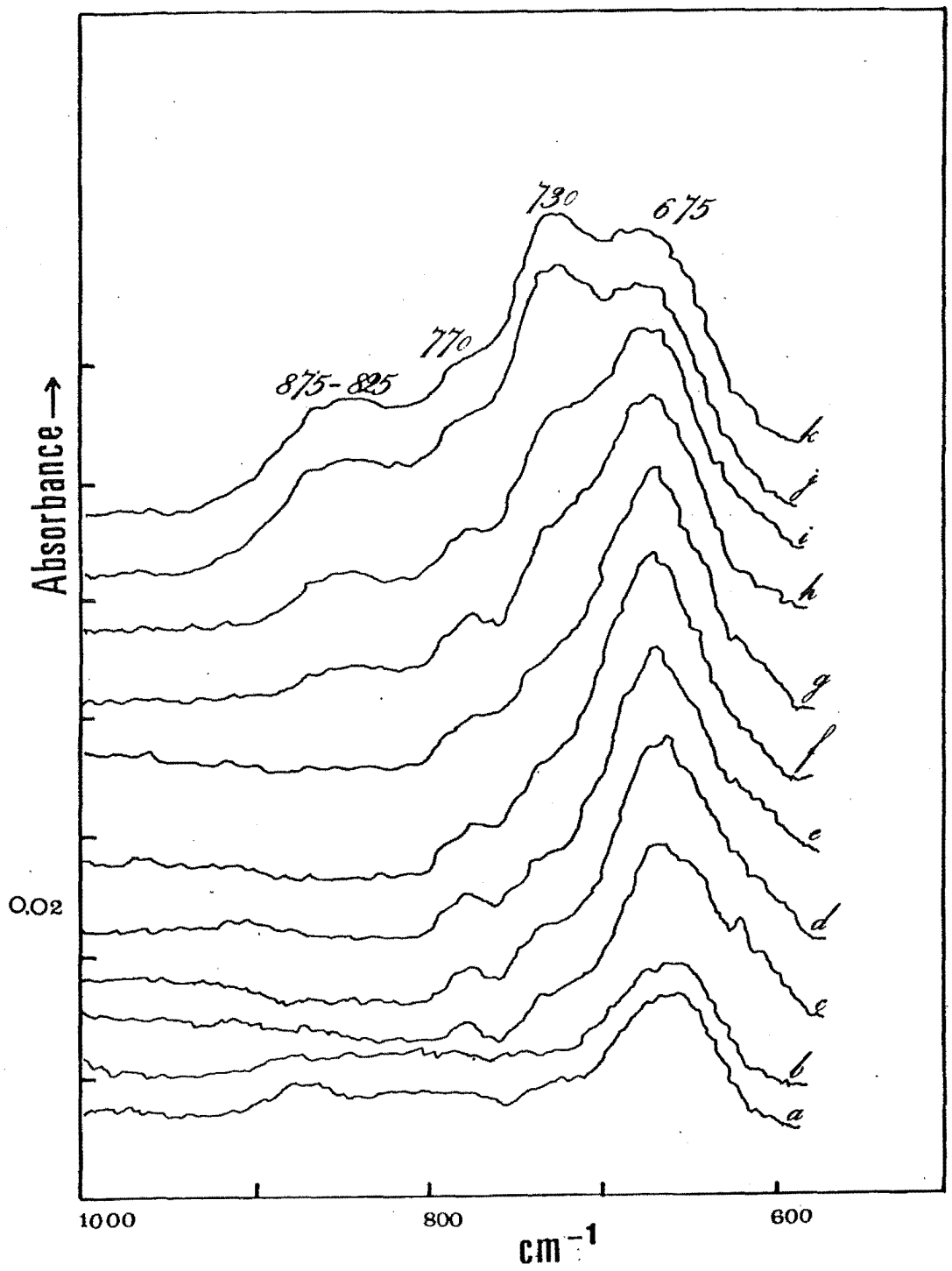

Figure 4.3 Spectra of water vapour adsorbed on germanium, at 27°C. (a) and (b) 1.3 Pa, (c) to (j) 773 Pa. (a) 15 min; (b) 35 min; (c) 1h 20 min; (d) 4h 20 min; (e) 20h 10 min; (f) 26h; (g) 28h 20 min; (h) 44h 10 min; (i) 54h 10 min; (j) 92h 10 min; (k) pumped 24h. Ordinates displaced.

the pumps and water vapour admitted at 773 Pa (5 Torr). Recordings were commenced and continued for about a week. The spectra obtained after subtracting the background are shown in figures 4.1 - 4.3.

It is evident from the spectra that there is an initial rapid interaction with the surface resulting in bands between 3600-3200 cm^{-1} (Fig. 4.1), 1980-60 and 1630 cm^{-1} (Fig. 4.2) and at 770, 730 and 675 cm^{-1} (Fig. 4.3). Very little detail can be seen in the broad band between 3600-3200 cm^{-1}, and since it was removed completely after pumping (trace e , Fig. 4.1), together with the 1630 cm^{-1} band (trace i , Fig. 4.2), they most probably are due to molecular water physically adsorbed on the surface. In contrast to the above bands the very weak bands appearing below 2000 cm^{-1} were stable to pumping (trace 1, Fig. 4.2 and trace k , Fig. 4.3). With increasing exposure the three absorptions below 1000 cm^{-1} show a small but significant growth. The 730 cm^{-1} band, which is initially obscured by the tail of the 675 cm^{-1} band, eventually grows to become the most intense band observable. A small decrease in the 675 cm^{-1} band can also be seen after a total of 30 hours exposure (trace h, Fig. 4.3). At this stage a broad plateau appears between 875-825 cm^{-1} on the same scan.

The 1980-60 cm^{-1} band which appears to have reached its maximum intensity within 10 minutes exposure shows completely opposite behaviour to the others on continued exposure. It is characterised by a steady decline in intensity which continues over a period of 90 hours after which the band is barely detectable (Fig. 4.2).

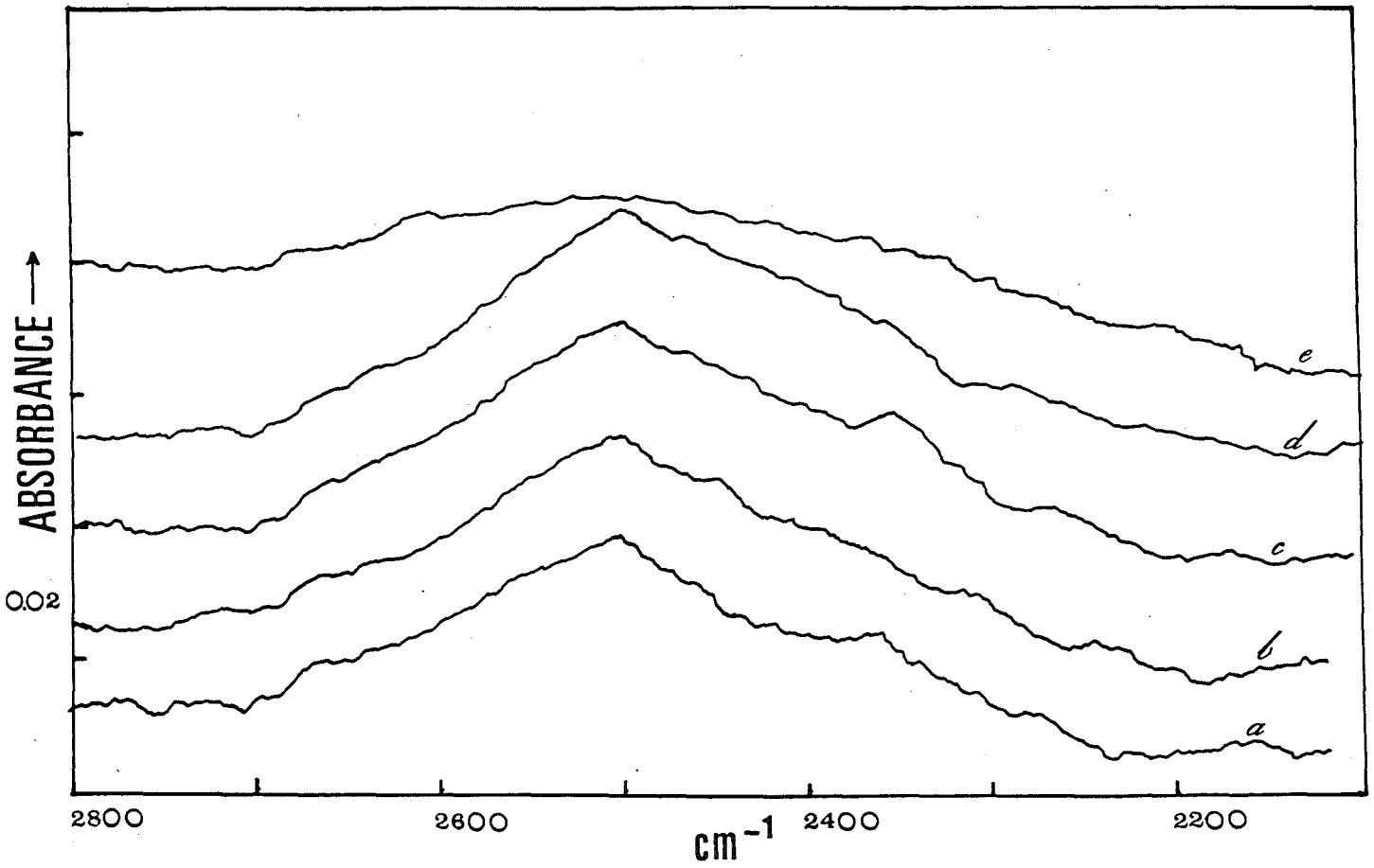

Figure 4.4 Spectra of D_2O^{16} adsorbed (at 773 Pa) on germanium, at 27°C. (a) 30 min; (b) 1h; (c) 6h 30 min; (d) 18h; (e) pumped 1h. Ordinates displaced.

Figure 4.5 Spectra of D_2O^{16} adsorbed (at 773 Pa) on germanium, at 27°C. (a) 10 min; (b) 30 min; (c) 4h; (d) 19h; (e) 30h; (f) pumped 1h. Ordinates displaced.

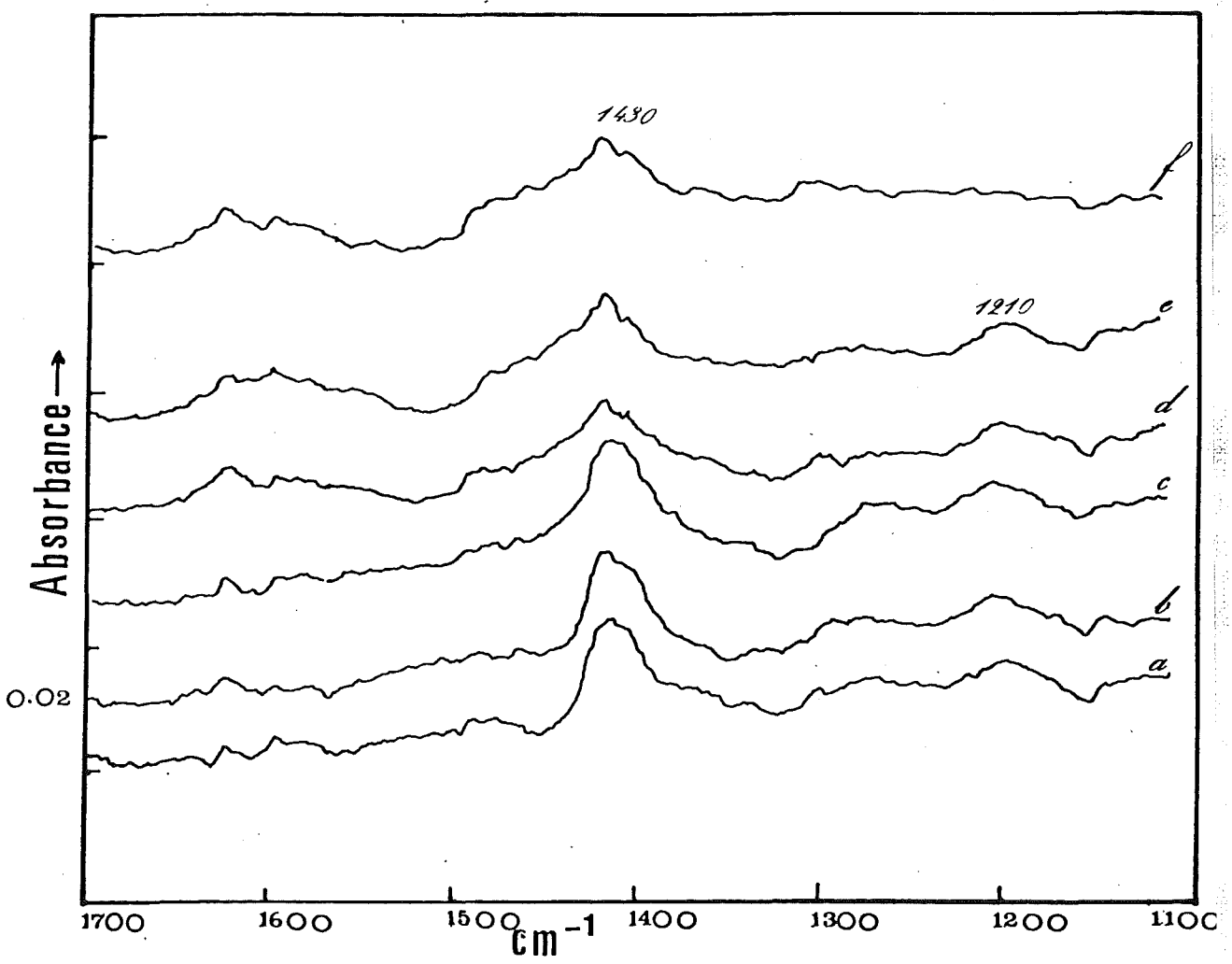

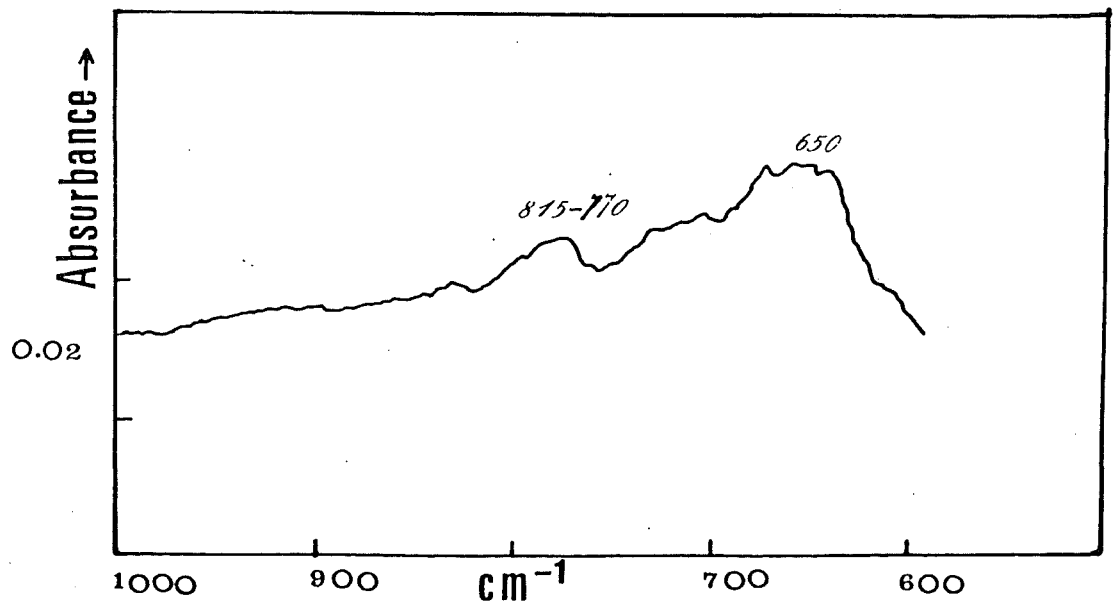

Figure 4.6 Spectra of D_2O^{16} adsorbed (at 773 Pa) on germanium, at 27°C. Recorded after 1 hour exposure. Ordinates displaced.

Several unsuccessful attempts were made to observe the spectra at very low exposures (i.e. below a pressure of 1.3×10^{-2} Pa (1×10^{-4} Torr). Significant changes in the spectra could only be seen at pressures above 1.3×10^{-1} Pa with the appearance of the bands below 2000 cm^{-1}, described earlier, but with the exception of the 1630 cm^{-1} band. The band centre of the previously described 675 cm^{-1} band is positioned at a much lower frequency, at about 650 cm^{-1} (trace, a,b, Fig. 4.3). Intensity changes, however, were not apparent even on continued exposure at pressures between 1.3×10^{-1} - 1.3 Pa (trace b, Fig. 4.2 and trace b, Fig. 4.3). Band growth or decrease only occurred at presures above 133.3 Pa (1 Torr).

4.32 Adsorption of D_2O^{16} on Germanium

The adsorption of deutrated water at the same pressure (773 Pa) on a set of freshly prepared films (cooled to $27^{o}C$) is shown in figures 4.4 - 4.6. A broad band, which is completely removed on pumping, is observed between 2700 and 2200 cm^{-1} (Fig. 4.4). In figure 4.5 the 1630 cm^{-1} band, observed previously with water, is replaced by one at 1210 cm^{-1}. This is similarly removed on pumping. A new band, which appears in place of the 1980-60 cm^{-1} band, can be seen at 1430 cm^{-1}. With increasing exposure this band shows a similar tendency to decrease as with the 1980-60 cm^{-1} band (Fig. 4.5).

Only slight changes in the spectra are apparent between 1000-600 cm^{-1} (Fig. 4.6). The band centre of the 675 cm^{-1} absorption (observed with water vapour) is

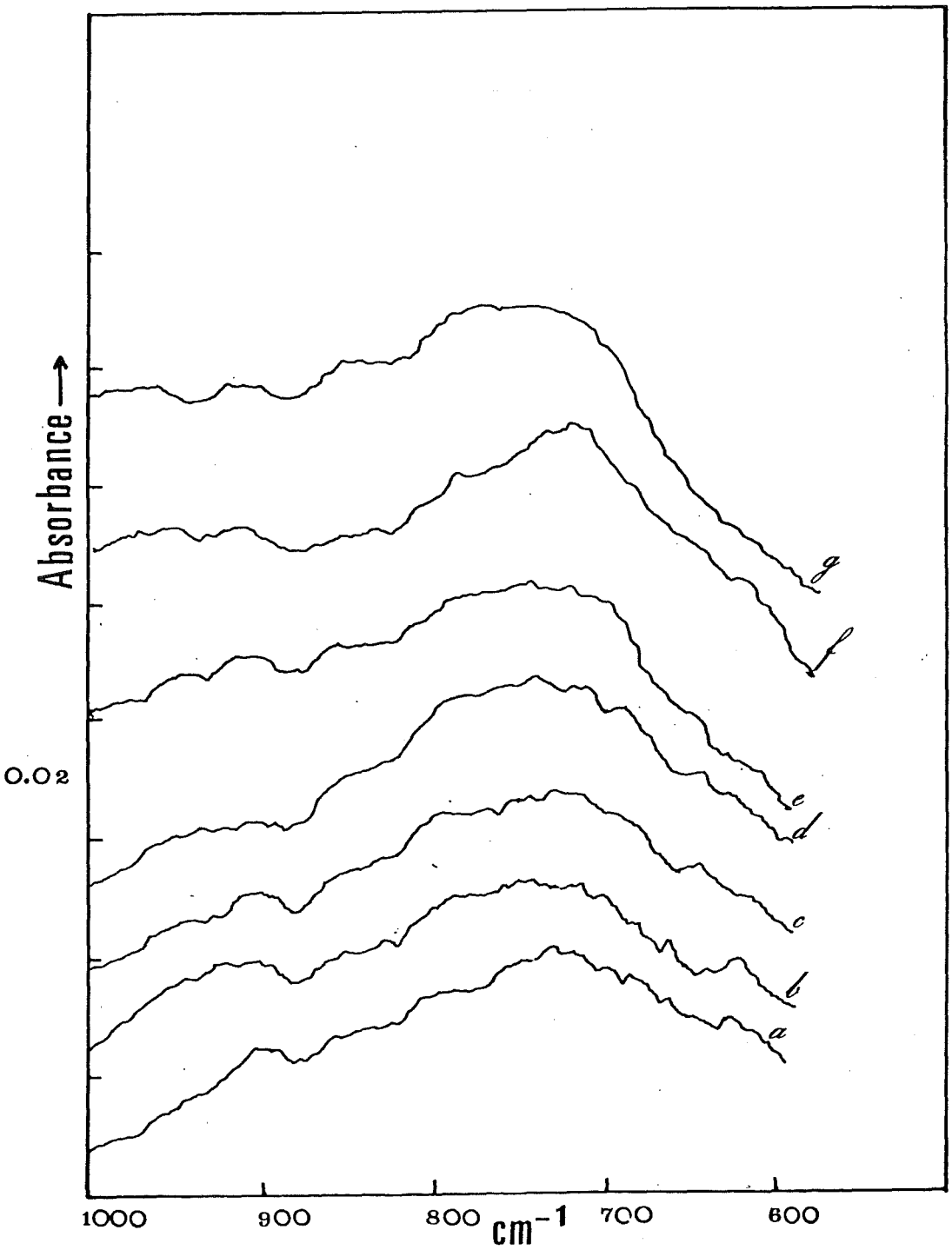

Figure 4.7 Spectra of O^{18} water adsorbed (at 773 Pa) on germanium, at 27°C. (a) 10 min; (b) 30 min; (c) 2h; (d) 4h 30 min; (e) 6h; (f) 26h; (g) 44h. Ordinates displaced.

shifted to 650 cm^{-1}, while the 770 cm^{-1} shows a small broadening between 815-770 cm^{-1}.

4.33 Adsorption of D_2O^{18} on Germanium

In order to try and resolve the bands due to germanium-oxygen vibrations O^{18} water was adsorbed on a set of clean films. The spectral changes below 1000 cm^{-1} are shown in figure 4.7. Because of the inherent broadness of the bands, absorptions due to the various germanium-oxygen species (i.e. Ge-O^{18} and Ge-O^{16}) are not resolved sufficiently to allow assignments to be made with any certainty.

4.34 Decrease of the 1980-60 cm^{-1} band

The decrease of the 1980-60 cm^{-1} band with increasing exposure, in contrast to the growth of the other bands, warranted a more detailed study. Since marked intensity changes occurred at high exposures the role of water vapour in influencing the decrease of the band was investigated; the study being confined mainly to the 1980-60 cm^{-1} band and the 675 cm^{-1} band, which seemed to show a parallel growth.

A set of four films were exposed to water vapour under identical conditions to that described in Section 4.31. After one hour the apparatus was evacuated to below 1.3 x 10^{-3} Pa (1x10^{-5} Torr) and isolated from the pumps. Difference spectra obtained from recordings made over a period of 60 hours are shown in figure 4.8. No

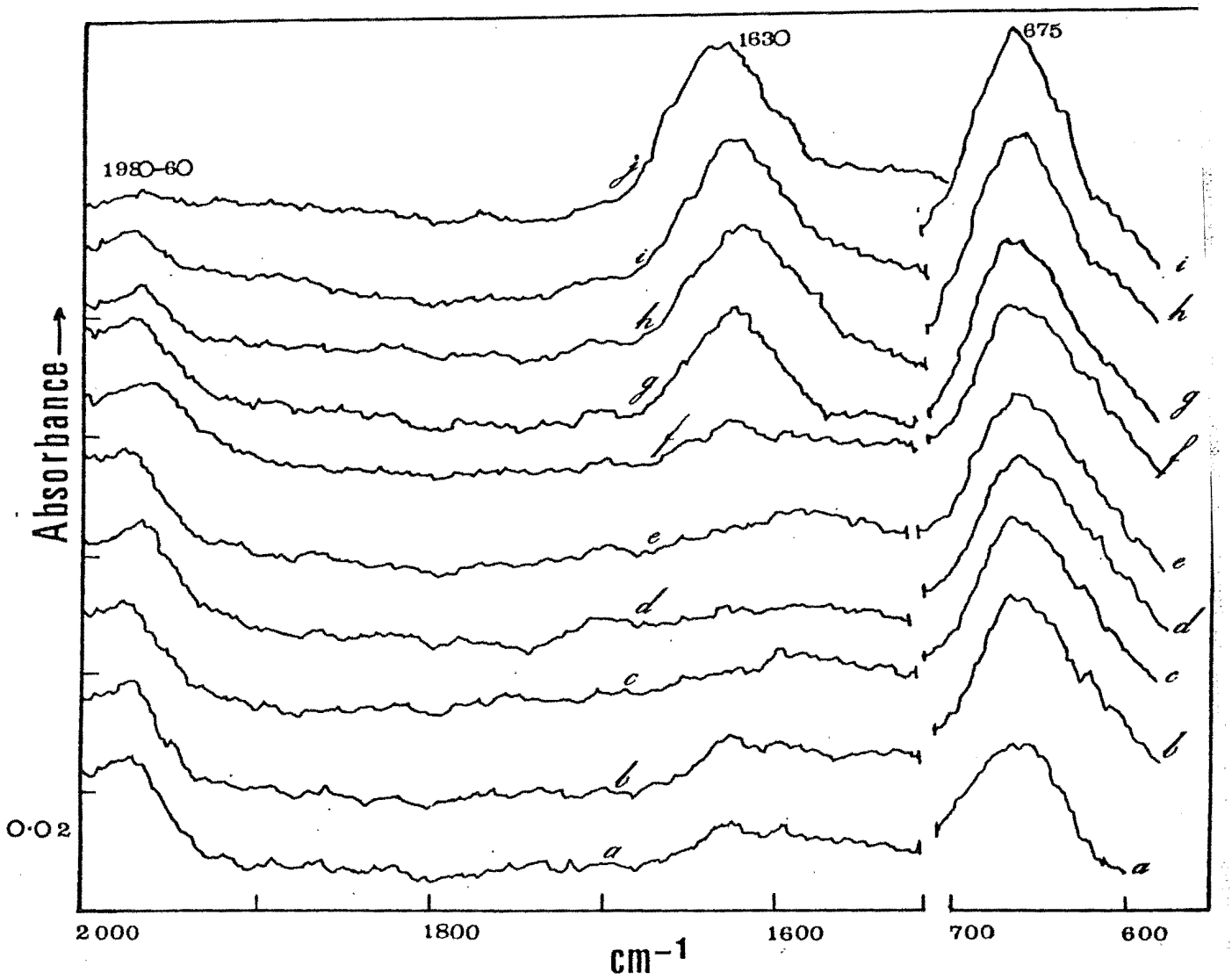

Figure 4.8 Influence of water vapour on the decrease of the 1980-60 cm^{-1}. Traces (a-e) after evacuating water vapour. Traces (f-j) after readsorbing water vapour at 773 Pa. (a) 10 min; (b) 1h 40 min; (c) 10h 30 min; (d) 25h; (e) 66h; (f) 5 min; (g) 1h 20 min; (h) 7h 20 min; (i) 30h; (j) 73h. Ordinates displaced.

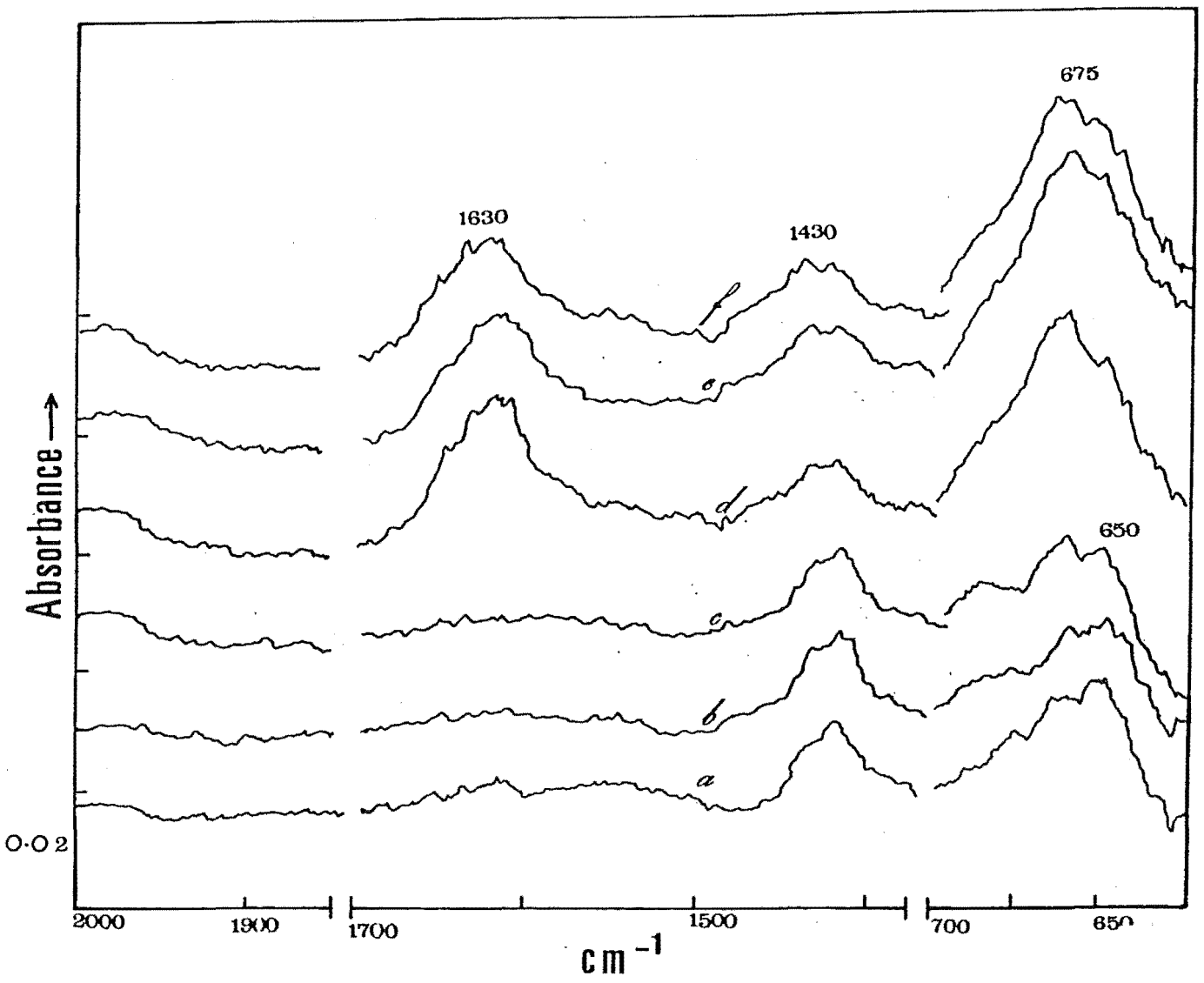

Figure 4.9 Spectra obtained by first adsorbing D_2O^{16} at 773 Pa (a-e) on germanium, at 27°C, followed by evacuation and adsorbing water vapour (d-f). (a) 10 min; (b) 30 min; (c) evacuated 1h; (d) 1h; (e) 20h; (f) 25h. Ordinates displaced.

significant changes are apparent in the 1980-60 cm^{-1} band (trace a to f). On readmitting water vapour at the original pressure (773 Pa) a steady decrease in the band is observed (trace g to j). An increase in the 675 cm^{-1} band is also evident (trace g to i).

Using a similar procedure as above D_2O^{16} was initially adsorbed on a set of films. After evacuation water vapour was admitted in its place. The changes in the spectra are shown in figure 4.9. The 1430 cm^{-1} band which appears on adsorption of D_2O^{16} gradually decreases in intensity (trace d to f) while a band centred at 675 cm^{-1} shows a small growth (trace d to f).

4.35 Temperature Dependence

Experiments were carried out at four different temperatures (25, 30, 38 and 45^{o}C) to characterise the temperature dependence of the rate of decrease of the 1980-60 cm^{-1} band. For each temperature a set of new films was always employed. Spectra were recorded over a period of 90 hours in the region between 2000-1800cm^{-1}, the pressure of water vapour being maintained at 773 Pa in each case. The difference spectra are shown in figure 4.10.

The areas under the curves, normalised by comparison with the initial value for each temperature, between 2000-1800 cm^{-1}, are plotted as a function of time in figure 4.11. Since extinction coefficients of absorption bands are known to vary with coverage, either linearly or non-linearly, it is not surprising

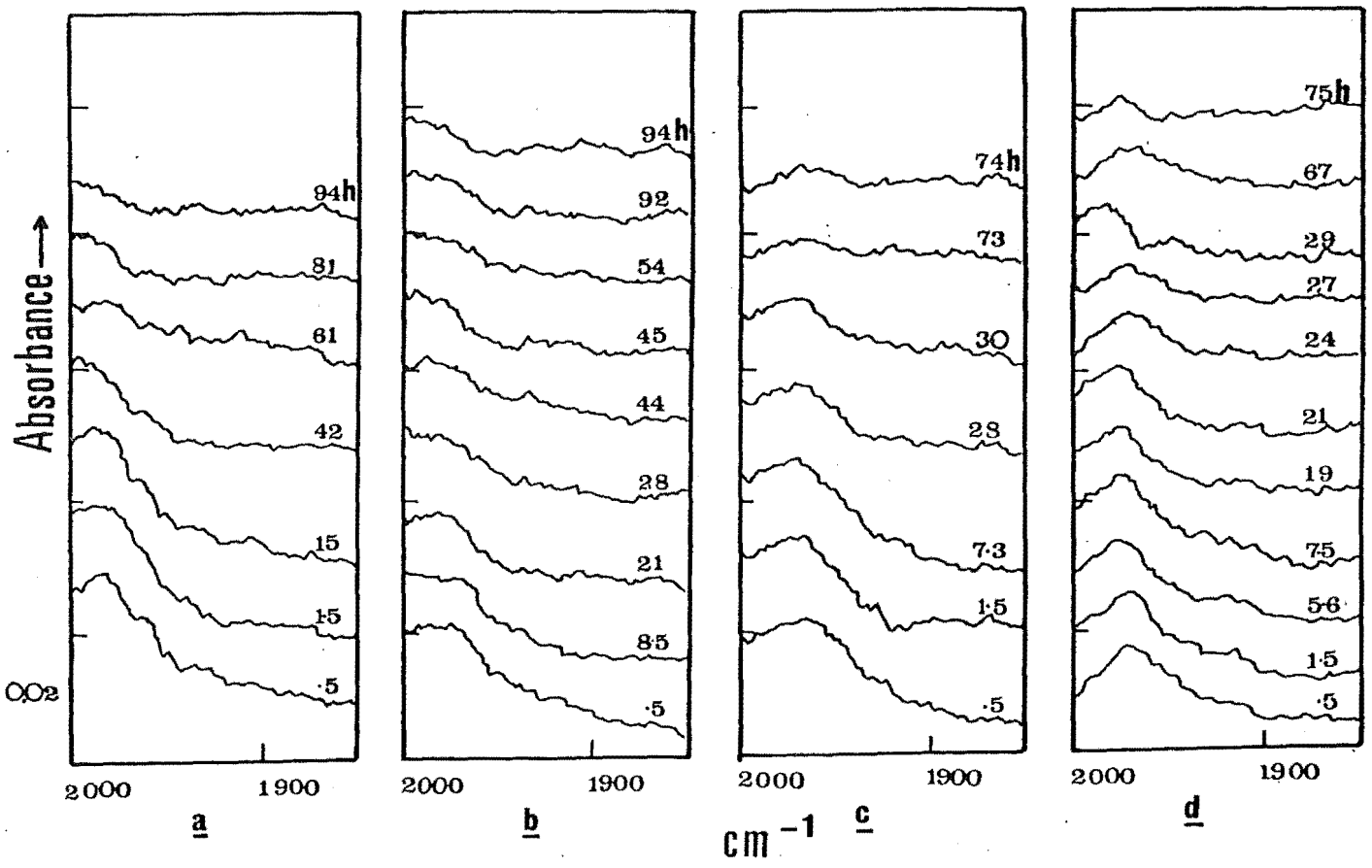

Figure 4.10 Spectra obtained in the 1980-60 cm^{-1} region from four separate runs (at 773 Pa) at increasing temperatures. (a) 25°C (b) 30°C; (c) 38°C; (d) 45°C. Ordinates displaced.

Figure 4.11 Relative band areas of the 1980-60 cm^{-1} band as a function of time, obtained from figure 4.10. O, 25°C; ▽, 30°C; □, 38°C; ◖ 45°C.

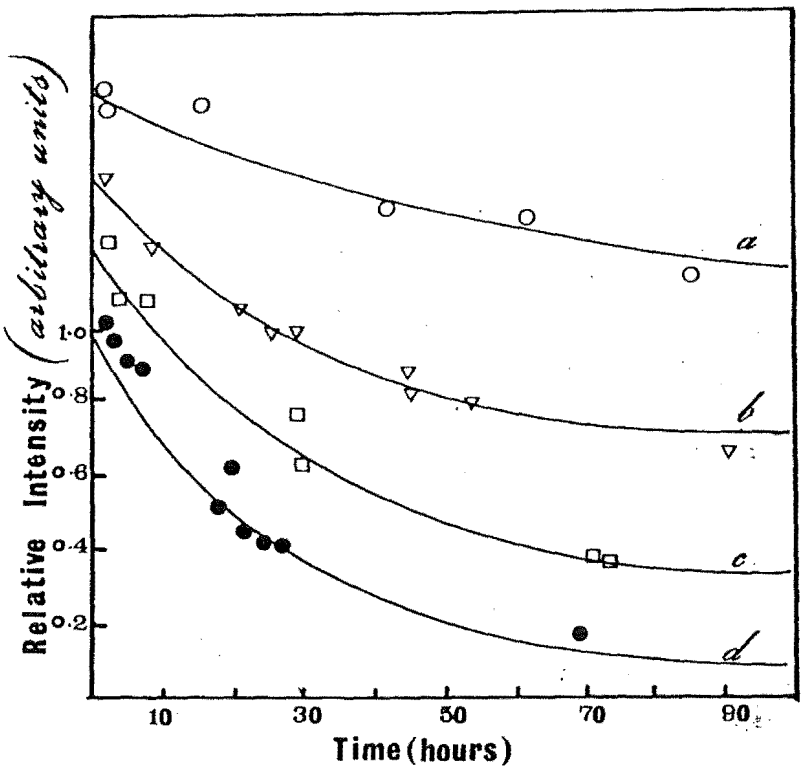

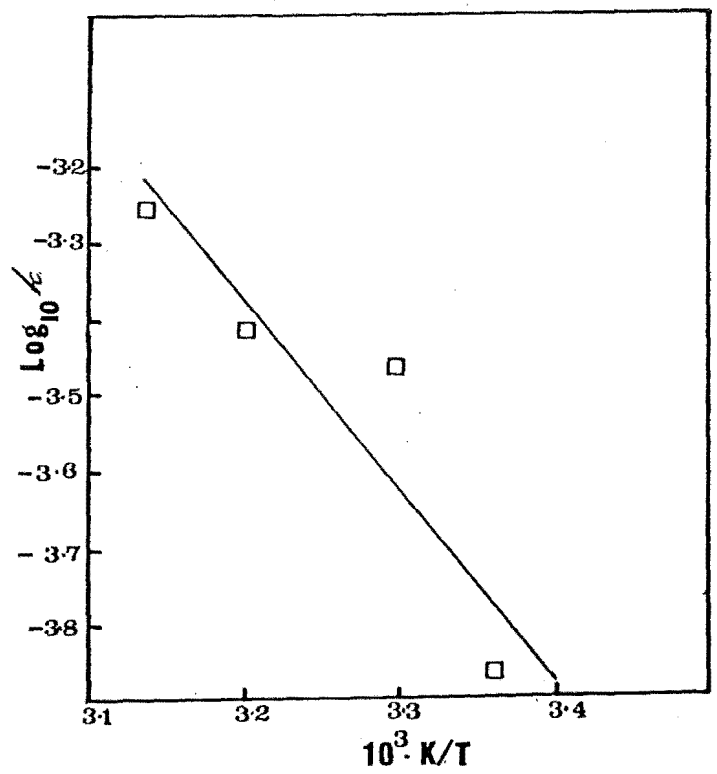

Figure 4.12 Dependence of the calculated rate constants on temperature.

that there are marked diviations from a smooth curve. Nevertheless, an estimate of the activation energy for the desorption process may be obtained if it is assumed that these variations are minimal.

By measuring the slopes at points along the curve the rates are obtained. If a further assumption is made that desorption occurs through a first order process (some justification for this will be given in a subsequent section, 4.5) then rate constants (k) may be evaluated (rate $= -kC$, where C is the relative intensity). To obtain the Arrhenius activation energy (Ea), given in 4c, rate constants are plotted against reciprocal temperature ($^1/_T$) in figure 4.12.

$$\log_{10} K = \frac{-Ea}{2.303RT} + \log A \qquad (4c)$$

where A is the pre-exponential factor and R the gas constant. A value of approximately 50 $kJ\ mol^{-1}$ is obtained from the slope of the line of best fit, obtained from a least squares calculation.

The validity of this estimate depends on the assumption that variations in the extinction coefficient are minimal, and the premise that the desorption is a first order process.

Table 4.1 : Summary of Water Vapour Adsorption on Evaporated Germanium Films

Treatment	Pressure (Pa)	IR Bands (cm^{-1})	Comments
Adsorption of H_2O^{16} at low exposures.	1.3×10^{-1} - 1.3	1980-60, 770, 730, 650	Bands stable to pumping.
Adsorption of H_2O^{16} at high exposures.	133.3	3600-3200, 1630	Bands are removed on pumping.
"	"	770, 730, 675	Significant growth of bands on continued exposure.
"	"	1980-60	Band decreases in intensity on continued exposure. Water vapour is necessary for decrease, activation energy for desorption 50 KJ mol^{-1}.
"	"	875-825	Appears after 30 hours exposure.
Adsorption of D_2O^{16}	"	1430	Replaces 1980 cm^{-1} band (observed with water).
"	"	650	Replaces 675 cm^{-1} band (observed with water).
"	"	815-770	Replaces 770 cm^{-1} band (observed with water).

4.4 Discussion

4.41 Identification of Bands

Since the bands appearing below 2000 cm^{-1}, with the exception of the 1630 cm^{-1} band, are not usually associated with the absorptions of molecular water they are likely to be due to dissociatedly adsorbed species resulting from the adsorption of water on germanium. Contamination of the surface, particularly by residual oxygen, may give rise to the bands below 1000 cm^{-1}.[1,5] However, as discussed in Section 3.2 (Chapter Three) the prepared surfaces would have remained free of contamination long enough to allow the recording of the background and the admission of the adsorbate vapour. No serious contamination is also expected from dissolved gases in the water used as it was thoroughly outgassed prior to admission.

The broad band between 3600-3200 cm^{-1} and the absorption at 1630 cm^{-1} are characteristic absorptions of water molecules, presumably physically adsorbed on the surface. However, because of the complete removal of these bands on evacuation it is difficult to decide if water chemisorbs non-dissociatively at monolayer level on the germanium surface.

If water dissociates on germanium and some evidence for this has been obtained previously by Boonstra,[126] then it would be expected that a number of species, such as Ge-H, Ge-OH and Ge-O, will exist on the surface. The

first of these may give rise to absorptions due to the υ(Ge-H) mode near 2000 cm^{-1}, as spectra published in the literature show.[128, 130, 131] The proximity of the 1980-60 cm^{-1} band to the absorption at 2010 cm^{-1}, attributed to the stretching vibration of germanium hydride bonds by Beckmann,[130] suggests that the 1980-60 cm^{-1} band may belong to Ge-H groups on the surface. The large shift in freguency of this band from the normally observed absorption at 2112 cm^{-1}, of the asymmetric stretching mode of GeH_4,[23] may be explained as due to the existence of additional surface groups, such as Ge-OH and Ge-O, which may influence the frequency of the Ge-H bond. Further support for this assignment comes from the spectra of D_2O adsorbed samples, which show a shift of the 1980-60 cm^{-1} band to 1430 cm^{-1}. A υ_H/υ_D ratio of approximately 1.38 is consistent with the isotopic shift when hydrogen is substituted by deuterium.

Since the existence of Ge-H is clearly demonstrated it is reasonable to expect other bands, due to surface hydroxyls and oxides, to occur at regions characteristic of these absorptions. The results illustrated in figure 4.1 show, however, that there are no bands attributable to surface hydroxyls, between 3600-3200 cm^{-1}. But in view of the typically low intensity of the 'stable' bands observed here the absence of these bands cannot be taken to mean that -OH groups are not present. Furthermore, extinction coefficients of the bands may be influenced by the asymmetrical force fields acting on the surface, thus affecting band shapes and intensities in an unpredictable manner.

Of the three bands appearing at 770, 730 and 675 cm^{-1}, the 730 cm^{-1} band seems to grow at a different rate to the other two. Thus it seems likely that they belong to two different species. Howe et al.[5] assigned a number of bands appearing below 1000 cm^{-1} to germanium-oxygen stretching vibrations when oxygen was adsorbed on evaporated films. During the early stages of oxidation two bands appeared at 780 and 690 cm^{-1}. The pair of bands reached their maximum intensity at exposures below 67 Pa-min ($5x10^{-1}$ torr-min) after which they were replaced by a band at 750 cm^{-1}. One may conclude at first that the 770 and 675 cm^{-1} bands are similar to those observed at the early stages of surface oxidation, mainly because of its proximity to the latter. However, there are two reasons why this is unlikely: (1) the bands (at 770 and 675 cm^{-1}) continue to grow at exposures greater than 67 Pa-min , and (b) the growth of the bands seems to depend on the presence of water vapour (O_2 content in the ppm range). A more plausible explanation would be that they belong to a transient species resulting from the dissociation of water.

Raman and infrared spectra of germanium compounds such as $(CH_3)_2Ge(OH)_2$[132] and SrH_2GeO_4[133] show bands at 673 cm^{-1} in the former and at 770 and 676 cm^{-1} in the latter, arising from stretching vibrations of Ge-O groups belonging to the $Ge(OH)_2$ entity. Therefore, the 770 and 675 cm^{-1} bands are tentatively assigned to ν(Ge-O) vibrations of surface Ge-OH groups.

The unusual shift of the apparent absorption, centered at 650 cm^{-1} at low exposures, to 675 cm^{-1} at higher exposures may occur as a result of hydrogen-bonding of surface hydroxyls. The shift upwards of about +25 cm^{-1} can be accounted for by an increase in the force constant, K_{Ge-O}, of Ge-OH; this may occur as a result of the enhancement of the $P\Pi - D\Pi$ bond of Ge-O. Similarly the substitution of the hydrogen of Ge-OH by deuterium will influence the degree of hydrogen-bonding, thereby making the Ge-O bond sensitive to deuterium substitution. In the case of SrH_2GeO_4.[133] deuterium substitution led to the shift of the 770 cm^{-1} band to 815 cm^{-1} and the 676 cm^{-1} band to 693 and 656 cm^{-1}. Somewhat similar behaviour is shown when D_2O is adsorbed on evaporated germanium. The 770 cm^{-1} band shows an apparent broadening between 815-770 cm^{-1} and the band centered at 675 cm^{-1} is replaced by one centered at 650 cm^{-1}.

It remains to account finally the bands appearing at 730 and 875-825 cm^{-1}. By comparison with the spectra published by Howe et al.[5] these bands may be assigned to the vibrations of germanium-oxygen species. The low intensity of the bands may possibly be due to asymmetrical force fields introduced by the other species adsorbed on the surface.

If the 730 cm^{-1} band is assigned to Ge-O (a band at 750 cm^{-1} is attributed by Howe et al.[5] to this species) then a likely mechanism for surface oxidation involves

the elimination of water between two surface hydroxyls, as in 4d below.

$$OH_{ads} + OH_{ads} \longrightarrow O^{-}_{ads} + \oplus^{V} + H_2O_{ads} \quad (4d)$$

where $\oplus^{V}$ represents a hole in the valence band.

Although one may expect a bridged species to occur, as in the case of silicas,[134] such a species will give rise to two bands, one due to the asymmetric stretch and the other due to the symmetric stretching vibrations of the bridge.[5]

The broadness of the 730 cm^{-1} band, observed on adsorbing O^{18} water, could possibly be a result of the overlapping of two absorptions at 730 and 690 cm^{-1} due to Ge-O^{16} and Ge-O^{18} respectively. On the other hand if GeO_2 was responsible for the band, then because $\left[O^{16}\right] \div \left[O^{18}\right]$ =~1.5 the greatest fraction of O^{18} atoms will be incorporated in $O^{16}Ge\ O^{18}$. Thus a prominent band should also occur at around 710 cm^{-1} (a shift 20 cm^{-1} from the GeO^{16} band). This is not evident.

The mechanism proposed in scheme 4d is consistent with electrical measurements which indicate an initial rise in p-type conductivity during water vapour adsorption.[125] Some of the positive holes near the surface, formed as a result of electron trapping by the acceptor levels of Ge-O^{-}, become ionised and effect a rise in the p-type conductivity of the surface.

The final stages of oxidation includes the incorporation of oxygen atoms into the bulk of the solid. A

Table 4.2 Infrared bands of H_2O adsorbed on Germanium

Group	This Work (cm^{-1})	Comparison Bands (cm^{-1})
H_2O	1630	1620[a]
Ge-H	1980-60	2010[b] 1986, 1970[c]
Ge-D	1430	1430[b]
Ge-OH	770, 675	673[d] 770, 676[e]
Ge-OD	815-770, 650	815, 693, 656[e]
$Ge-O^-$	730	750[f]
O^{2-} incorporated	875-825	840[f]

[a] Liquid-phase; [b] ref (130); [c] ref (128); [d] ref (132); [e] ref (133); [f] ref (5)

band at 840 cm^{-1} has been attributed to Ge-O-Ge groups in the lattice of germanium.[5] The appearance of the 875-825 cm^{-1} band, at the latter stages of exposure can similarly be attributed to bulk oxidation (4e).

$$O^-_{ads} \longrightarrow O^{2-}_{incorporated} + \oplus^{v} \qquad (4e)$$

The frequencies of the various bands observed, together with the comparison bands, are summarised in Table 4.2.

4.42 Desorption of Hydrogen

The observed decrease in intensity of the Ge-H band, at 1980-60 cm^{-1}, may occur as a result of the removal or loss of the adsorbed H atoms. Desorption of hydrogen atoms into the gas-phase, at 27°C, does not occur readily in view of the high activation energy for desorption of hydrogen on germanium (159 KJ mol^{-1}).[17,135] This is apparent if the average lifetime (τ) of adsorbed hydrogen is calculated from the inverse rate expression, given by de Boer[136] (equation 4f).

$$\tau = \tau_o \exp(\Delta Q_{des}/RT) \qquad (4f)$$

where τ_o is related to the time of oscillation perpendicular to the surface, and is of the order of 10^{-13} sec.,[136] Q_{des} is the activation energy for desorption and R and T have their usual meanings. The average lifetime obtained is greater than 10^5 secs (> 1 week). It is seen in figure 4.2, however, that the Ge-H band begins to

decrease within 2-3 hours of exposure to water vapour.

Experiments performed with the total exclusion of water vapour show that for the decrease to occur water vapour should be present, at pressures greater than 133.3 Pa. It is unlikely that hydrogen is being displaced by water molecules since the energy dissipated by the adsorption of water (-96 kJ mol^{-1})[15] is considerably lower than the activation energy for desorption of hydrogen. Such displacements do not occur even when oxygen is adsorbed on hydrogen-covered germanium surfaces, as shown by the experiments of Maxwell and Green.[137]

The decrease in intensity of the 1980-60 cm^{-1} band, coupled with a concomitant increase of the 675 cm^{-1} band, suggests an inter-relationship between the two. It can also be inferred from the results obtained when D_2O was adsorbed, and subsequently replaced with water vapour, that Ge-D groups are being replaced by Ge-OH groups during this interaction. Thus a reaction between strongly adsorbed deuterium (or hydrogen) atoms and physically adsorbed water molecules, such as in scheme 4g below, could conceivably account for the decrease of the Ge-D (or Ge-H) band, and the corresponding growth of the Ge-OH band during the interaction.

$$H_2O + \underset{|}{\overset{D}{Ge}} \longrightarrow \underset{|}{\overset{OH}{Ge}} + HD \qquad (4g)$$

As HD (or H_2) is not adsorbed to a significant extent on germanium, it would desorb into the gas-phase.[17,135]

Although such a reaction has not been proposed previously for interactions on germanium surfaces, a number of studies on surfaces such as tungsten,[138] nickel,[139] iron and copper[140] have shown that a mechanism similar to 4g above is responsible for the production of H_2 over these surfaces (at high coverages of water vapour).

A simple calculation of the free energy (ΔG_a) for reaction 4g shows that it is thermodynamically feasible, provided that the surface coverage (θ) is high (i.e. approaching unity). The free energy can be evaluated from the expression given in equation 4h below.

$$\Delta G_a = \Delta H_a - T \Delta S_a \qquad (4h)$$

ΔH_a is the enthalpy change in reaction 4g. This may be evaluated if scheme 4g is represented by the sum of schemes 4i and 4j below.

$$H_2O + 2Ge \longrightarrow \underset{Ge}{OH} + \underset{Ge}{H} + \Delta H_b \qquad (4i)$$

$$H_2 + 2Ge \longrightarrow 2\ \underset{Ge}{H} + \Delta H_c \qquad (4j)$$

Thus, $\Delta H_a = \Delta H_b - \Delta H_c$ if both reactions 4i and 4j take place under similar coverages. If the difference in entropy between adsorbed H atoms and adsorbed -OH groups (entropies of both are small) is ignored then $\Delta S_a = -59$ J mol^{-1} deg^{-1} (i.e. the difference in standard entropies of H_2 and gaseous H_2O at 298^oK).[141] It

follows that $-T\ \Delta S_a = \sim 17$ kJ mol^{-1}. Consequently in order that there shall be a decrease of free energy for reaction 4g ΔH_a must be less than -18 kJ mol^{-1}. At coverages below $\theta = 0.1$ the heat of adsorption of hydrogen on germanium is about -96 kJ mol^{-1},[17,135] close to the value obtained for water vapour adsorption on various germanium surfaces.[15,124] Thus $\Delta H_a \simeq 0$ and the reaction would not be expected to proceed (as $\Delta G_a \approx +17$ kJ mol^{-1}). On the other hand the heat of adsorption of hydrogen decreases significantly at high coverages,[135] approaching a value of 0 at $\theta = 1$. The value obtained for water vapour is substantially higher at these coverages. At $\theta = 0.71$, ΔH_b is between -54 and -67 kJ mol^{-1}, although these values have been obtained for interaction on surfaces of single crystals[142] or oxide covered surfaces.[124] Nevertheless, if a conservative estimate of -20 kJ mol^{-1} is used for ΔH_c and -54 kJ mol^{-1} for ΔH_b then at high coverages (i.e. $\theta \geq 0.7$) $\Delta H_a = 34$ kJ mol^{-1}. Thus, $\Delta G_a = -17$ kJ mol^{-1} and reaction 4g is thermodynamically favourable. These calculations are valid provided the pressure of water vapour and hydrogen are equal near the surface (the pressure of H_2 in equilibrium with the surface will be appreciable if the coverage is sufficiently high).

The proposed mechanism is different, however, to that suggested by Ertl and Giovanelli.[12] It was thought by them that recombination of pairs of adsorbed H atoms was responsible for the release of hydrogen. On the other hand, kinetic data obtained by the two workers

indicate that hydrogen is produced through a first order process, thus ruling out the suggested recombination process. This inconsistency was not explained. However, in view of the complicated kinetics often encountered in adsorption processes, it would be difficult to decide between reaction mechanisms on the basis of kinetic results alone.

Reaction 4g is consistent with the observed first order kinetics if it is assumed that the rate of reaction (equation 4k) is independent of the pressure of water vapour, at high coverages.

$$\text{Rate} = \frac{d\,P_{H_2}}{d\,t} = K\ P_{H_2}^{1} P_{H_2O}^{0} \qquad (4k)$$

where P_{H_2O} is the partial pressure of water vapour and P_{H_2}, the partial pressure of hydrogen. However, no experiments were performed to substantiate this. The only real basis for this argument being the similarity in the order of magnitude of the activation energy (≈ 50 KJ mol^{-1}) to that obtained by Ertl and Giovanelli[12] (71 ± 13 KJ mol^{-1}). The lower value obtained in this work may be a result of an enhancement of the reaction rate by the heterogeneous nature of evaporated films. Alternatively, desorption of small amounts of adsorbed H atoms, through the reduction of surface area due to oxidative sintering[67] (since oxidation is evident within the first hour of exposure) may be responsible.

At elevated temperatures it is conceivable that the increased mobility of adsorbed H atoms will enhance

their recombination. Thus it is possible that there is more than one mechanism responsible for hydrogen production, with reaction 4g predominating at high coverages.

CHAPTER FIVE

INTERACTION OF AMMONIA WITH EVAPORATED GERMANIUM FILMS

5.1 Review of Studies of the Adsorption of Ammonia

The adsorption of ammonia on metal catalysts has been studied extensively in the past in relation to the kinetics of decomposition on these surfaces. It is not surprising that kinetic information on this subject is well documented[143-145] in view of the importance of these studies to the synthesis of ammonia; the book by Anderson[146] provides a concise review on this aspect.

It is generally found that with most metals studied the decomposition yields surface residues[147] such as $-NH_2$, -NH-, $\geqslant N$, and -H resulting from a number of adsorption processes, as summarised below:

$$NH_{3(g)} \longrightarrow NH_{2(ads)} + H_{(ads)} \qquad (5a)$$

which proceeds with very low activation energy.

$$NH_{2(ads)} \longrightarrow NH_{(ads)} + H_{(ads)} \qquad (5b)$$

and

$$NH_{(ads)} \longrightarrow N_{(ads)} + H_{(ads)} \qquad (5c)$$

the last two reactions are activated, and thus occur at high temperatures.

Very few studies have been carried out on germanium, but there seems to be a general correspondence in the nature of the adsorption with metal surfaces.[16] The volumetric studies of Boonstra et al.[126] show that, on

clean surfaces, for every molecule of ammonia adsorbed a total of 6 germanium surface atoms are precluded from further participation. This would suggest that complete dissociation occurs with the result that the nitrogen atom is adsorbed to three surface atoms and the hydrogen atoms each to a single surface atom. However, as the rate of hydrogen evolution is found to vary at different temperatures,[126] above 100°C, various stages are presumably involved in the disintegration. Each stage may have with it an "activated complex" which decomposes with the liberation of hydrogen. Reactions 5a-5c above may play an important role in the disintegration process. Molecular hydrogen may form through the recombination of pairs of adsorbed H atoms or alternatively through a reaction with molecular ammonia, at high coverages.

LEED[148] (low energy electron diffraction) data on (111) and (100) surfaces of germanium yield different diffraction patterns during adsorption at 25 and 200°C. This suggests that different surface residues are present at the two temperatures. At the lower temperature molecular ammonia may adsorb forming a co-ordinate bond with the surface. This can be inferred from electrical measurements[149] which show a similar character in the p-type conductivity changes during ammonia adsorption at low exposures to that found for water vapour adsorption. The existence of a donor species is suggested, as there is a partial restoration of the p-type conductivity when the gas-phase is removed on pumping.

On oxidised surfaces the amount adsorbed is found to be independent of the state of oxidation[126] suggesting that the "activated complexes" may involve subsurface germanium atoms as well.

5.2 Previous Infrared Studies of Adsorbed Ammonia

Infrared studies of the adsorption of ammonia on various silica surfaces have been numerous.[150,151] Bands have been identified in both the stretching (3600-2700 cm^{-1}) and deformation (1700-1100 cm^{-1}) regions, corresponding to adsorbed NH_3, $-NH_2$ and -NH- groups. A comprehensive review on these studies is given in the book by Little.[21]

The infrared spectrum of ammonia adsorbed on germanium is not expected to be too different to those already obtained with silica surfaces; although only one such study, using germania-gel as the adsorbent, has been reported in the literature.[16]

With germania-gel[16] three groups of bands have been identified, corresponding to ammonia physically adsorbed, co-ordinated and dissociatedly adsorbed. The first group, which is easily removed on pumping at 25°C, consists of bands at 3420 cm^{-1} (asymmetric ν(N-H)), 3312 cm^{-1} (symmetric ν(N-H)), 1610 cm^{-1} (asymmetric δ(N-H)) and finally one at 1260 cm^{-1} (symmetric δ(N-H)).

Bands, which remain after pumping at 25°C for several days, have been assigned[16] to ammonia co-ordinated to surface germanium atoms. They appear at 3363 cm^{-1} (asymmetric ν(N-H)), 3267 cm^{-1} (symmetric ν(N-H)),

1600 cm^{-1} (symmetric δ(N-H)). One other band due to the rocking mode of ammonia is observed at 700 cm^{-1}. The five bands show good correspondence with those of typical amine complexes.[23] The two ν(N-H) bands are similar to those attributed to NH_3 co-ordinated to surface boron atoms on porous glass[152] and boric-oxide impregnated silica.[153] The bands arising from the bending modes are close to those of ammonia co-ordinated to surface aluminium atoms.[21]

A reaction between NH_3 and surface GeO_2, giving a primary amine ($-NH_2$) and a surface hydroxyl, is thought to be responsible for a third group of bands at 3467 cm^{-1} (asymmetric ν(N-H)), 3393 cm^{-1} (symmetric ν(N-H)) and 1535 cm^{-1} (the bending mode, δ(N-H)). These are removed only after evacuation at 100°C. Bands similar to the deformation vibration at 1535 cm^{-1} have been observed at 1555 cm^{-1} with silica,[21, 152] and at 1560-1510 cm^{-1} with alumina surfaces.[21]

A lone band at 3397 cm^{-1} has been tentatively assigned to a secondary amine (-NH-) thought to arise as a result of the elimination of water between surface hydroxyls and the primary amine.

It has been suggested[154] that weak bands appearing between 3000-2800 cm^{-1} may be due to NH_4^+ adsorbed on the surface. However, no bands due to the bending modes (between 1500-1400 cm^{-1}) were observed as the gel absorbed strongly below 1500 cm^{-1}.

(b) 4h; (c) 17h. (d-f) from a separate run (at 665 Pa), (d) 30 min; (e) 2h 30 min; (f) pumped 18 hours. Ordinates displaced.

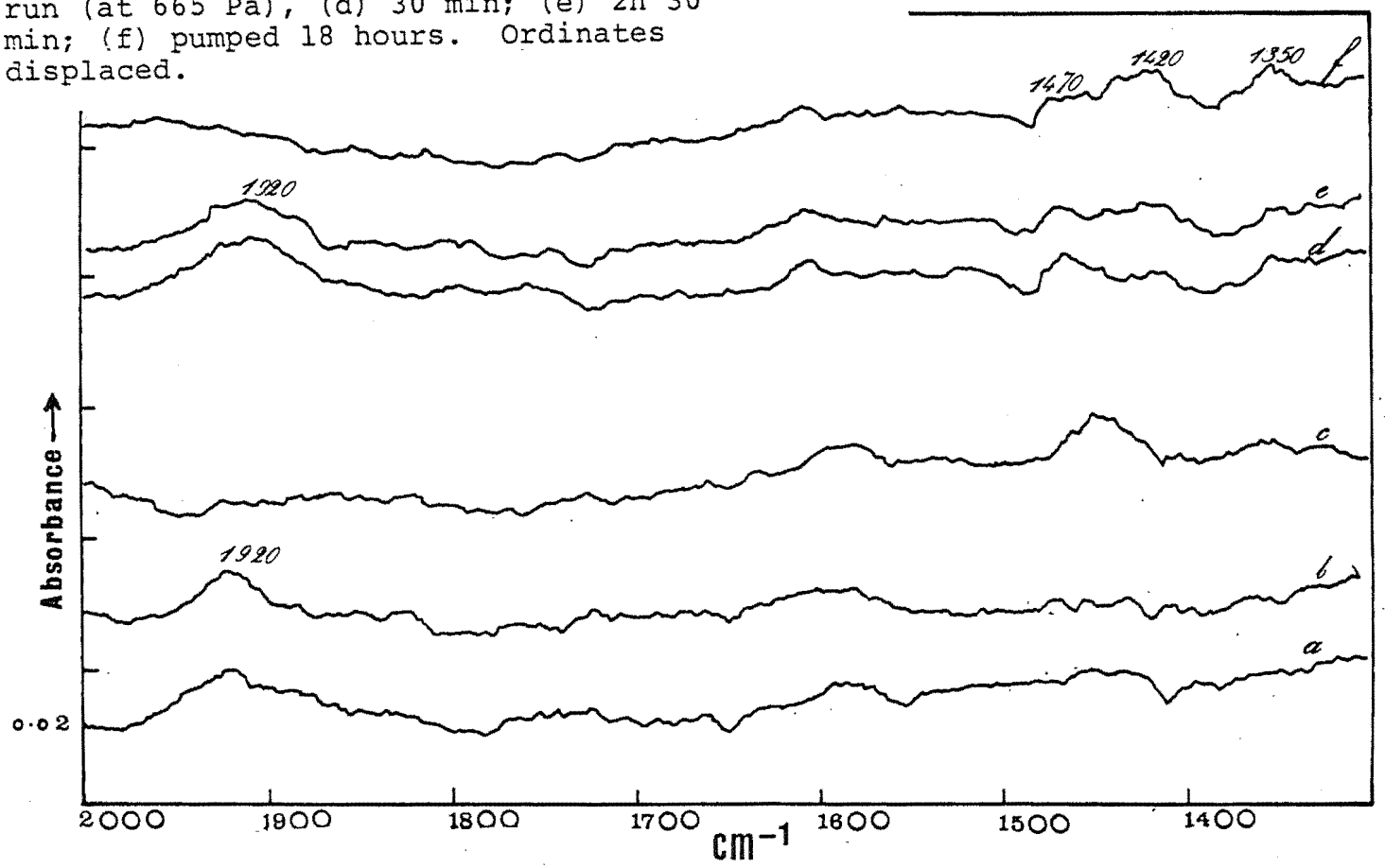

Figure 5.2 Spectra of ammonia adsorbed (at 13.3 Pa) on germanium, at 27°C. (a) 10 min; (b) 1h 30 min; (c) pumped 30 min. Ordinates displaced.

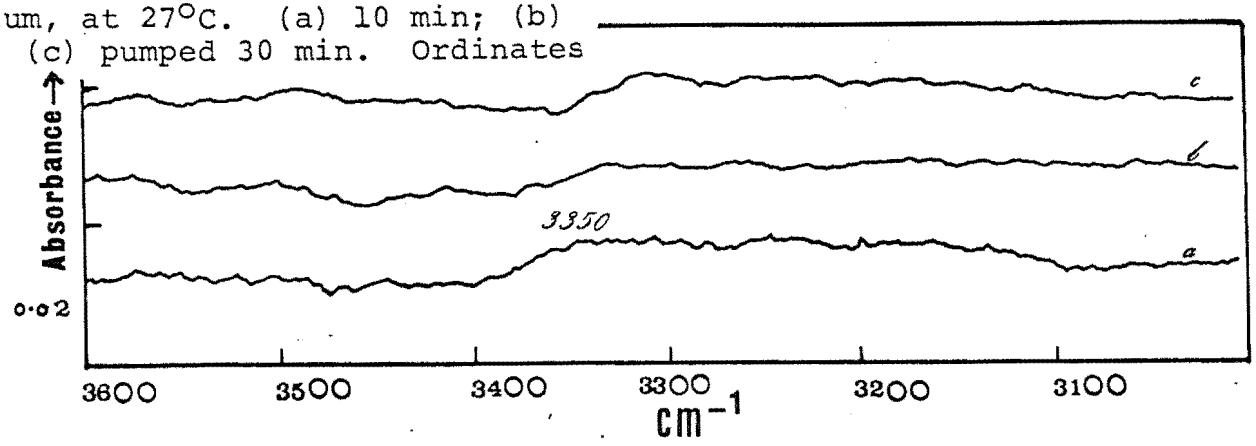

5.3 Infrared Spectra of Ammonia Adsorbed on Evaporated Germanium Films

A preliminary study of ammonia adsorption has been made on both clean and oxidised surfaces. The adsorption was followed at low and high pressures, mainly in the spectral range between 3600-3000 cm^{-1} and 2000-1000 cm^{-1}.

5.31 Adsorption at Low Pressures

Ammonia was admitted at a pressure of 67 Pa (5 x 10^{-1} torr) after a set of four films were freshly prepared and cooled to about 27°C. The resulting difference spectra are shown in figures 5.1 and 5.2.

A very weak band which appears at 1920 cm^{-1} is seen to disappear completely after a total of 17 hours exposure (Fig. 5.1, trace a to c). In a separate experiment, ammonia was admitted at a slightly higher presure (665 Pa) and the bands recorded over a period of 24 hours. Here, however, the cell was evacuated after an initial equilibration of 4 hours. The 1920 cm^{-1} band is seen to decrease, as in the previous case, and is completely removed after pumping for 17 hours (trace d to f). Weak bands are also discernible at 1470, 1420 and 1350 cm^{-1} at these exposures (trace a to f). However, they are not removed on pumping (trace f).

In the spectral region between 3600-3000 cm^{-1} a broad band of low intensity can be seen between 3400-3100 cm^{-1} with an apparent maximum at 3350 cm^{-1} (Fig. 5.2). When the gas-phase is removed a residual absorption remains between 3350-3100 cm^{-1} (trace c).

Figure

Spectra of ammonia adsorbed (at 5.3 x 10^{3} Pa) on germanium, at 27°C. (a) 20 min; (b) 1h 30 min; (c) 6h 30 min; (d) 13h; (e) 15h; (f) 26h; (g) pumped 12h. Ordinates displaced.

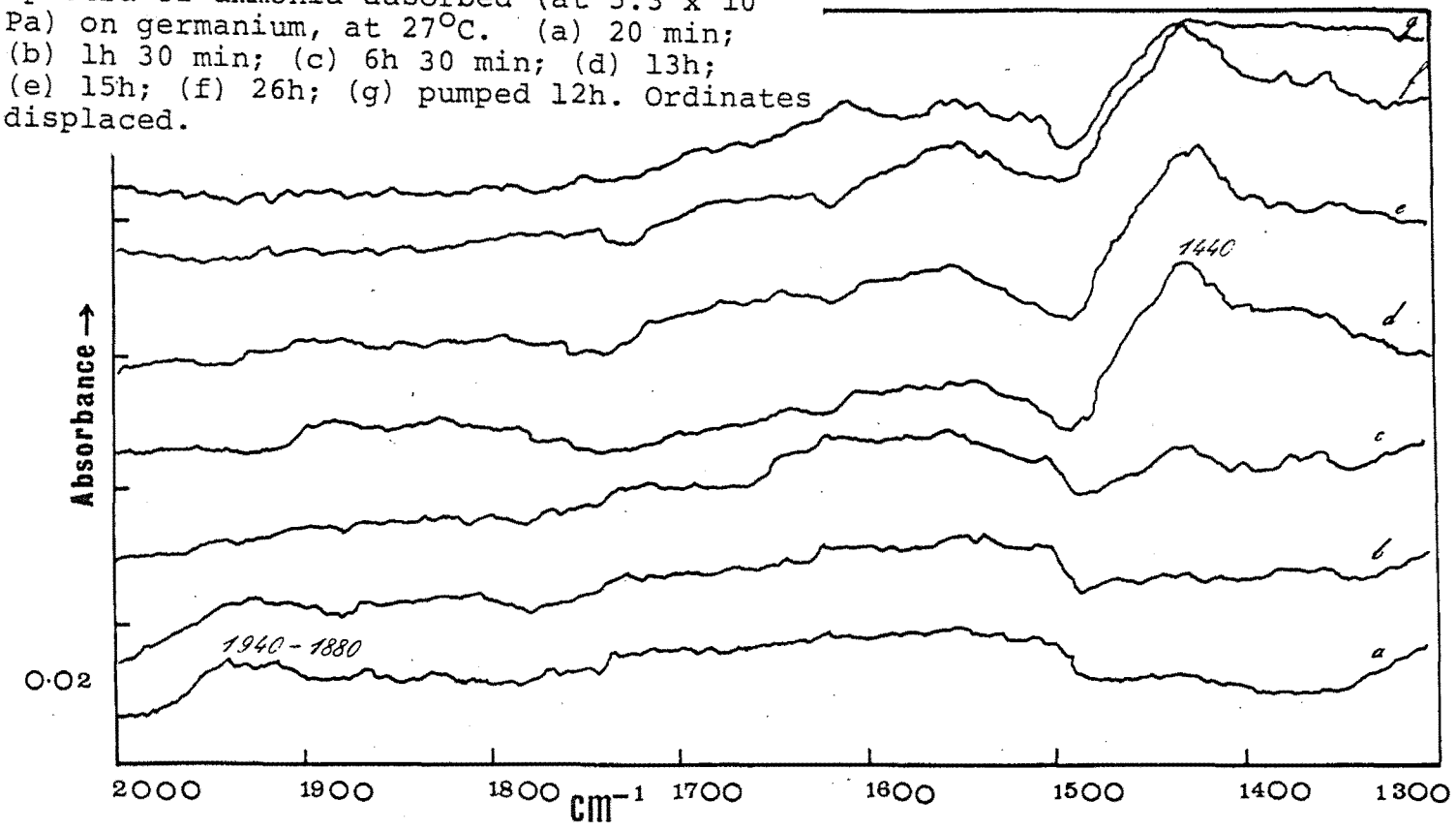

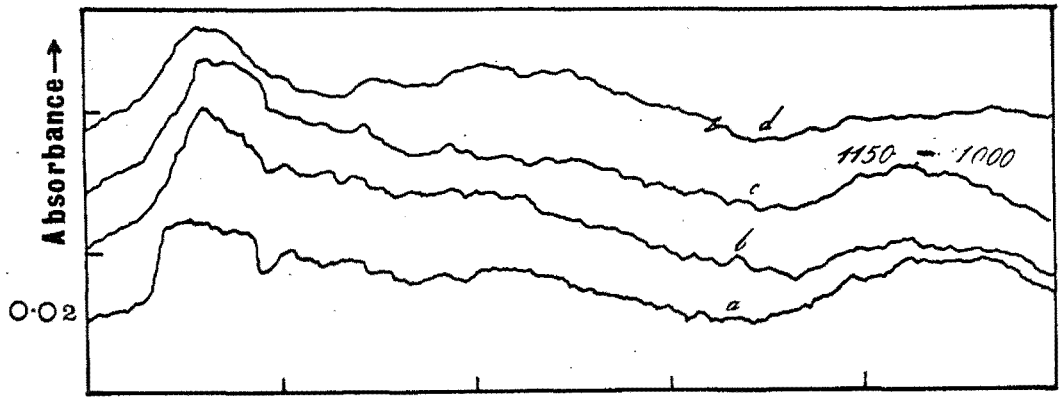

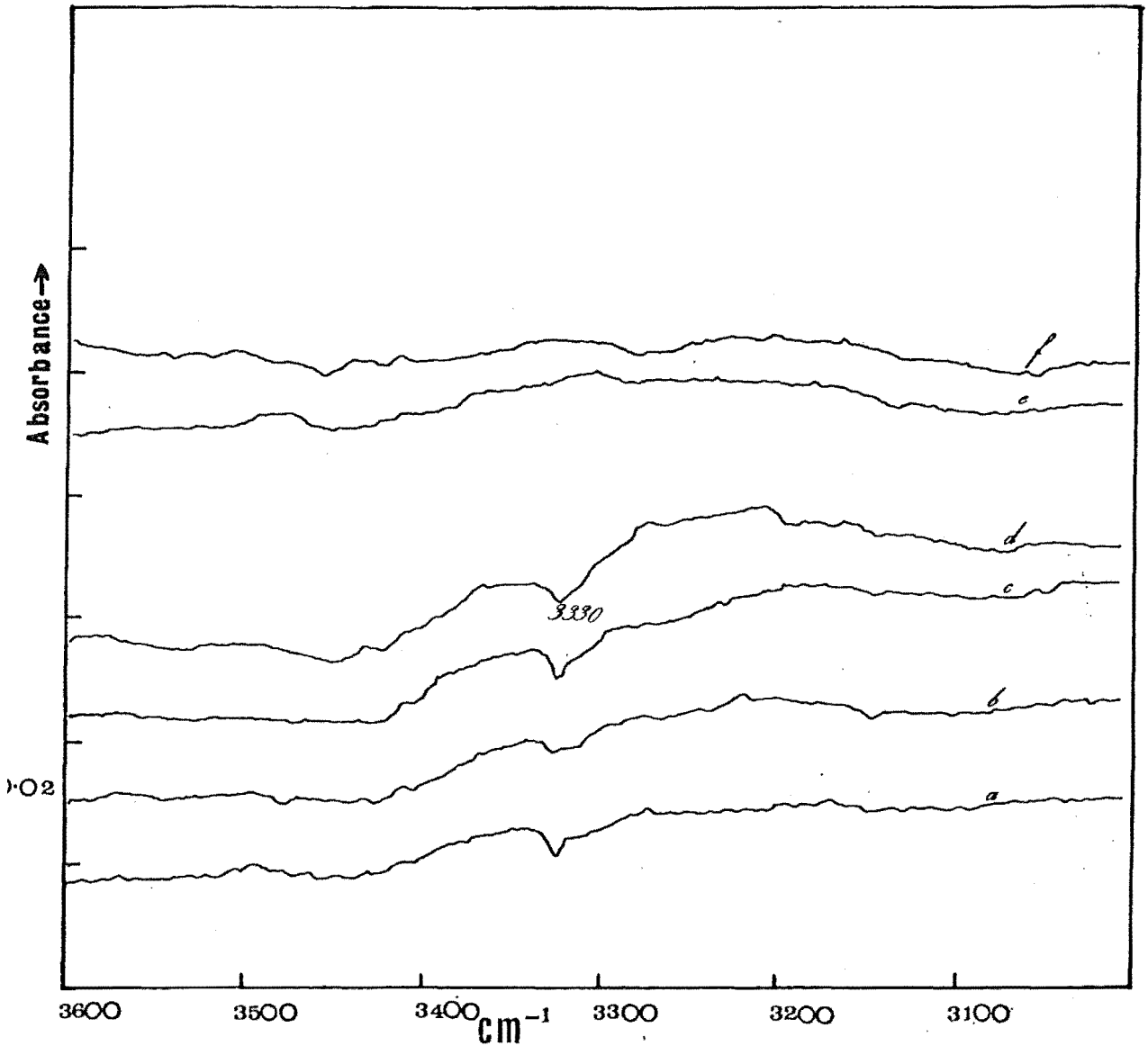

Figure 5.5 Spectra of ammonia adsorbed (at 5.3×10^3 Pa) on germanium, at 27°C. (a) 30 min; (b) 2h; (c) 7h 10 min; (d) 14h; (e) pumped 30 min; (f) pumped 24h. Ordinates displaced

5.32 Adsorption at High Pressures

Figure 5.3 shows the resulting difference spectra after exposure of four germanium films to ammonia at 5.3×10^3 Pa. An extremely weak band appears between 1940-1880 cm^{-1}, but which disappears within an hour of exposure (trace a to c). The relatively strong band at 1440 cm^{-1}, which appears to have shifted from the absorption at 1420 cm^{-1} at low pressures, is the predominant band at these exposures. It broadens considerably during exposure (trace d to f) and continues to grow in intensity. On pumping, at 27°C, for 24 hours the band is diminished slightly (0.5-0.75 of its original intensity — trace g).

In one run where the investigation was extended to cover the spectral region between 1500-1000 cm^{-1} a broad absorption is also observed between 1150-1000 cm^{-1} (Fig. 5.4). This band grows progressively with exposure but diminishes markedly on pumping for 24 hours, whereas the 1440 cm^{-1} band is reduced only slightly (Fig. 5.4, trace f).

The difference spectra obtained in the fundamental stretching region is shown in Figure 5.5. A broad band between 3430-3160 cm^{-1}, with an apparent maximum at 3330-40 cm^{-1}, appears soon after ammonia is admitted. After evacuation for 24 hours a band centered at 3240 cm^{-1} remains. A small absorption at 3470 cm^{-1} which is evident at the early stages of exposure also remains after pumping for 24 hours. The negative infrared absorption at around

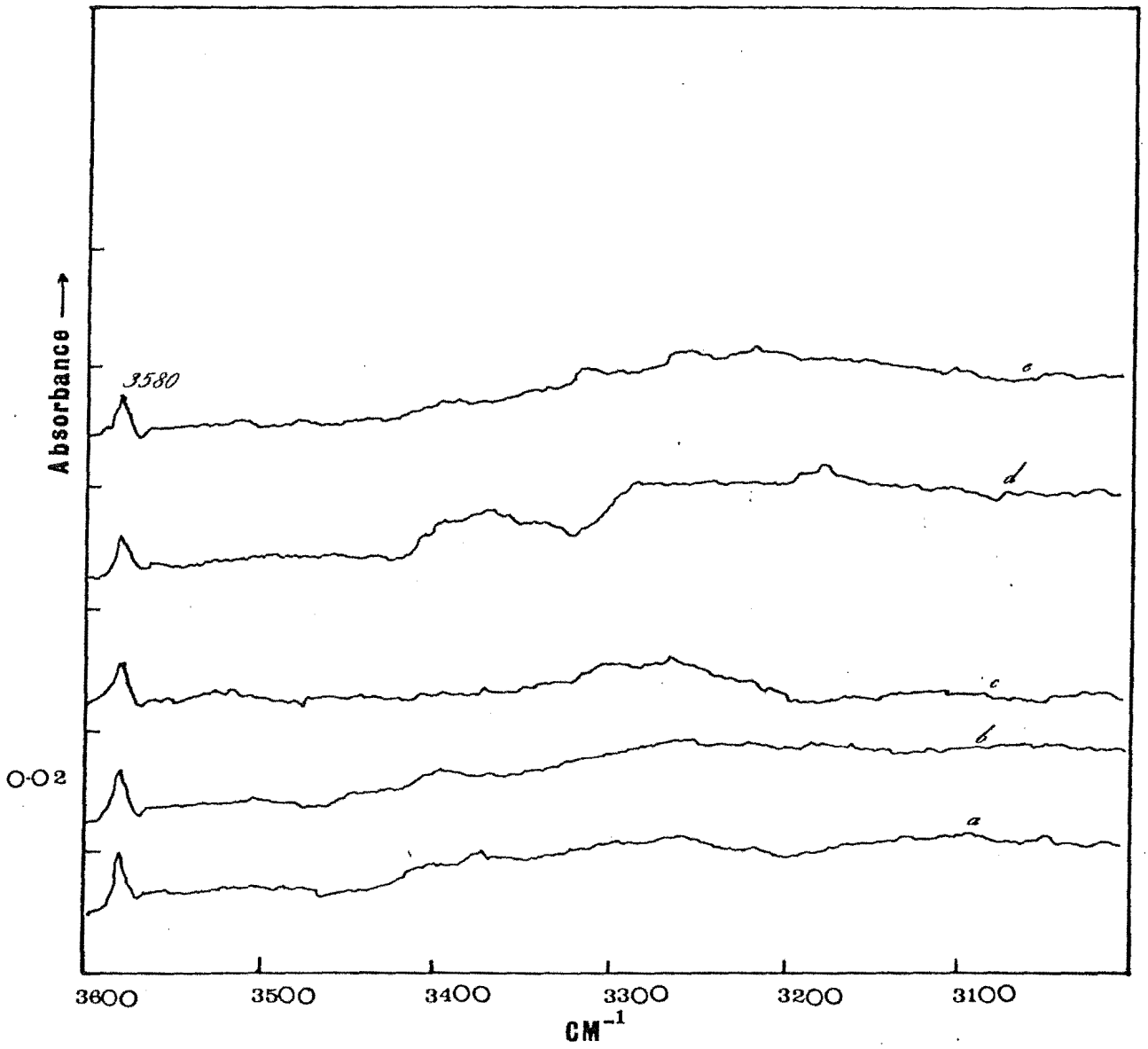

Figure 5.6 Spectra of ammonia adsorbed (at 5.3×10^3 Pa) on oxidised germanium, at $27^{\circ}C$. (a) 15 min; (b) 19h; (c) 23h; (d) pumped 30 min; pumped 1h. Ordinates displaced.

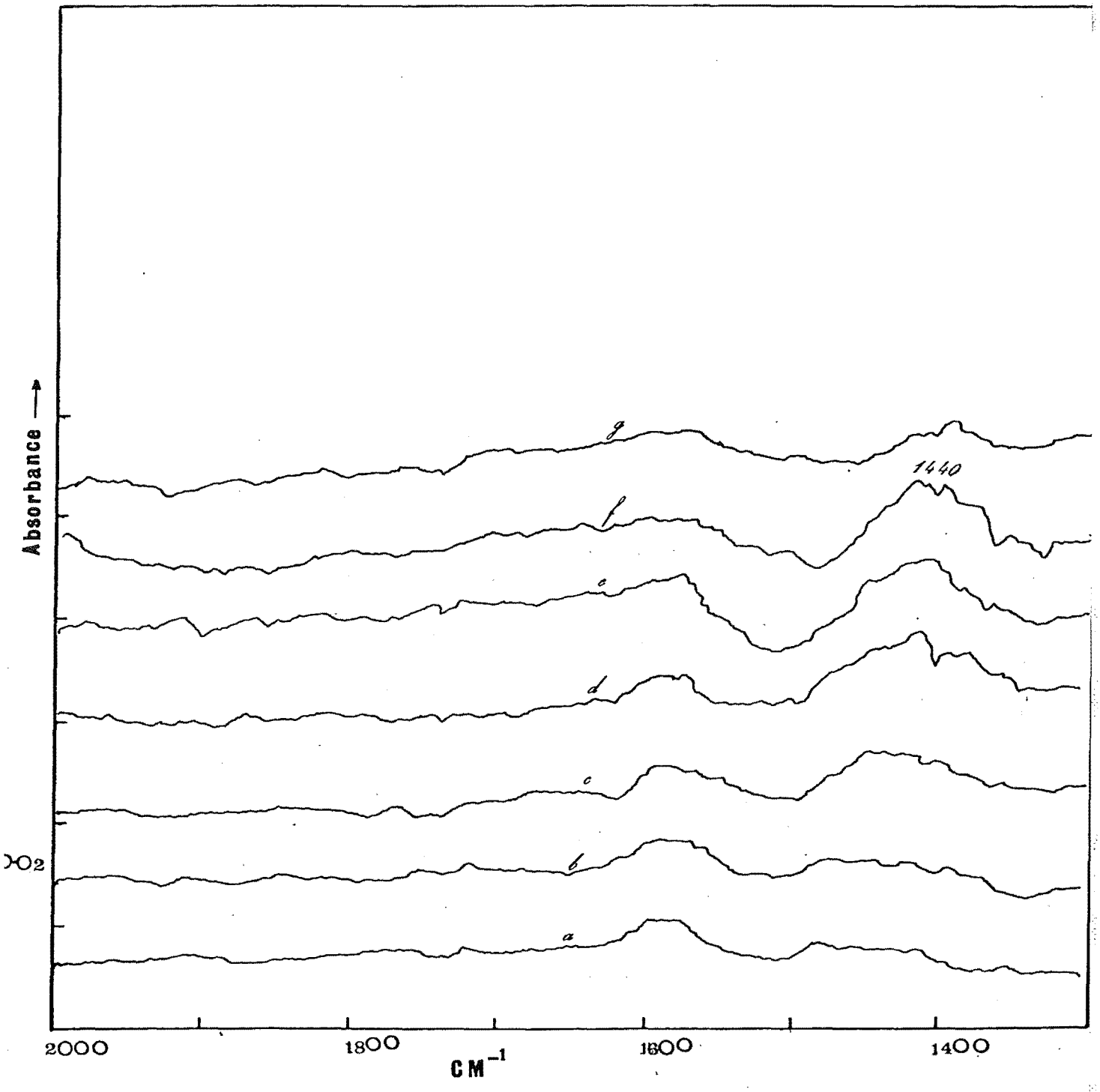

Figure 5.7 Spectra of ammonia adsorbed on germanium, at 27°C. (a-e) at 133.3 Pa and (d-f) at 5.3×10^3 Pa. (a) 5 min; (b) 30 min; (c) 18h; (d) 40 min; (e) 4h; (f) 24h; (g) pumped 4 days. Ordinates displaced.

3330 cm^{-1} is due to the gas-phase adsorption of ammonia. Incomplete cancellation of the gas-phase bands, due to a path-length difference, is responsible for this absorption.

5.33 Adsorption on Oxidised Surfaces

A set of four films were prepared and then oxidised at 13.3 Pa ($1x10^{-1}$ torr) by exposure to oxygen. Ammonia was then admitted at a pressure of 173 Pa (1.3 torr). The resulting difference spectra are shown in figures 5.6 and 5.7.

A very sharp band appears at 3580 cm^{-1} together with a small absorption between 3440-3250 cm^{-1} (Fig. 5.6). On pumping the latter disappears but the former remains unperturbed.

In figure 5.7 the 1920 cm^{-1} band is not apparent but there are weak absorptions at 1470, 1420 and 1350 cm^{-1}. At higher exposures ($>4x10^{3}$ Pa) the band at 1440 cm^{-1} shows a significant growth over a period of 24 hours (trace d to f), however, it is almost completely removed on pumping for 4 days (trace g).

5.4 Discussion

5.41 Adsorption on Clean Surfaces

It is evident from the non-uniform behaviour of the bands under various conditions that a number of different modes of adsorption occur on the surface. These include dissociative and molecular adsorption.

The band at 1920 cm^{-1}, which appears very near the 1980-60 cm^{-1} band observed with water vapour as the adsorbate (Chapter 4), can be assigned to υ(Ge-H) surface bonds. The shift to lower frequencies by about -40 cm^{-1} can be attributed to the influence of the more electropositive nitrogen atom (compared to oxygen in the case of water) on the surface. This is in accord with the findings of Mathis et al.[131] that in over 40 germanium compounds studied the frequency of the Ge-H stretching vibration decreased as the substituents on germanium become less electronegative.

It should be noted that the 1920 cm^{-1} band shows a similar tendency to diminish with time as in the previous study with water vapour; the rate of disappearance is, however, considerably faster. At low exposures, or on evacuation, this band is completely removed within 20 hours, whereas at high exposures it is only observed momentarily and disappears within one hour of exposure. Thus the initial dissociative adsorption (scheme 5d below) is evidently followed by further reaction to remove the adsorbed H atoms.

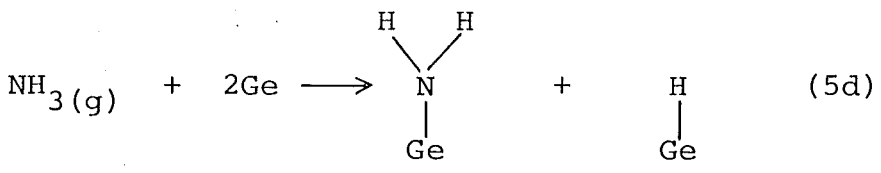

(5d)

At low exposures or on evacuation a reaction scheme, similar to that proposed for water vapour adsorption, is not feasible (see discussion, Chapter 4). As alternatives, reactions 5e and 5f below should be considered.

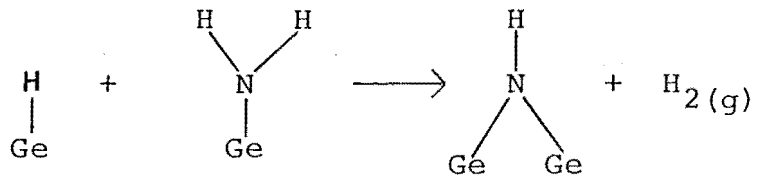

(5e)

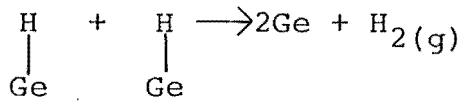

(5f)

If the first scheme proceeds to a significant extent then a band corresponding to the secondary amine formed can be expected in the fundamental stretching region, possibly near 3397 cm^{-1} (tentatively assigned to -NH- groups on GeO_2 by Low and Matsushita).[7] However, unless this band is sufficiently intense it would be hidden in the broad absorption, due to the fundamental modes of the adsorbed ammonia, that is observed between 3400-3100 cm^{-1}. Blomfield and Little[152] have expressed doubts about the formation of a secondary amine group on silica surfaces at room temperature and believe that bands previously assigned to this species are due to a $-NH_2$ group. Furthermore, studies on metal surfaces have shown that secondary amine formation requires considerable activation[143] and it is not expected that such a species would form readily at room temperature. Thus, scheme 5e seems unlikely. Recombination as shown by scheme 5f would be a more plausible explanation for the removal of hydrogen; a greater degree of H atom mobility can be expected at low surface coverages.

At high exposures the decrease of the Ge-H band can be attributed to a reaction between gas-phase or physically adsorbed ammonia and adsorbed hydrogen, as in scheme

5g below, to produce a primary amine.

$$NH_{3(g)} + \begin{matrix} H \\ | \\ Ge \end{matrix} \longrightarrow \begin{matrix} NH_2 \\ | \\ Ge \end{matrix} + H_{2(g)} \qquad (5g)$$

As shown by thermodynamic calculations in the previous chapter, a reaction similar to this is favoured at high coverages.

One further possibility, i.e. the formation of ammonium ions, as in 5h below, should also be considered.

$$NH_{3(g)} + \begin{matrix} H \\ | \\ Ge \end{matrix} + \ominus^{V} \longrightarrow \begin{matrix} NH_4^{+} \\ | \\ Ge \end{matrix} \qquad (5h)$$

It is possible that the bands observed below 1500 cm^{-1}, which occur in the region corresponding to the asymmetric bending mode of adsorbed ammonium ions[154] (between 1500-1300 cm^{-1}) are due to such a species. However, as no corresponding band due to the asymmetric stretch of this group was observed (between 3100-2800 cm^{-1}) the latter scheme must remain speculative.

The incomplete removal of the 1470-1420 cm^{-1} band after pumping suggests that it may comprise of overlapping absorptions by more than one species. The shift in the band maximum at 1420 cm^{-1} to 1440 cm^{-1}, as the coverage increases, can be attributed to hydrogen bonding. H-bonding between the adsorbed species shifts the deformation bands to higher frequencies while lowering the corresponding frequencies of stretching modes, as indicated by the absorption bands of ammonia in going from the gaseous state

to the crystalline state.[155]

The species removed by pumping at 25°C is likely to be physically adsorbed ammonia. It is possible that the maximum, evident at 1470 cm^{-1}, is due to this species although the equivalent found in the spectra of germania-gel[16] occurs at 1610 cm^{-1}. The 1440 cm^{-1} centered band which remains even after pumping can be attributed to co-ordinated ammonia, while the absorption centered at 1350 cm^{-1}, which shows a different rate of growth to the former band, can be assigned to a Ge-NH_2 group. Pumping at 25°C diminishes the former (although this may be due to the removal of the overlapping band of physisorbed ammonia), whereas the latter band remains unperturbed. The corresponding bands for the two species appear at 1600 and 1535 cm^{-1} respectively in the spectra of GeO_2.[16]

The shift in frequency of over +150 cm^{-1} cannot be explained readily, but it is conceivable that stronger binding of the nitrogen atoms to energetically more favourable edge and corner atoms would reduce the N-H bond order thereby lowering the frequency. Atoms in edge or corner positions are expected to be more variable in bonding character than those in plane surfaces, thus the broader nature of the bands. Evaporated films can be expected to have a large distribution of these sites as they are composed essentially of small crystallites (Section 3.1, Chapter 3). The same reasoning would not, however, apply to physisorbed molecules as they are displaced somewhat from the surface.

The appearance of a band between 1150 and 1000 cm^{-1}, which can be assigned to the symmetric bending modes of physisorbed and co-ordinated ammonia, provides further evidence for the existence of the two species on the surface. On germania-gel[16] the corresponding bands appear at 1260 and 1210 cm^{-1} respectively. The bands are much higher in frequency than the gas-phase symmetric deformation[155] at 980 cm^{-1}, but the shift is consistent with the greater degree of hydrogen-bonding in the adsorbed state.

Although bands in the fundamental stretching region are of low intensity some tentative assignments can be made. A weak absorption at 3470 cm^{-1} which persists, even after evacuation, can be assigned to the asymmetric stretch of Ge-NH_2 by comparison with the spectra of Low and Matsushita.[16] The symmetric stretch cannot be distinguished, however, the maxima at 3340-40 cm^{-1} which is evident in the same scan is possibly due to the asymmetric stretch of co-ordinated ammonia. The broad band centered at 3240 cm^{-1}, observed after high exposures followed by evacuation, could possibly be due to the symmetric stretch of co-ordinated ammonia. No other absorptions are resolved sufficiently to make any assignments with confidence.

The various frequencies together with the comparison bands are summarised in Table 5.1

Table 5.1 Infrared Bands of NH_3 Adsorbed on Germanium

Group	This Work (cm^{-1})	Comparison Bands (cm^{-1})
Perturbed (Ge-OH) ϑ symm.	3580	3550[a]
($Ge-NH_2$) ϑ asymm.	3470	3467[b]
Co-ordinated ($Ge-NH_3$) ϑ asymm.	3330-40	3363[b]
Co-ordinated ($Ge-NH_3$) ϑ symm.	3240	3267[b]
(Ge-H) ϑ symm.	1920	1980-60[c] 2010[d]
Physically adsorbed ($Ge...NH_3$) δ symm.	1470	1610[b]
Co-ordinated ($Ge-NH_3$) δ symm.	1440	1600[b]
($Ge-NH_2$)δ	1360	1535[b]
Physically adsorbed ($Ge...NH_3$) δ symm.	1150-1000	1260, 1210[b] 980[e]

[a] ref (128); [b] ref (16); [c] This Work, see Chapter 4 (Sect. 4.5);

[d] ref (130; [e] ref (155).

5.42 Adsorption on Oxidised Surfaces

The appearance of a sharp band at 3580 cm^{-1}, which can be assigned to H-bonded surface hydroxyls by comparison with the spectra of Low et al.,[128] together with a weak absorption between 1470-1350 cm^{-1}, suggests that some dissociative adsorption is occuring. On oxidised surfaces the corresponding reaction is

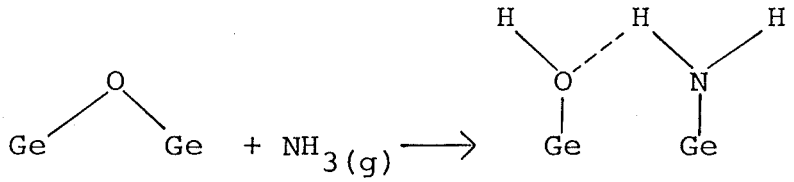

(5i)

where the broken line indicates hydrogen bonding between the two species.

The 1360 cm^{-1} band, due to Ge-NH_2, is observed to grow only slightly with time. There may be two reasons for this: a) there is no further reaction between gas-phase ammonia and the surface resulting in the formation of a primary amine, and b) decomposition may be limited by the availability of sterically suitable sites on the oxide surface.

At high exposures the deformation band centered at 1440 cm^{-1} increases strongly to almost the same intensity as with the clean surface. This suggests that co-ordination with subsurface atoms must be occuring to a significant extent. A large concentration of these sites directly accessible to adsorbate molecules, is available for adsorption if one considers, for example, the structure of the clean (111) germanium surface (as suggested by the LEED studies of Lander and Morrison).[156] If the oxide

layer is 2 or 3 atoms thick then it can be considered to be epitaxial, as shown in 5j, where the first oxide layer is presumed to chemisorb on the basic hexagon.

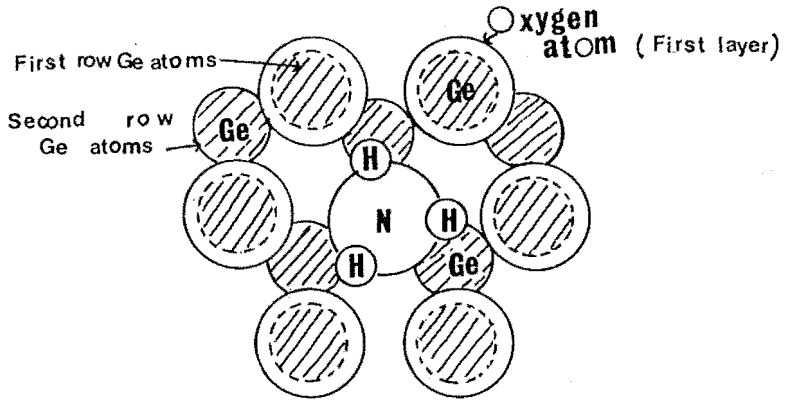

(5j)

As the second layer germanium atoms do not have available bonding orbitals needed to dissociate adsorbate molecules, only undissociated species will exist in the centre of the hexagon. Ammonia, if it resides within the hexagon centre, will have its nitrogen atom directed downwards to facilitate electron exchange between the pair of donor electrons and the germanium lattice. The hydrogen atoms which are then directed upwards will be conveniently placed for H-bonding with alternate chemisorbed oxygen atoms. The almost complete removal of the band, after pumping at 25^{o}C for 4 days, suggests that the degree of electron exchange is limited with subsurface atoms as compared with atoms on the bare surface.

Bands in the stretching region cannot be assigned as they are not distinguished clearly.

CHAPTER SIX

INTERACTION OF CARBON DIOXIDE ON EVAPORATED GERMANIUM FILMS

6.1 Review of Studies on the Adsorption of Carbon Dioxide on Germanium

Electrical measurements show that carbon dioxide acts as an acceptor, at low exposures,[157,158] with the result that similar changes in the p-type conductivity occur as in the case of water vapour,[125] oxygen[13] or ammonia[149] adsorption on germanium.

The kinetics of the adsorption of carbon dioxide on evaporated germanium films have been investigated by Bennett and Tompkins,[17] who found a direct proportionality between the pressure and the rate of uptake after an initial rapid sorption stage. At -78°C they found that the interaction was mainly non-dissociative, whereas at temperatures above 0°C carbon monoxide was released as a result of dissociation. The germanium films were found to sinter to some extent suggesting that the dissociatedly adsorbed oxygen atom was incorporated into the lattice by a place-exchange mechanism, similar to that observed in the case of molecular oxygen.[67]

By anology with the results of Eischens[159] from the infrared spectra of carbon-dioxide adsorbed on nickel it was suggested[17] that the initial adsorption complex is a carboxylate-like ion. However, data for carbon dioxide adsorption on metal surfaces are conflicting. For example,

Eischens and Pliskin[160] obtained two different results with reduced-nickel surfaces; in one case carbon dioxide was found to dissociate only at 100°C while in another dissociation occurred at 25°C. The disparity in the results shows that adsorption is sensitive to the properties of the surface, and it may also be that the mode of adsorption is not the same in each case.

Subsequent breakdown of the adsorbed complex is thought to be responsible for the release of carbon monoxide and the oxidation of the surface. As the d-band of germanium is completely filled[166] carbon monoxide is not expected to chemisorb to form metal-carbonyl type species.

On oxidised surfaces the interaction is mainly reversible; the small permanent uptake reported by Law[161] may have been due to the presence of 'free' germanium atoms on the surface as a result of place-exchange with overlying chemisorbed oxygen.[67]

There have been no reports in the literature of any infrared study relating to the adsorption of carbon dioxide on germanium.

6.2 Infrared Spectra of Carbon Dioxide on Evaporated Germanium Films

A preliminary study of the interaction of carbon dioxide on germanium has been made. The spectral region below 2400 cm^{-1} was monitored for likely absorptions due to various possible species arising from the adsorption. These include bands due to molecular carbon dioxide

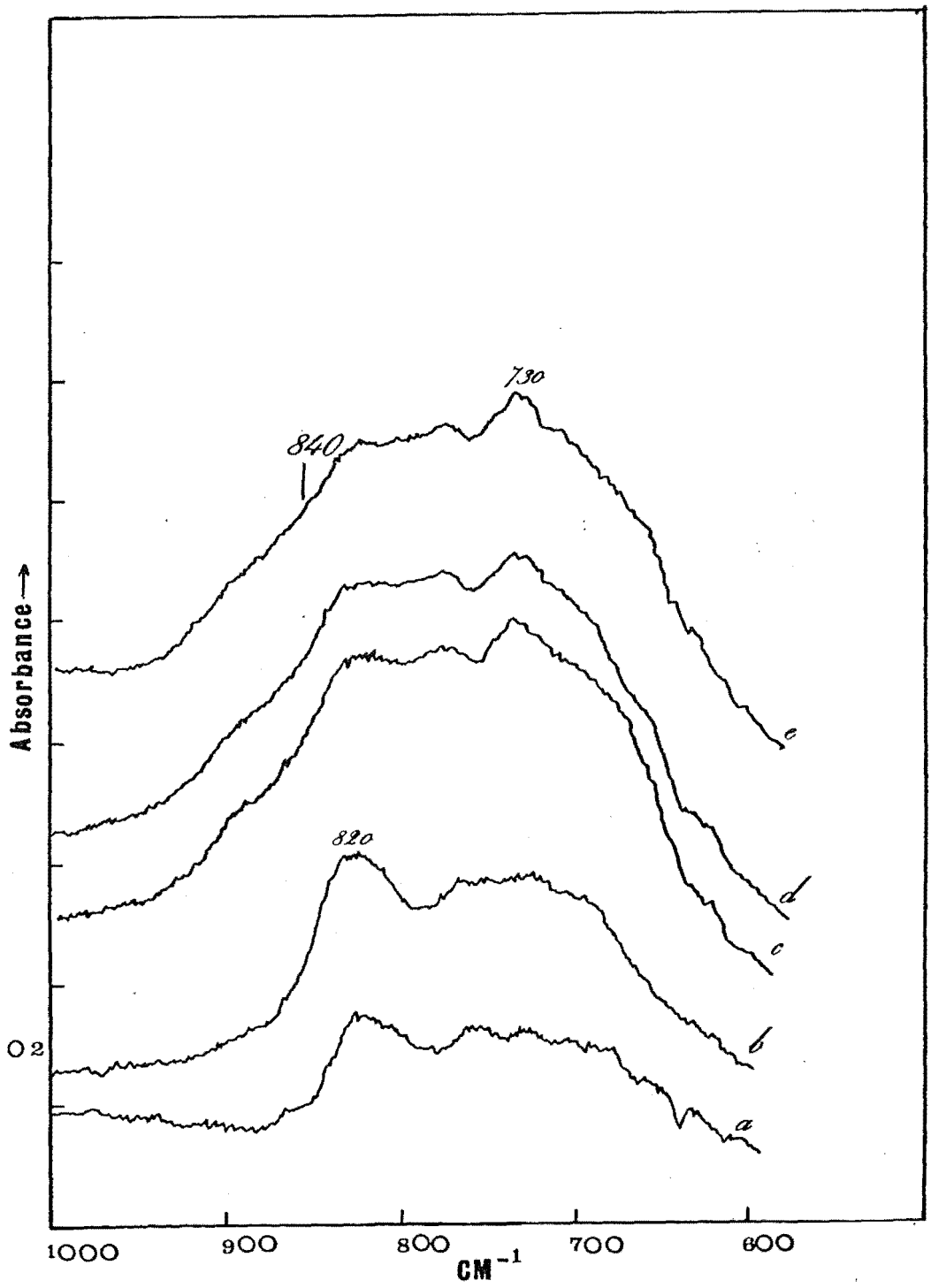

Figure 6.1 Spectra of carbon dioxide adsorbed (at 133.3 Pa) on germanium, at 27°C. (a) 20 min; (b) 4h; (c) 16h; (d) 20h; (e) 48h. Ordinates displaced.

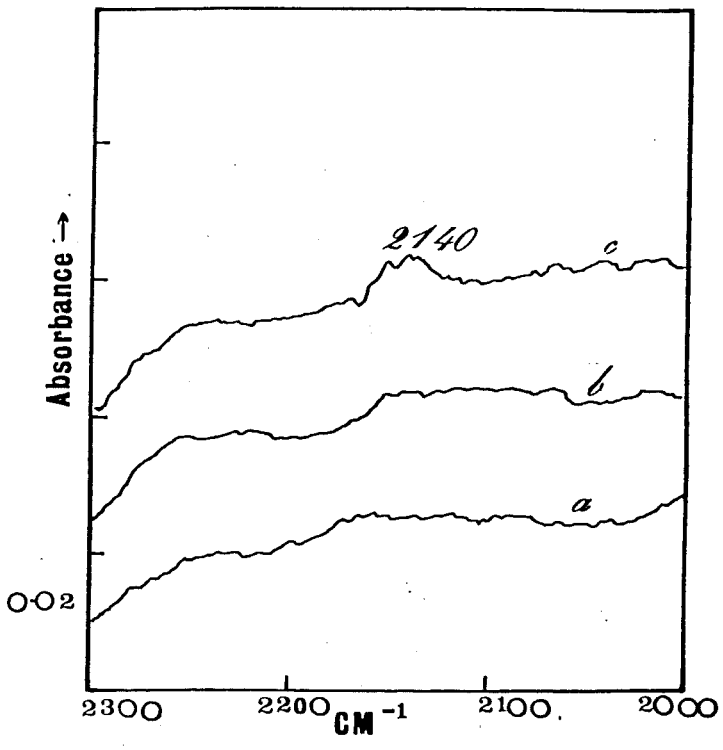

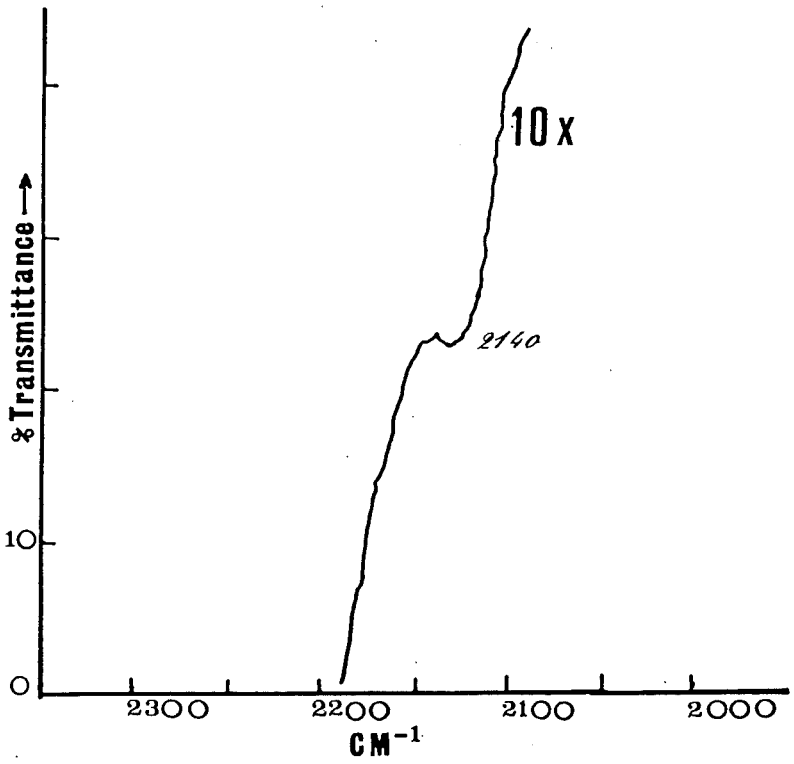

Figure 6.2 Spectra of carbon dioxide adsorbed (at 133.3 Pa) on germanium. (a) 1h, 25°C; (b) 4h, 40°C; (c) 18h, 70°C. Ordinates displaced. Also reproduced is a chart recorder scan at 10x scale expansion.

(2349 cm^{-1}),[162] carbon monoxide (2143 cm^{-1})[162] and oxygen adsorbed as a result os dissociation (between 900-600 cm^{-1}).[1,5] A region between 1600-1100 cm^{-1} was also examined for likely absorptions due to carbonate or carboxylate-type species.[163] Spectral intensities have also been measured, between 820-730 cm^{-1}, in order to obtain a correlation with the pressure dependence of the amount adsorbed.

6.21 Adsorption of Carbon Dioxide

Figure 6.1 shows the spectral changes (between 1000-600 cm^{-1}) observed after admitting carbon dioxide to a set of freshly prepared films. Already at low pressures (133 Pa) a relatively strong band emerges at 820 cm^{-1} within 20 minutes of exposure. A weaker band is also evident between 760-670 cm^{-1}. With increasing exposure both bands grow in the same ratio at first but within a few hours the band envelope changes in a complicated manner with the 760-670 cm^{-1} absorption growing more rapidly than the former. After a total of 16 hours there appears a maximum at 730 cm^{-1}, while the band at 820 cm^{-1} broadens considerably. A very weak band at around 2140 cm^{-1}, observed after several hours exposure is shown in figure 6.2. Spectra recorded on chart paper, using the scale expansion (10x), is also shown in the same figure for clarity. No other bands were apparent between 4000-600 cm^{-1}. On evacuation of the gas-phase the 2140 cm^{-1} band diminished slightly but the other bands remain unperturbed.

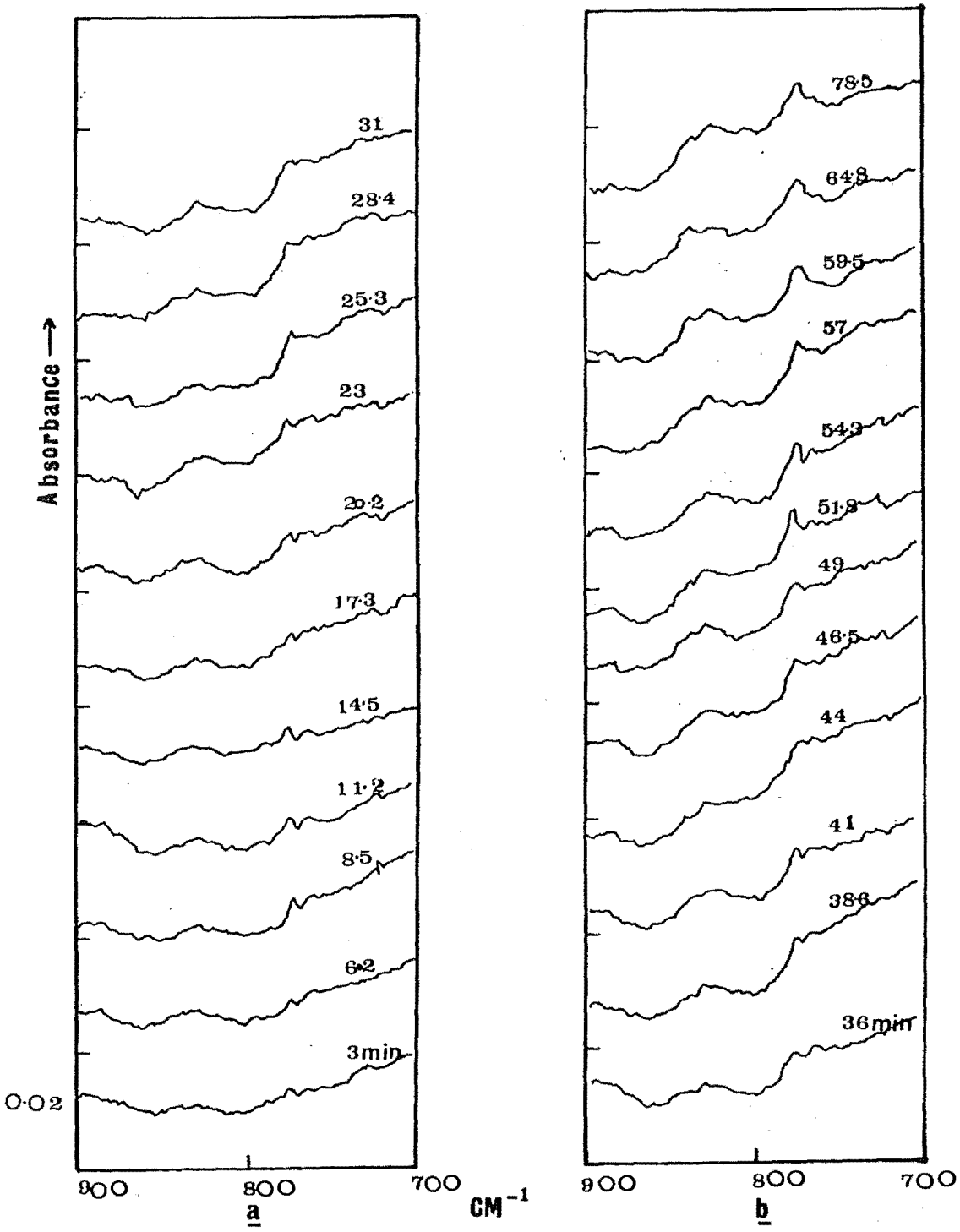

Figure 6.3 Spectra obtained after adsorbing carbon dioxide on germanium at two pressures. (a) 20 Pa; (b) 133.3 Pa. Ordinates displaced.

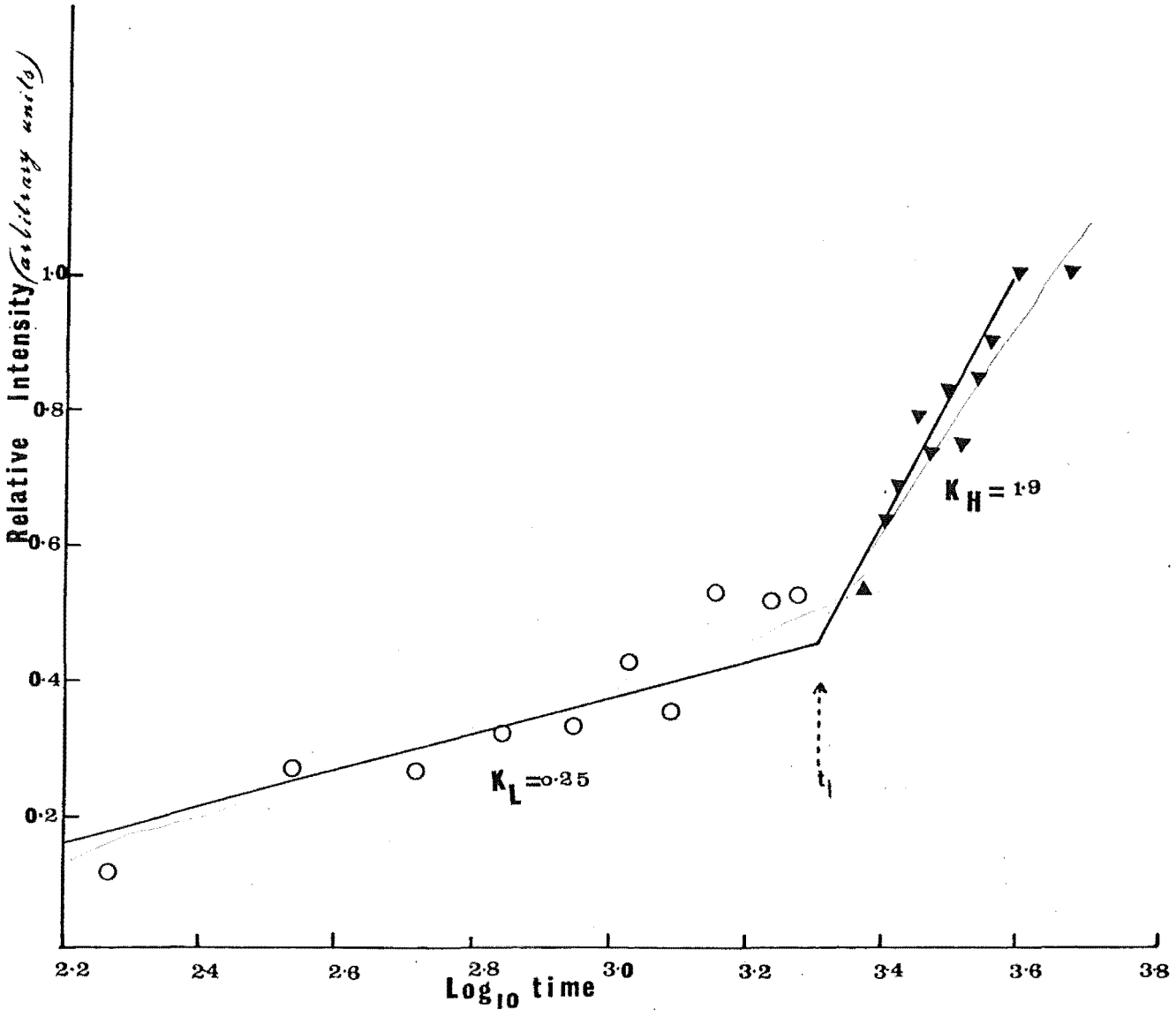

Figure 6.4 Plot of peak heights (normalised), obtained from Fig. 6.3, versus logarithm of time.

On heating the films, at temperatures between 50-100°C after adsorption, the 2140 cm^{-1} band is intensified slightly (Fig. 6.2, trace b,c) but no other changes are apparent elsewhere. This band does not, however, decrease on pumping after heating.

6.22 Pressure Dependence

Experiments were carried out to determine the pressure dependence of the bands appearing below 1000 cm^{-1}, viz. the 820 and 730 cm^{-1} bands. The procedure used is essentially the same as that employed by Bennett and Tompkins.[17] Although precise interpretation of infrared measurements is difficult, because of likely variations in extinction coefficients with surface coverage, some obvious trends may nevertheless be obtained.

A set of freshly prepared films, cooled to about 27°C, were exposed to carbon dioxide at a pressure of 20 Pa (1.5×10^{-1} Torr) after a background spectrum was recorded. Spectral recordings were then begun and continued over a period of 80 minutes. At some time t_I the pressure was increased to 133 Pa (1 Torr) and the recordings continued for a further 40 minutes. The difference spectra are shown in figure 6.3.

As is the case with oxygen[67] the amount adsorbed is found to follow Elovich type kinetics,[17,67] i.e,

$$q = k \log t + c \qquad (6a)$$

where q is the amount adsorbed in time t., k and c are constants. Thus a plot of the peak heights (assumed proportional to the amount adsorbed) versus the logar-

Figure 6.5 Plots of log (r/p^n), where n = 0, ½, 1, 2, versus the relative peak heights, q(≃ the amount adsorbed). $r = dq/dt$

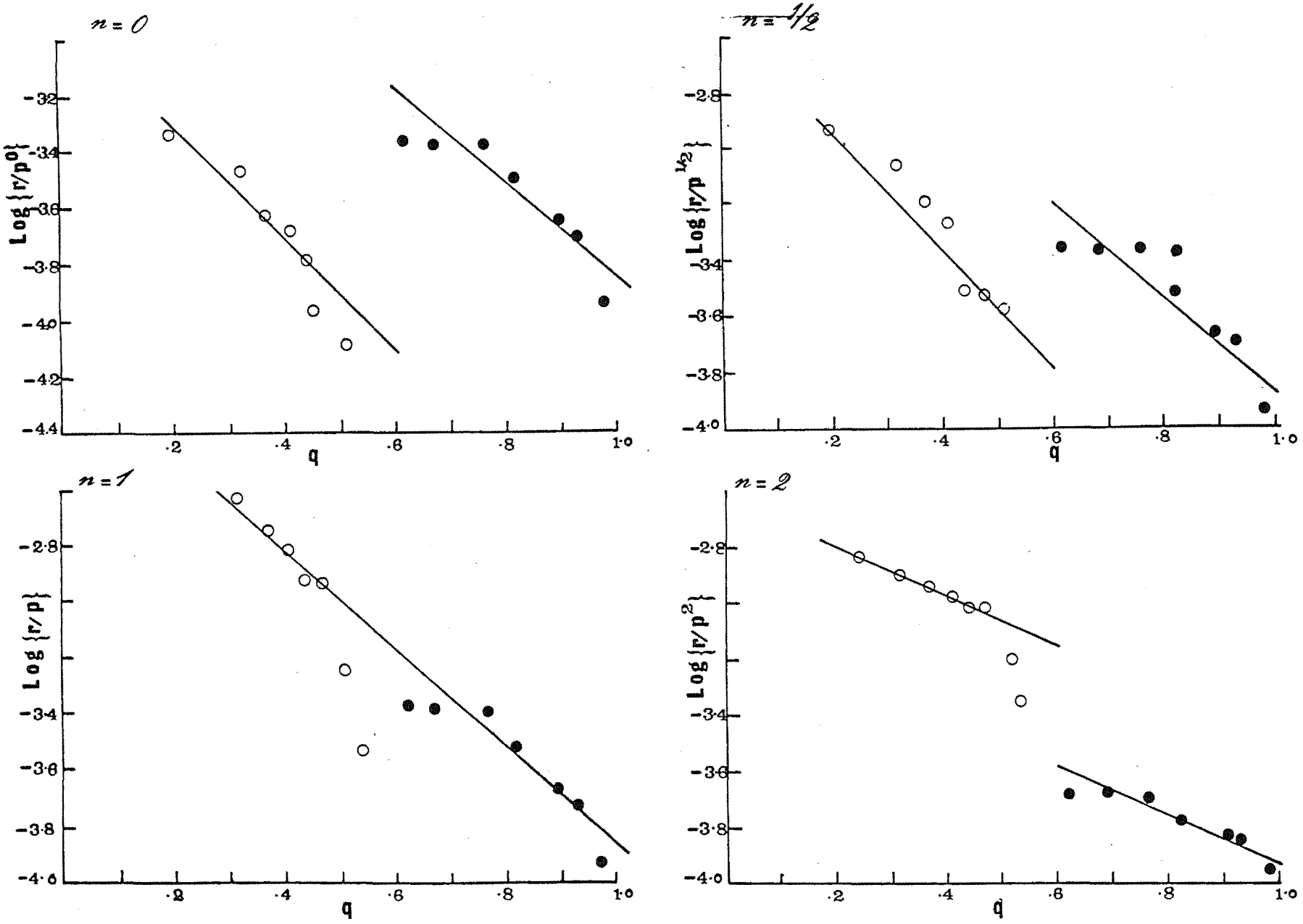

rithm of time should yield straight lines with slopes K_L for the lower pressure region and K_H for the higher pressure region. This is shown in figure 6.4. Each point has been obtained by summing the peak heights of the 820 and 730 cm^{-1} bands and normalising them with respect to the final value. The two lines through the points of best fit are drawn so that they intersect at t_I; the amount adsorbed at t_I should be the same at the two pressures as no instantaneous uptake is expected to occur.[67]

If it is assumed that the rate (r) is a function of the amount adsorbed (q) and pressure (p) (i.e. $r = f(q,p)$, where q and p are independent variables, then as shown by Bennett and Tompkins[67] at time t_I,

$$\left(r_H \div r_L\right) = \left(p_H \div p_L\right)^n = \left(K_H \div K_L\right) \qquad (6b)$$

where H denotes the higher pressure range and L the lower pressure range. A comparison of the slopes yields a value for n of approximately 1.30, which therefore can be interpreted as a direct linear dependence of rate on the pressure. Thus the rate equation can be written as,

$$dq/dt = ap \exp(-bq) \qquad (6c)$$

where a and b are constants. The validity of this equation can be further substantiated by plotting $\log_{10}\left\{\left(dq/dt\right) / p^n\right\}$ versus q. Figure 6.5 shows a number of plots obtained with different values for the exponent of p. If the initial premise that f(p) and f(q) are independent variables is valid then linearity should be maintained with no discontinuities when the pressure is

increased. This is found to hold reasonably well with n=1, whereas with n=½, 0, 2 there are marked deviations from a straight line after increasing the pressure.

6.3 Discussion

The direct proportionality shown by the peak heights of the bands appearing below 820 cm^{-1}, to the carbon dioxide pressure, suggests that these bands are due to CO_2 adsorbed molecularly or dissociatedly. The observed bands are summarised in Table 6.1. If the bands did arise as a result of residual oxygen then it would be anticipated that the amount adsorbed will be proportional to the square root of pressure.[67] There are two further reasons why it is unlikely that the bands are due to oxygen: a) the carbon dioxide was thoroughly freed of impurities by repeated vacuum sublimation, and b) the initial stages of oxygen adsorption results in bands at 780 and 690 cm^{-1} on germanium;[1,5] a band near 840 cm^{-1}, attributed to oxygen dissolved in the lattice, appears only after several hours exposure to air at atmospheric pressure.[1,5]

Although with metals a carboxylate type structure (6d) has been proposed[159]

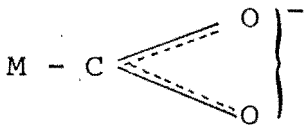

(6d)

for the adsorption complex such a possibility can be ruled out as no bands were observed due to this species. The carboxylate ion if present is expected to show strong absorptions near 1600-1500 cm^{-1} due to the asymmetric stretch, and between 1400-1350 cm^{-1} due to symmetric

Table 6.1 Infrared Bands of Carbon Dioxide Adsorbed on Germanium

Group	This Work (cm^{-1})	Comparison Bands (cm^{-1})
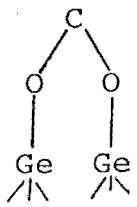	820	880[a] 837[b]
$Ge-O^-$	730	730[c] 750[d]
O^{2-} (incorporated)	840	840[d]
CO (physically adsorbed)	2140	2143[e]

[a] ref. (164); [b] ref. (165); [c] This work (Chapter 4);

[d] ref. (1,5); [e] gas-phase (ref.162).

stretching vibrations of the OCO group.

A carbonate type species which may result if the surface is covered with a monolayer of oxygen can similarly be ruled out as this species is also expected to absorb between 1500-1300 cm^{-1}.

Thus it does not seem unreasonable to assign the 820 cm^{-1} band to germanium-oxygen bond stretching vibrations resulting from carbon dioxide being adsorbed, through its oxygens, on the germanium surface, as in 6e below.

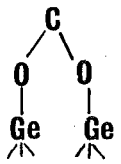

(6 e)

Some support for this assignment is obtained by comparing the Ge-O stretching vibrations of organo-germanium compounds such as acetoxygermane[164] ($H_3GeOCOCH_3$) and trimethylacetoxygermane ($(CH_3)_3GeOCOCH_3$);[165] the band corresponding to this absorption appears at 880 cm^{-1} with the former and at 837 cm^{-1} with the latter.

Carbon dioxide adsorbed in this fashion is suitably placed to accept electrons during the subsequent decomposition of the complex. According to Bennett and Tompkins[17] decomposition occurs to some extent at $0^{o}C$, with the slow evolution of carbon monoxide. On p-type surfaces the general process of decomposition may be written as,

$$CO_{2\ (ads)} \longrightarrow CO_{(ads)} + O^{-}_{(ads)} + \oplus^{v} \qquad (6f)$$

The positive hole $\oplus^{v}$ released may eventually contribute to the rise in p-type surface conductivity as indicated by electrical measurements. The 730 cm^{-1} band, which seems to grow strongly at latter stages of the interaction, can be assigned to $Ge\text{-}O^{-}$ (see Section 4.41, Chapter 4) arising from reaction 6f. Subsequent incorporation of adsorbed oxygen into the lattice of germanium results in the appearance of a band at 840 cm^{-1}. This probably accounts for the broader nature of the absorption at 820 cm^{-1}, at the latter stages.

Carbon monoxide, released through the decomposition of the adsorption complex, does not adsorb irreversibly on germanium as the d-band of germanium[166] is completely filled. However, as suggested by Bennett and Tompkins[17] enhanced physical adsorption may occur as in p-type metals, such as copper, silver and gold.[167] It is possible that the band centered at 2140 cm^{-1}, which is close to the gas-phase absorption of carbon monoxide at 2143 cm^{-1},[162] is due to a carbon monoxide species weakly interacting with the surface, probably through dipolar forces. The enhancement of the band at high temperatures and its incomplete removal on pumping, after heating the films, suggests that the adsorption occurs through an activated process.

CHAPTER SEVEN

INTERACTION OF OXYGEN WITH EVAPORATED SILICON FILMS

7.1 Review of Oxygen Adsorption Studies on Silicon

It is generally acknowledged that the kinetics of adsorption of oxygen on silicon occurs as a two step process,[168-170] in a similar manner to oxygen adsorption on germanium.[67] Gas-volumetric measurements on powders[13] and evaporated films[169] indicate an initial rapid sorption process up to monolayer coverage, followed by a slow process above exposures of 1.3×10^{-1} Pa-min (1×10^{-1} torr-min) during which the rate of adsorption decreases exponentially with increasing amounts of gas adsorbed. The kinetics of the slow step is of the Elovich type and can be written as

$$q = A \log t + B \qquad (7a)$$

where q is the amount adsorbed at time t.

Law[169] investigated the pressure dependence of the rate of the slow uptake and found it to vary as the square root of pressure. Thus the overall rate of uptake (dq/dt) for the slow process can be written as

$$dq/dt = ap^{\frac{1}{2}} \exp(-bq) \qquad (7b)$$

where p is the oxygen pressure and a and b are constants.

There is considerable disparity, however, in the values quoted in the literature for the extent of adsorption at monolayer coverage. Green and Maxwell,[168] who measured the rates of sorption on vacuum crushed surfaces,

found the uptake to terminate at an oxygen take-up equivalent to about 1.5 oxygen atoms per surface silicon atom. The logarithmic rate law in this case was obeyed only over a short period of between 10-80 minutes. Carossela and Comas[171] obtained a value of 1 oxygen per 2 surface silicon atoms from their proton activation studies. Schlier[172] interpreted his results of LEED studies of oxygen adsorption on silicon single crystals, cleaned by argon ion-bombardment, also as an adsorption of 2 oxygens per surface silicon atom. But the results of Wolsky[173] are in complete contradiction. His results suggest the ratio to be closer to 1 oxygen per 2 surface silicon atoms.

Perhaps the most extended determination of the absolute amount adsorbed at monolayer coverage comes from the studies of Boonstra[13] who found the oxygen to silicon ratio, at monolayer coverage, to be close to unity. Recent ellipsometric data[174] On (111) and (100) surfaces of silicon is in agreement with this value.

The destruction of non-integral order spots in LEED studies[172] indicates a reconstruction of the surface due to oxygen adsorption. The surface is thought to rearrange to a more 'relaxed' state and the structure is found to be similar to that of the underlying planes. No additional spots were observed during the early stages of adsorption that could be attributed to an oxide layer (for both (111) and (100) surfaces). At high exposures an amorphous oxide layer is evidently formed.

Electrical measurements by Boonstra[13] show that the p-type conductivity of the surface rises to a maximum up to exposures between 1.3×10^{-5} and 1.3×10^{-6} Pa (10^{-7} - 10^{-8} torr) or at coverages below 0.01 monolayer. If exposure to oxygen is continued, the conductivity decreases to the intrinsic value. The formation of acceptor-like surface states during the initial stages is evidently followed by the setting up of donor levels, at coverages greater than 0.01 monolayer. The work function values[175] of all surfaces of cleaved silicon show an upward rise by between 0.3 and 0.4 eV upon exposure to oxygen, but it begins to decrease only at coverages greater than 0.1 monolayer.

In view of the large variety of different and often contradictory results no complete picture has emerged on the nature of the adsorbed species. However, several authors[18,19] have considered various models for the initial adsorption process in the light of results obtained by a variety of techniques. An average heat of adsorption of 912 $\overset{k}{K}J\ mol^{-1}$ obtained calorimetrically by Brennan et al.,[176] for coverages up to 0.8 oxygen atoms per surface silicon atom, closely parallels the heat of formation of SiO and SiO_2[141] molecules (879 $\overset{k}{K}J\ mol^{-1}$). Thus it is likely that silicon forms predominantly covalent bonds with adsorbed oxygen. In a recent study Meyer and Vrraking[18] interpreted their ellipsometric results to indicate a definite 'surface oxide' layer. The measured polarizability of the surface species was found to correspond to Si-O groups rather than to a layer of adsorbed oxygen atoms. Thus the top layer of silicon is incorporated in the adsorbed layer.

Surface structures analogous to those suggested by Green and Liberman,[177,178] for germanium surfaces, were considered for both (100) and (111) surfaces. Strain energy calculations in terms of bond types, bond lengths and bond angles of germanium compounds suggest that for minimum strain a bridged oxide structure is favoured on (100) surfaces and a peroxide-like complex on (111) and (110) surfaces. According to Meyer and Vrraking[18] the model for the (100) surface, where each silicon has associated with it two 'free valencies' (or dangling bonds), consists of chains of Si-O units, as shown below.

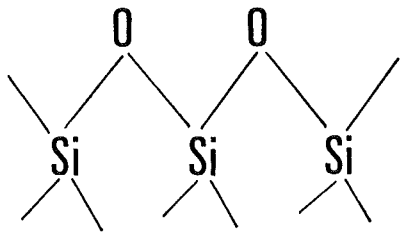

(7c)

(100) surfaces

An alternative structure has been proposed for (111) surfaces as the peroxide-like model does not provide a continuous oxide layer; the authors regard this as necessary for subsequent bulk oxide formation which would otherwise require the breaking of the O-O bond. With this model the -Si-O-Si- chains are maintained as a result of structural rearrangements whereby second layer silicon atoms are also utilized in the bonding, as shown below.

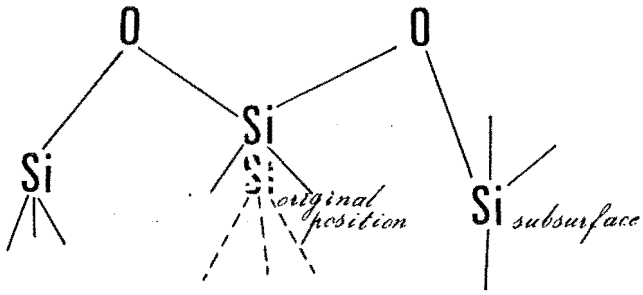

(7d)

(111) surfaces

The strain induced by the formation of an oxygen bridge between two neighbouring surface atoms is thought to assist the breaking of the Si-Si bonds. The subsequent relaxation of the surface structure is in accord with LEED data.[172]

An identical electron loss spectrum for both (111) and (100) surfaces obtained by Ibach and Rowe[179] suggests that the electronic states at monolayer coverage are similar for both surfaces. Thus the mode of adsorption is presumably the same in both surfaces giving some support to the above model.

During the early stages of adsorption the formation of SiO_3^- groups, which have been detected at coverages below 0.01 monolayer by secondary ion mass spectroscopy (SIMS),[180] can also be explained in terms of the alternative model. It is believed that the acceptor levels associated with this species is responsible for the observed rise in p-type conductivity at coverages up to 0.01 monolayer.

Contrary views are held by Ibach et al.[19] They favour the peroxide-like structure for (111) surfaces on the basis

of their High Resolution Electron Spectroscopy (HRES) results. Energy losses were observed at 94, 130 and 175 meV (758, 1049 and 1411 cm^{-1}) in the vibrational spectrum, corresponding to three vibrational modes, of the adsorbed species. The energy losses were observed at coverages between 0.2 and 0.6 monolayer. Since they reached their maximum intensity at the same exposure (1.1×10^{-2} Pa-min) they are thought to arise from only one binding state of adsorbed oxygen. By considering the vibrational modes of various surface structures, which are likely to have components of their dipole moments oriented perpendicular to the surface plane (since energy losses in HRES only occur as a result of the interaction of low energy electrons with adsorbed species having dipole moments, or their components, normal to the surface) it was suggested that the most likely structures would be peroxide-like, as in 7e and 7f below.

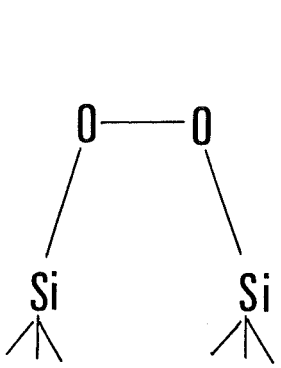

(7e)

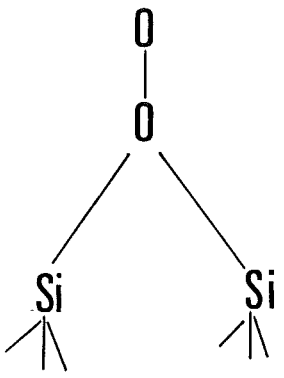

(7f)

Other models, including the silicon-oxygen bridge, were ruled out on the basis of their vibrational modes which are fewer in number than suggested by HRES.

As the HRES technique is not sensitive at very low coverages the existence of precursor states that saturate below 0.01 monolayer is a possibility that cannot be ruled out. A constant sticking coefficient, even at coverages up to 0.8 monolayer, suggests that the adsorbed species may also be mobile.

It is interesting to note that Bennett and Tompkins[67] also suggest molecular adsorption at coverages close to monolayer on germanium surfaces. The decrease in p-type conductivity has been attributed to the elimination of all dangling bonds resulting in the formation of O_2^- ions; the O_2^- ions are presumably adsorbed in a similar manner to the structures shown in 7e and 7f.

The slow step, during which the logarithmic uptake occurs, corresponds to the formation of the bulk oxide. Optical constants, measured ellipsometrically,[181] indicate a shift into the direction of the bulk optical constants during oxygen adsorption beyond a monolayer. From these measurements the thickness of the bulk oxide layer was calculated to be approximately 0.3nm at exposures above 2×10^{-2} Pa-min. This suggests an oxygen uptake corresponding to one or two monolayers at room temperature ($25^{\circ}C$).

From their infrared spectral measurements, obtained during steam oxidation of silicon wafers, Ligenza and Spitzer[182] suggest that the actual oxidation and its rate-limiting step occur at the silicon-oxygen interface. Only 30% of the adsorbed O^{16} atoms were found to exchange with

O^{18} indicating that a high concentration of the oxygen penetrates the film to the Si-O interface. This rules out the Mott and Cabrera[183] mechanism of oxide formation on metal surfaces, which involves the diffusion of metal ions or metal vacancies which are subsequently oxidised by oxygen ions.

An alternative mechanism has been suggested by Lanyon and Trapnell[184] and more specifically by Green and Liberman[178] for oxide formation in germanium. This involves 'place exchange' of adsorbed oxygen with the underlying metal or semiconductor atoms, as in 7g.

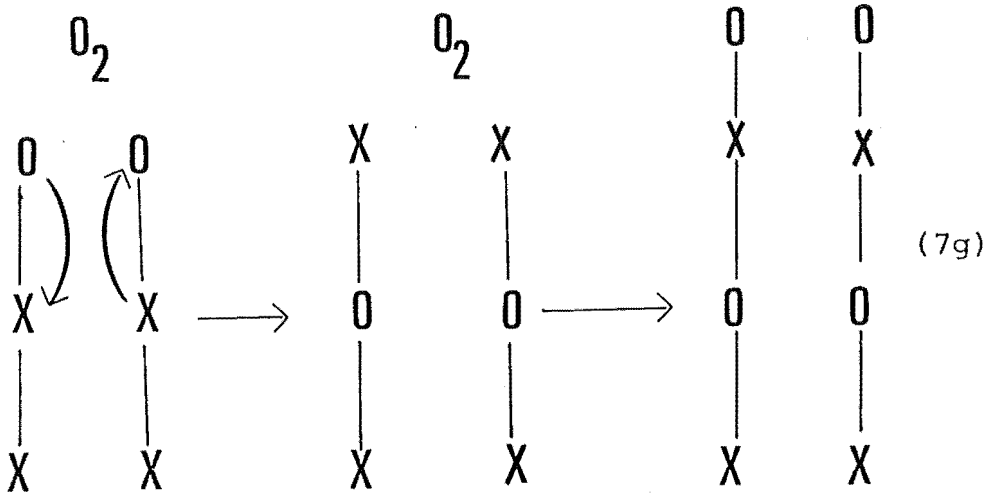

(7g)

According to Green and Liberman the driving force for place exchange in germanium is the lattice strain in germanium-germanium bonds caused by the initial monolayer adsorption.

Bennett and Tompkins[67] have suggested an alternative model for heterogeneous germanium surfaces (like evaporated

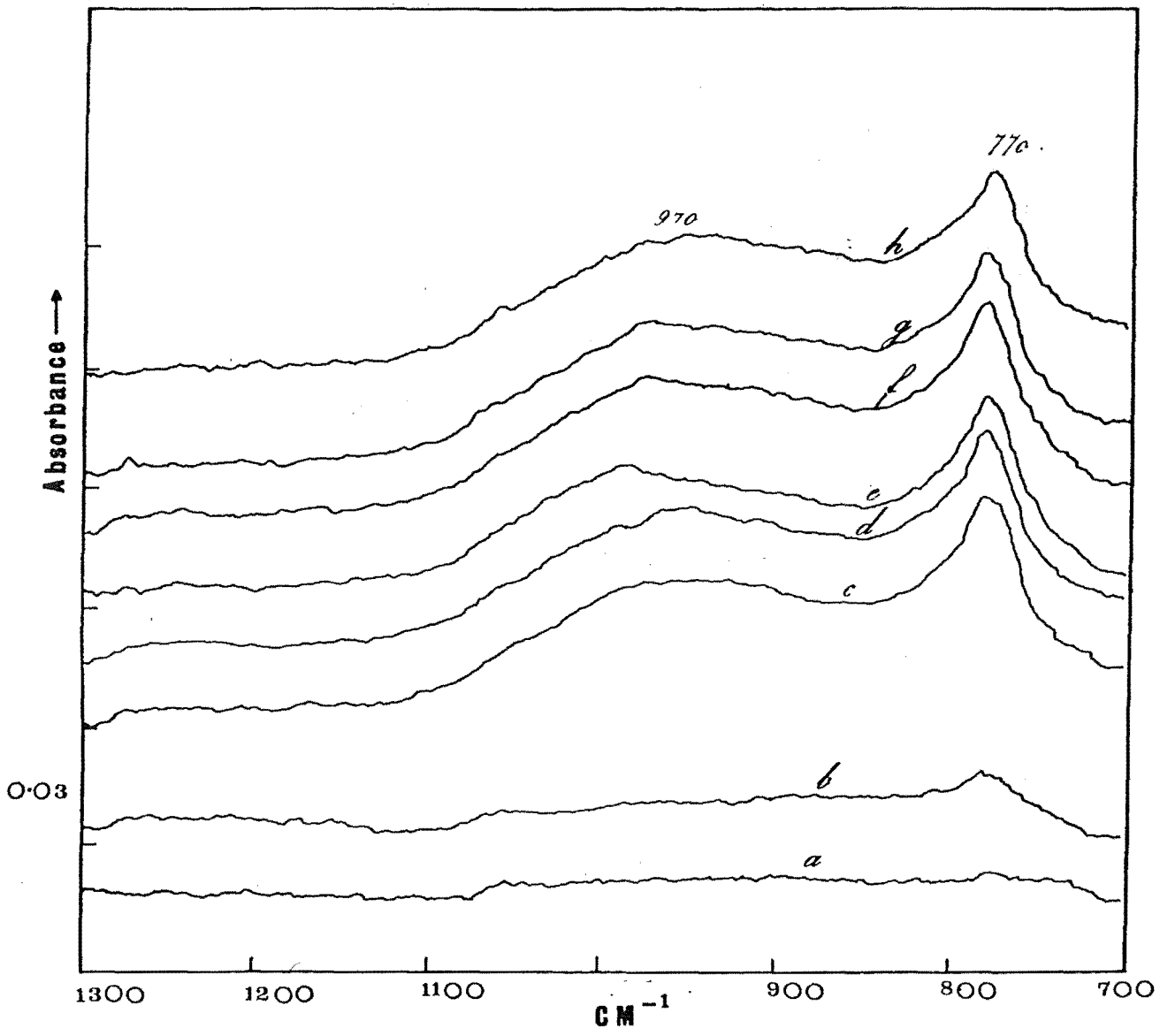

Figure 7.1 Spectra of oxygen adsorbed on silicon, at 27°C. (a) 3×10^{-6} Pa, 5 min; (b) 8×10^{-6} Pa, 20 min; (c) 4×10^{-5} Pa, 15h; (d) 1.3×10^{-1} Pa, 15 min; (e) 1.3×10^{-1} Pa, 1h; (f) 1.3×10^{-1} Pa, 4h; (g) 1.3×10^{-1} Pa, 18h; (h) 1.3×10^{-1}, 24h. Ordinates displaced.

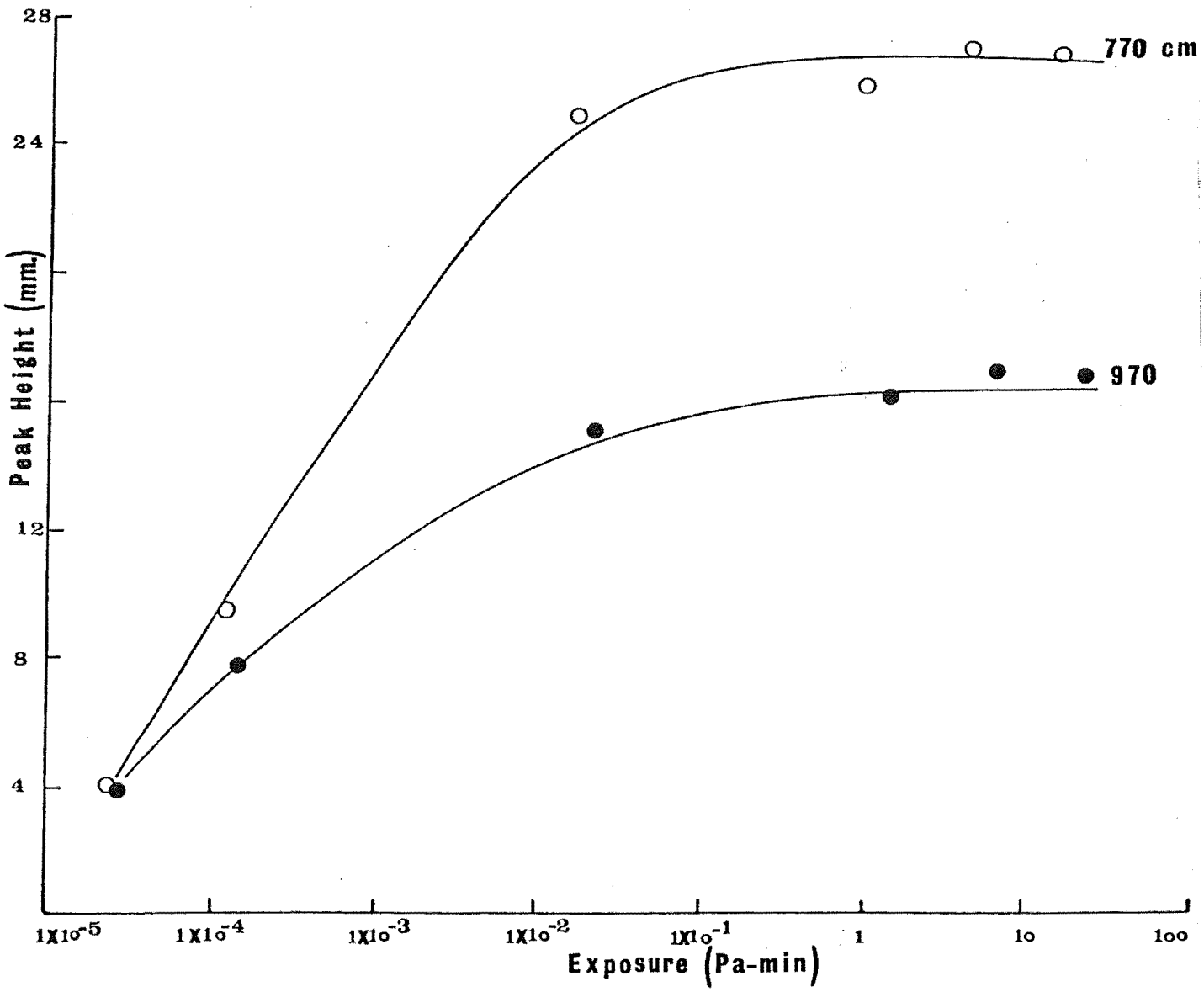

Figure 7.2 Peak heights of 770 and 970 cm^{-1} bands plotted against exposure to oxygen.

films) in view of the small effect of pressure on the rate of oxygen uptake (proportional to $P^{\frac{1}{2}}$) which indicates that the whole surface is not active in the rate process. The two workers regard place exchange as occurring at singularities (eg. defects or steps) where as a result of the abnormal electron density O_2^- ions are formed readily. Subsequent dissociation of O_2^- is followed by incorporation of adsorbed oxygen atoms by place exchange. A similar mechanism is likely to be operative on silicon surfaces as O_2^- ions produced by ion pumps or ion gauges have been found[179,181] to enhance the rate of oxidation above monolayer coverage.

7.2 Infrared Spectra of Oxygen Adsorbed on Evaporated Silicon Films

The infrared bands due to the silicon-oxygen stretching vibration of oxygen-containing silicon compounds occurs in the region between 1400-600 cm^{-1}. The study has therefore been conducted principally in this region in order to observe absorption bands corresponding to various possible species arising from the interaction.

7.21 Adsorption at Low Pressures

A set of four films were prepared, as described earlier (Section 2.32, Chapter 2) and a background recorded immediately after preparation. Spectral recordings were continued between 1400-600 cm^{-1}, while argon was allowed to flow continuously to the pumps at 1.3×10^{-1} Pa. The difference spectra are shown in figure 7.1 (trace a to e). Since the stated oxygen content of the argon is approximately

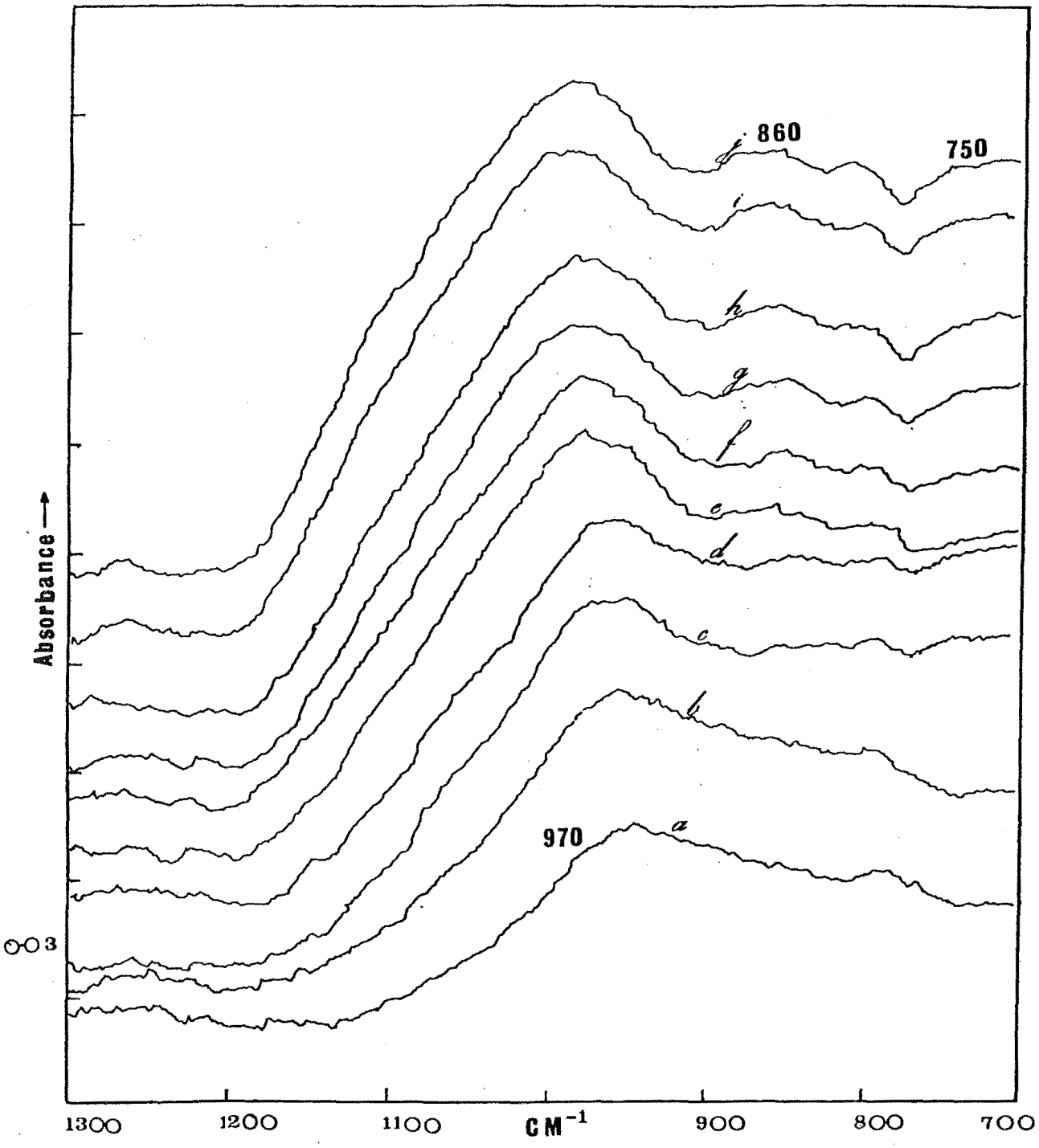

Figure 7.3 Spectra of oxygen adsorbed on silicon films, at 27°C, at increasing pressure. (a) 13.3 Pa, 20 min; (b) 13.3 Pa, 3h; (c) 773 Pa, 3 min; (d) 773 Pa, 20 min; (e) 773 Pa, 3h; (f) 3 x 10^3 Pa, 4 min; (g) 3 x 10^3 Pa, 1h 25 min; (h) 3 x 10^3 Pa, 4h; (i) 1 x 10^4 Pa, 30 min; (j) 1 x 10^4 Pa, 3h. Ordinates displaced.

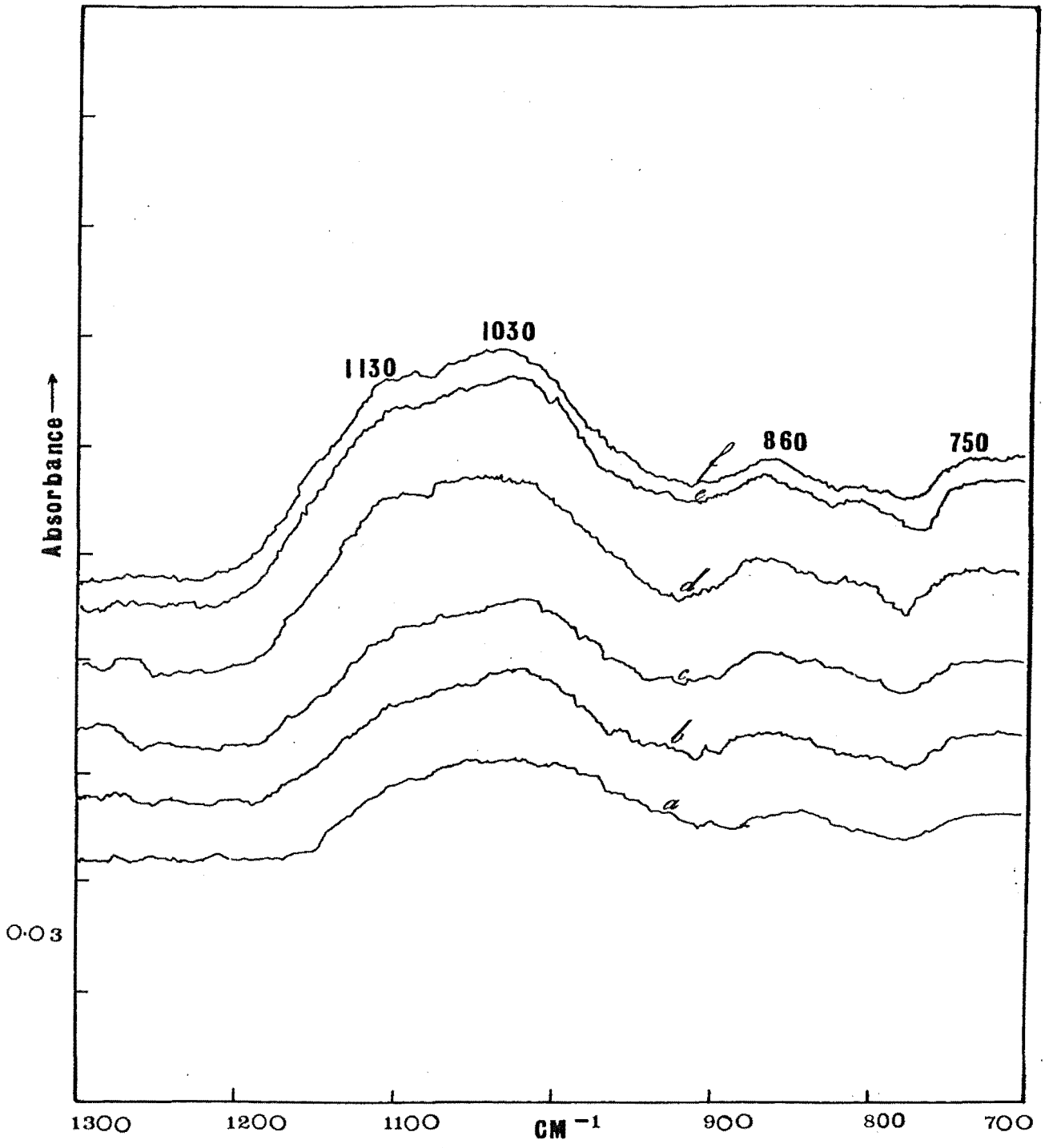

Figure 7.4 Spectra obtained by subtracting the low-pressure band (trace a) of Fig. 7.3. (a) 773 Pa, 20 min; (b) 773 Pa, 3h; (c) 3×10^3 Pa, 1h; (d) 3×10^3 Pa, 4h; (e) 1×10^4 Pa, 30 min; (f) 1×10^4 Pa, 3h. Ordinates displaced.

10 ppm the partial pressure of oxygen would have been in the 10^{-6} Pa (10^{-8} torr) range. Already at very low exposures a band, which is weak at first, emerges at around 770 cm^{-1}. It reaches maximum intensity after a total of 15 hours exposure. Further exposure to oxygen at 1.3 x 10^{-1} Pa ($1x10^{-3}$ torr), after removal of the argon buffer, results in no significant change in the band height (trace f to h).

A second band, which is much broader in nature and centered at around 970 cm^{-1}, is apparent after 20 minutes exposure. It also appears to reach its maximum intensity after a total of 15 hours exposure (trace e) with very little change occuring with further exposure to oxygen at 1.3 x 10^{-1} Pa (trace f to h).

The band heights of both absorptions are plotted against exposure in figure 7.2. The levelling off of the curve at around 1 x 10^{-1} Pa-min may indicate that saturation or monolayer coverage has been attained. Although the initial slopes of the two curves are different both bands reach maximum intensity at about the same exposure.

In a separate run exposure of freshly prepared films to oxygen, between 1.3 Pa and 1 x 10^{4} Pa, was investigated. The resulting difference spectra are shown in figure 7.3. At high exposures the band centre of the 970 cm^{-1} band seems to shift to higher frequencies. The band broadens considerably while an increase in the band height it also apparent. A small maximum at 860 cm^{-1} (and possibly a much weaker one near 750 cm^{-1}) in the band envelope is also evident.

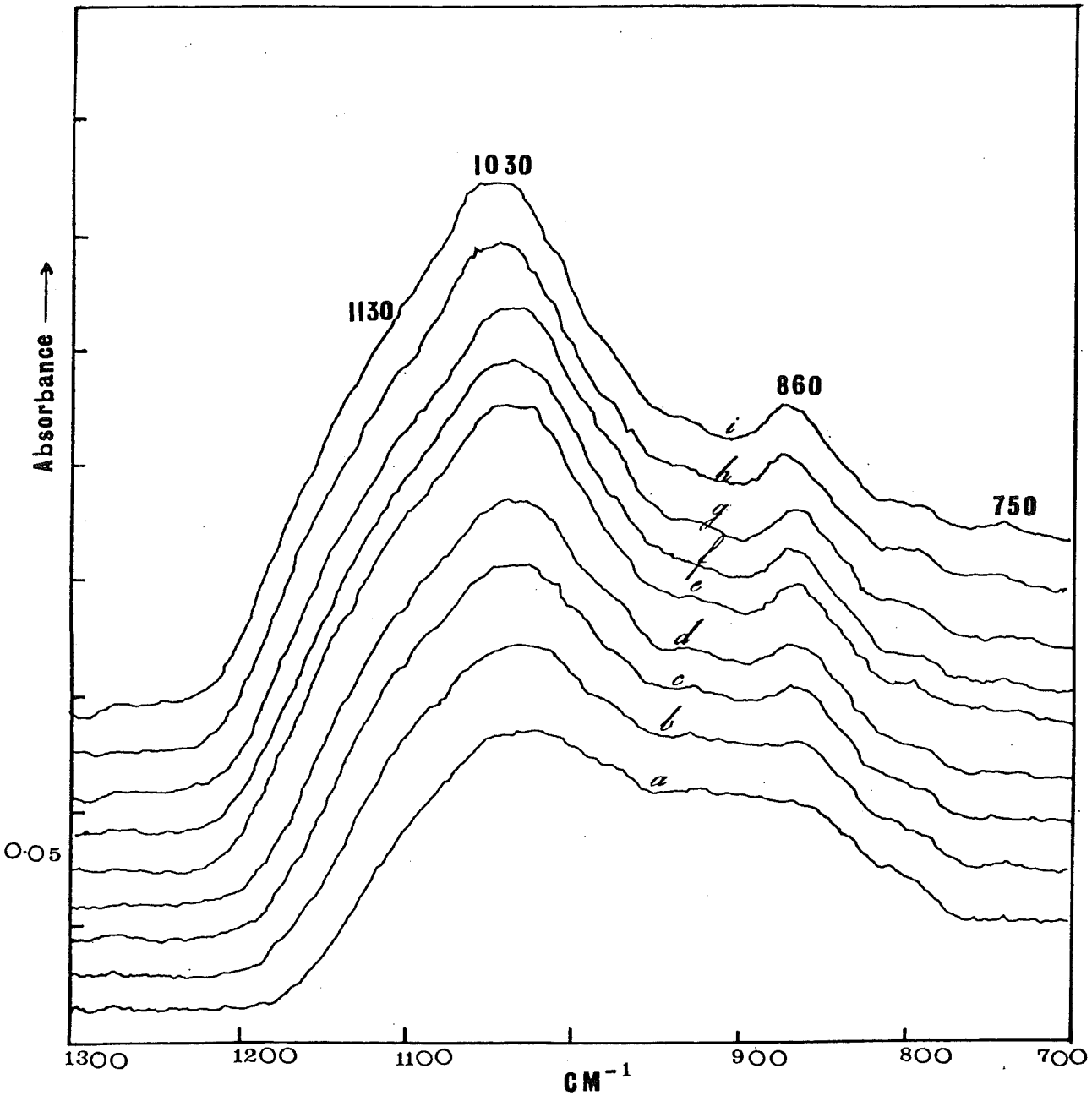

Figure 7.5 Spectra of silicon exposed to dry air at atmospheric pressure (1×10^5 Pa), at 27°C. (a) 2 min; (b) 10 min; (c) 1h; (d) 2h, 20 min; (e) 18h, 20 min; (f) 27h; (g) 49h; (h) 97h; (i) 103h. Ordinates displaced.

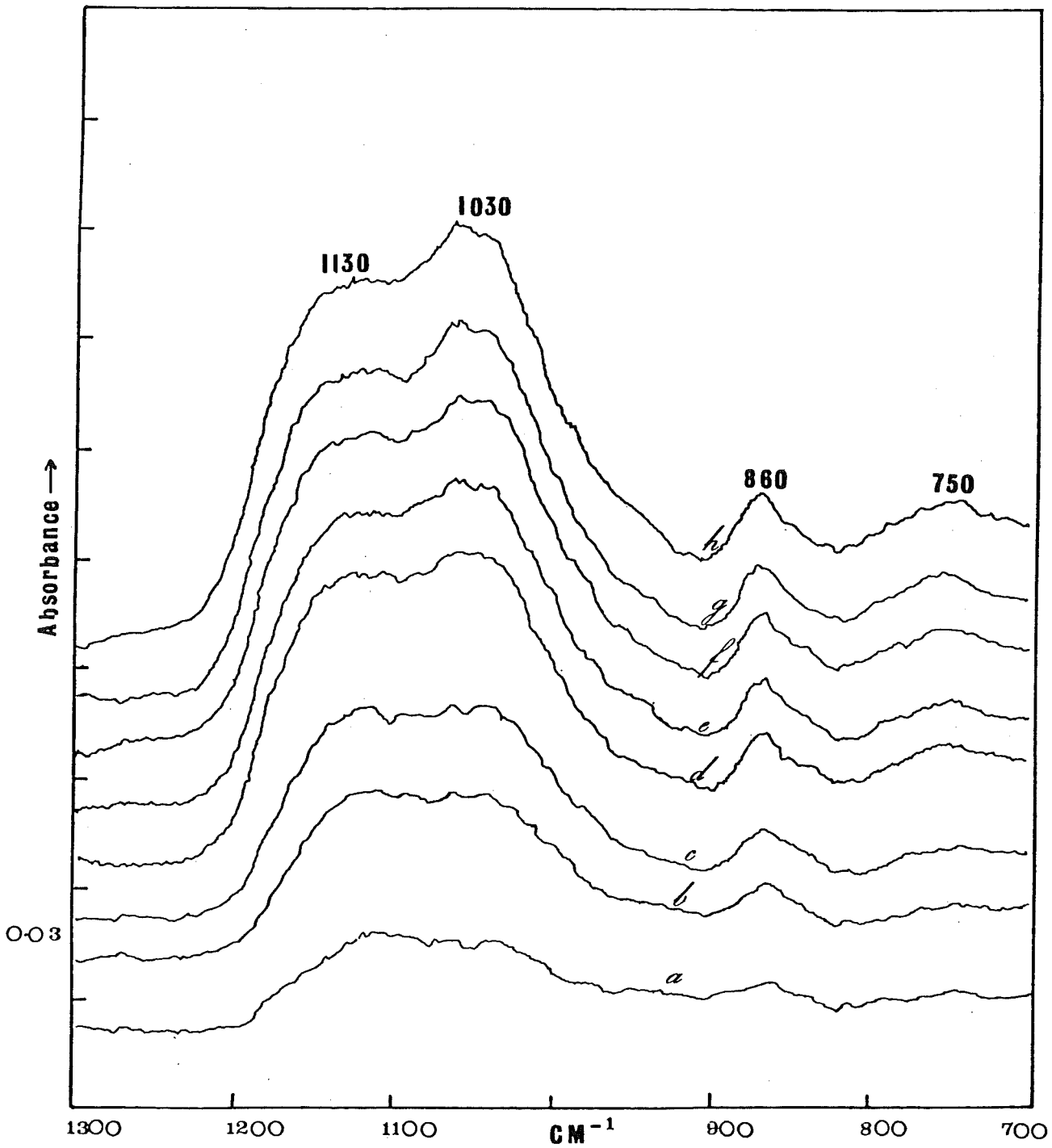

Figure 7.6 Spectra obtained by subtracting the 2 min band in Fig. 7.5 (trace a). (a) 10 min; (b) 1h; (c) 2h, 20 min; (d) 18h, 20 min; (e) 27h; (f) 49h; (g) 97h; (h) 103h. Ordinates displaced.

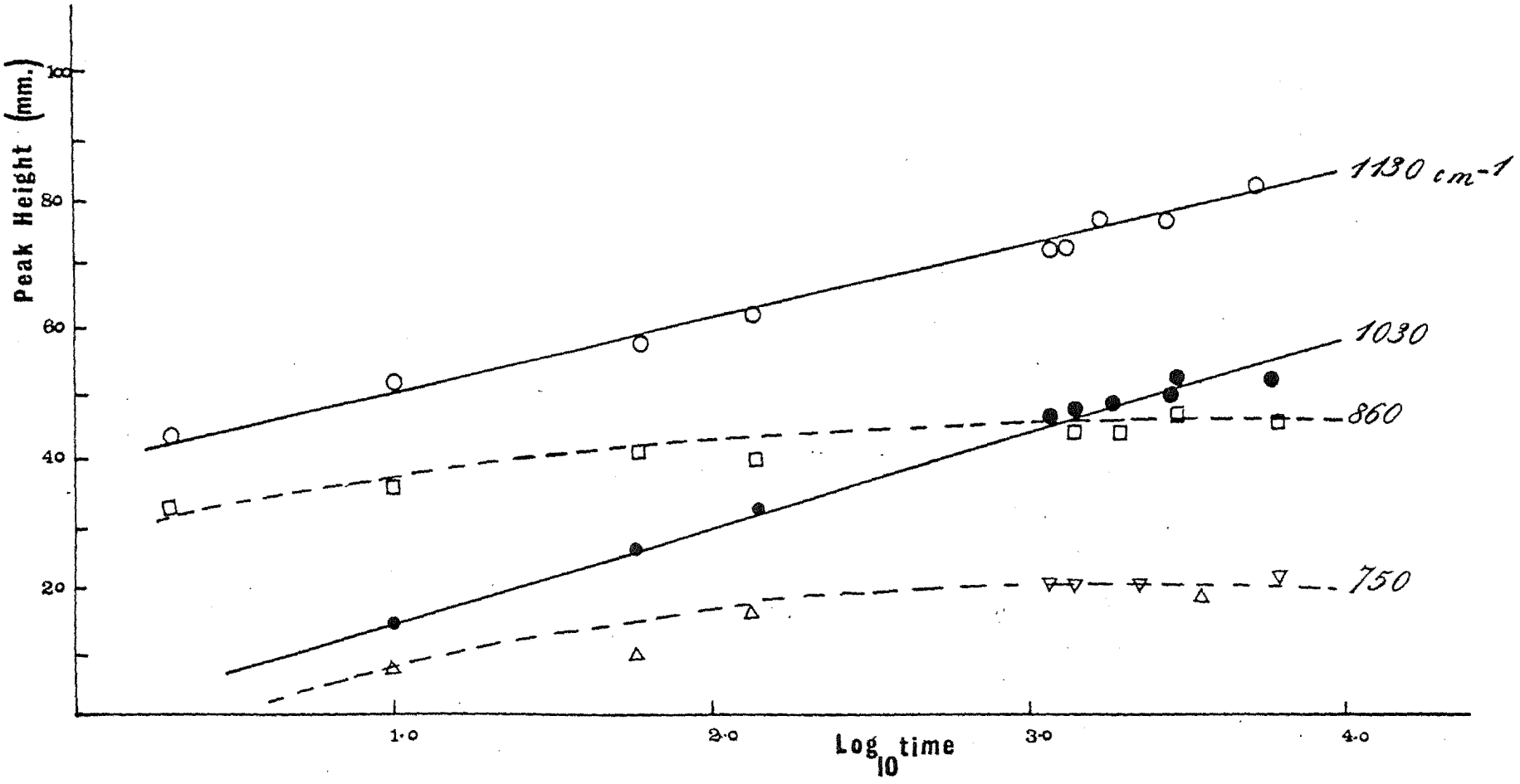
Peak Height (mm.)
100
80
60
40
20
1·0
2·0
3·0
4·0
Log10 time
1130 cm-1
1030
860
750

The bands are seen more clearly if the spectrum obtained at exposures below 13.3 Pa is subtracted from those recorded at higher exposures. This is shown in figure 7.4. It is observed in these spectra that bands positioned at 1130, 1030, 860 and 750 cm^{-1} begin to appear after exposure to oxygen at 1.3×10^4 Pa-min. (100 torr-min.).

7.22 Adsorption at Atmospheric Pressure

Figure 7.5 shows the resulting difference spectra obtained after exposure to dry air of a set of freshly prepared films, after they were allowed to cool to about $27^{o}C$. A strong band centered at around 1030 cm^{-1}, together with an absorption at 860 cm^{-1}, is seen within 2 minutes of exposure. They continue to grow strongly over a period of 100 hours. A shoulder near 1130 cm^{-1} in the band envelope is also apparent after prolonged exposure.

The growth of the bands can be seen more clearly by subtracting the spectrum appearing after 2 minutes exposure from the rest of the spectra. Figure 7.6 shows the growth of the 1130, 1030 and 860 cm^{-1} bands in air at atmospheric pressure. A small absorption is also apparent at around 750 cm^{-1} in the spectra. A shift towards higher frequencies of all the bands is apparent as the exposure increases. This occurs to a greater extent with the 1130 and 1030 cm^{-1} bands (which shift by $> + 20$ cm^{-1}) than with the 860 and 750 cm^{-1} bands (which shift by + 10 cm^{-1}).

The peak heights of the bands are plotted as a function of exposure time in figure 7.7. Both the 1130 and 1030 cm^{-1}

bands appear to grow in a logarithmic manner with time. The 860 and 750 cm^{-1} bands on the other hand show a non-linear growth in the logarithmic plot, and reach maximum intensity between 100-1000 minutes of exposure.

Thus it appears that there are two major stages in the adsorption of oxygen on silicon as indicated by the observed spectra:

a) the appearance of bands at 960 and 770 cm^{-1} which reach their maximum intensity at exposures around 1×10^{-1} Pa-min;

b) the appearance of bands at 1130, 1030, 860 and 750 cm^{-1} at exposures greater than 1.3×10^{4} Pa-min. The first two bands grow in a logarithmic manner on exposure to air at atmospheric pressure, while the latter two seem to reach their maximum intensity between 100-1000 minutes exposure to air at atmospheric pressure.

7.3 Discussion

As both the 960 and 770 cm^{-1} bands reach their maximum intensity at an exposure close to monolayer coverage it is likely that they belong to the same species, saturating at monolayer coverage. Although the 960 cm^{-1} band is not evident in the spectrum until approximately 20 minutes after the appearance of the 770 cm^{-1} band, this may be due to the effect of asymmetrical force fields enhancing or diminishing the intensity of vibrational modes.

Both frequencies are very close to the vibrational frequencies corresponding to the energy losses observed

at 94 and 130 meV (758 and 1049 cm^{-1}) in HRES, by Ibach et al.[19] The two bands observed in this work similarly reach their maximum intensities at an exposure around 10^{-2}-10^{-1} Pa-min.

A band near 980 cm^{-1} observed at very low exposures ($\sim 1.3 \times 10^{4}$ Pa-min.) in the case of germanium films, was assigned by Howe et al.[5] to the O-O stretch of O_2^- ions adsorbed on the surface; no other bands were apparent at these exposures.

It is therefore not unreasonable to assign the two bands to a peroxide-like species of the type suggested by Ibach et al.[19] (see Section 7.1). The absence of a band corresponding to the energy loss at 175 meV (1411 cm^{-1}), which appears as a shoulder in the HRES spectra, is possibly due to the very low intensity of this absorption, resulting from a very small dipole moment associated with the vibration. The energy loss of this vibration is found to be consistently small in several studies using HRES.[185,186]

Any species formed during the very early stages, for example, SiO_3^-, which is thought to saturate at coverages below 0.01 monolayer, cannot be precluded as the concentration of such a species would have been insufficient to give a detectable absorption.

The strong absorptions at 1130 and 1030 cm^{-1}, which show logarithmic growth, are evidently characteristic of oxide growth within the bulk of silicon. By comparison with the absorption bands of various silicon-oxygen species,

summarised in Table 7.1, the pair of bands may be attributed to oxygen dissolved in the lattice of silicon. The configuration of this species is well established;[187] the interstitial oxygen atom is bonded to two adjacent silicon atoms in a non-linear Si-O-Si unit (see 7h below), similar to the silicon-oxygen configuration in quartz[189] and siloxanes.[188]

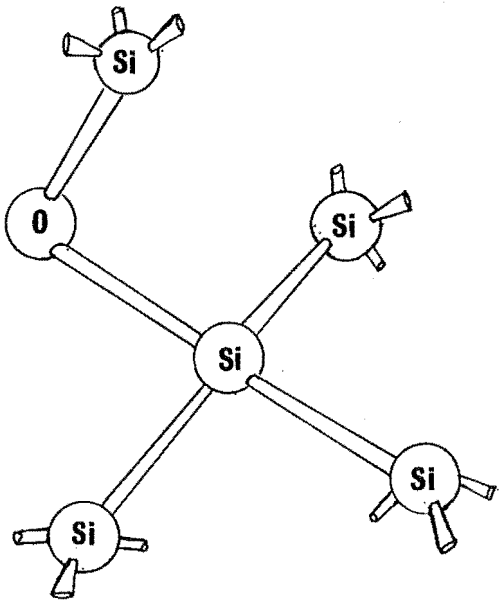

(7h)

The asymmetric stretching vibration of this structure normally occurs at 1106 cm^{-1} and is observed to be the most intense; the symmetric stretch absorbs at 1205 cm^{-1}.[187] The corresponding vibrations in α-quartz are at 1065 and 1162 cm^{-1}.[189] Rakov et al.[190] have found that the frequency of the 1106 cm^{-1} band is shifted to lower frequencies (to about 1080 cm^{-1}) if the thickness of evaporated films of silicon-oxide is reduced substantially. This may explain the much lower frequencies of the two bands at 1130 and 1030 cm^{-1}, as the thickness of the films used in this work is comparable to that of the very thin films used by Rakov et al.[190] for which the frequency lowering was observed.

Table 7.1 Infrared Bands of Silicon-Oxygen Species

Species	Bands (cm^{-1})	References
Si_2O_2 (in N_2 matrix, 15°K)	804,766	(193)
Si_3O_3 (in N_2 matrix, 15°K)	972,631	(193)
O_2 dissolved in Si lattice	1205 (symm. ϑ) 1106 (asymm. ϑ) 515 (δ)	(187)
SiO_2 (in α-Quartz)	1162,1065	(189)
SiO_2 (in α-βCristobalite)	1192, 1085	(189)
O_2 on Silicon (High Resolution Electron Spectroscopy)	1411, 1049 758	(19)
O_2 adsorbed on Si (Peroxide-like species)	960, 780	This Work
O_2 adsorbed on Si (bridge species)	860, 750	This Work
O_2 dissolved in Si	1130, 1030	This Work

The upward shift in frequency (of 10 & 20 cm^{-1}) of both bands, with time, is probably due to film sintering. This is in accord with the observations of Villemant and Kover[191] and Kubota and Kamoshida[192] who found similar shifts in the Si-O band frequencies on heating silicon-oxide crystals.

It seems possible therefore that a structure, similar to that in 7h, is responsible for the pair of bands at 1130 and 1030 cm^{-1}. The logarithmic growth of these bands with time is consistent with the observed logarithmic rate of uptake involving the incorporation of oxygen into the lattice of silicon.

The two bands at 860 and 750 cm^{-1}, which are observed above 1 x 10^4 Pa-min. exposure and show non-logarithmic growth, are possibly due to a species associated with the transition from monolayer adsorption to bulk incorporation. By comparison of the band frequencies with those of polymeric silicon-oxides held in argon or nitrogen matrices[193] (see Table 7.1) it seems reasonable to conclude that these may be due to a silicon-oxygen bridge structure, as below.

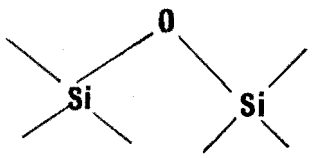

(7i)

It is not possible, however, to say whether bulk incorporation of oxygen is preceeded by the formation of such a species.

CHAPTER EIGHT

SUMMARY AND CONCLUSIONS

Infrared spectroscopy has been used as a tool to elucidate the nature of the adsorbed species on both germanium and silicon surfaces exposed to a variety of gases and vapours. Various mechanistic schemes have also been proposed for the interactions, which show that adsorption is a dynamic process involving not only the adsorbate-adsorbent interface but the bulk and the adsorbed phases as well. The technique, based on that originally developed in the fifties by a number of workers[2,47,48] and improved more recently by Howe,[1] has proved to be versatile as a wide range of adsorbate-adsorbent interactions have been studied in this and in previous investigations. Furthermore, because no strong electrical fields or radiation is involved, adsorption processes could be studied with no constraints placed on the surface, as some of the newer and more sophisticated techniques inevitably require.[12,15,19,194] Infrared spectroscopy does not allow a complete characterisation of surface processes, however, when augmented with date obtained from other techniques it enables a better description of the adsorption processes.

8.1 Summary

a) At room temperature the interaction of water vapour on germanium results in dissociative adsorption, with the formation of Ge-H, Ge-OH and Ge-O groups. No evidence for non-dissociative adsorption of water at monolayer coverage has been found, although this cannot be ruled out as bands due to this species may not have been sufficiently intense

to be detected. The extent of dissociative adsorption cannot be stated catagorically, as correlation of band intensities with the concentration of the adsorbed species was not possible without a knowledge of extinction coefficients. But little doubt exists that dissociation occurred at bare sites as only these have 'free valencies' or 'dangling bonds' necessary for the dissociation of molecules.

The reaction processes which appear to proceed after initial dissociative adsorption are given below.

i) $H_2O_{(ads)} \longrightarrow H_{(ads)} + OH_{(ads)}$

ii) $H_{(ads)} + H_2O_{(ads)} \longrightarrow OH_{(ads)} + H_{2(g)}$

iii) $OH_{(ads)} + OH_{(ads)} \longrightarrow O^-_{(ads)} + \oplus^{v} + H_2O_{(ads)}$

iv) $O^-_{(ads)} \longrightarrow O^{2-}_{(incorporated)} + \oplus^{v}$

The results show that hydrogen production on germanium, at room temperature and at high coverages, occurs through a surface reaction between adsorbed H atoms and water. No evidence was found for surface recombination between pairs of adsorbed H atoms as suggested by Ertl and Giovanelli.[12] The oxidation of the surface appears to be preceded by the formation of Ge-OH groups; direct evidence for this has been obtained. An intermediate stage involving surface hydroxyls provides an explanation for the differences in the thermal desorption peaks observed by Sinharoy and Henzler[15] during surface oxidation of germanium by water vapour and molecular oxygen.

b) Various modes of adsorption are indicated when germanium is exposed to ammonia at room temperature. Dissociative adsorption is evident at the early stages with the formation of Ge-H and Ge-NH_2 groups. Bands due to ammonia co-ordinated to surface atoms and physically adsorbed ammonia have also been tentatively identified. The rapid disappearance of the Ge-H group may have been due to recombination of pairs of H atoms, or alternatively due to further reaction with ammonia. It was not possible to unequivocally decide between the two processes. Adsorption on oxidised surfaces also results in some dissociative adsorption, with the formation of surface hydroxyls instead of Ge-H groups as on the bare surface.

c) A different mode of adsorption to that suggested previously by Bennett and Tompkins,[17] for carbon dioxide adsorption on germanium, is indicated by the results obtained in this work. The initial adsorption is thought to produce a surface complex with the carbon dioxide molecule being adsorbed upright on the surface. Kinetic data, although highly suspect because of the possible variation of extinction coefficients with coverage, is in agreement with the results of Bennett and Tompkins for the pressure dependence of the rate of carbon dioxide uptake by germanium. Some evidence for dissociation of the adsorbed complex is suggested by the appearance of germanium-oxygen bands and a weak band which is probably due to physically adsorbed carbon monoxide.

d) The initial stage of oxygen adsorption on silicon results in two bands which correlate well with the HRES

data reported by Ibach et al.[19] These are identified as belonging to peroxide-like silicon-oxygen species. Oxidation at higher exposures gives rise to two other pairs of bands showing logarithmic and non-logarithmic growth. The species showing logarithmic growth is tentatively identified as belonging to oxygen dissolved in the silicon lattice, while the species showing non-logarithmic growth is possibly due to silicon-oxygen bridge species. The bridge species probably occurs as an intermediate during the transition of the adsorbed oxygen to the bulk phase, although this cannot be confirmed with the obtained results.

8.2 Suggestions for Future Work

a) One of the major drawbacks of infrared spectroscopy, as applied to surface chemistry, is the difficulty in correlating band areas with the concentration of the adsorbed species. This is mainly due to a lack of knowledge of extinction coefficients in many instances. Future studies should be directed towards the preparation of well defined surfaces and the determination of extinction coefficients. This would enable quantitative measurements to be made of surface reactions in progress.

b) Because of the large dead-volume of the apparatus, no quantitative determination of the amount adsorbed can be made using techniques such as gas-volumetry. A feasible method is the measurement of surface conductivity[13] which would give a good estimation of the amount adsorbed from the conductivity changes during adsorption. Since it is evident from the studies in this work that different surface species predominate at different coverages or exposure, it

may be possible to correlate conductivity changes with the individual surface species.

c) It was often found necessary in this work to compare infrared band intensities of samples prepared in separate runs. A more precisely controlled method of film preparation would therefore be preferable if any ambiguities are to be removed. A relatively simple technique that can be incorporated in the existing vacuum-evaporation system would be a calibrated quartz crystal oscillator[46] located near the substrate plates. Film thickness and the rate of deposition can be monitored more accurately with this arrangement; the source temperature and hence the rate of deposition could be controlled automatically by linking the crystal output via a microprocessor to the peripheral electrical equipment.

d) Studies should also be directed towards the determination of electrical parameters characteristic of the prepared films. One such parameter is the semiconductor band gap (or the mobility gap in amorphous materials). This would provide a reference for the comparison of adsorption processes of surfaces prepared or conditioned in different ways (e.g. thermally evaporated films, sputtered films, or vacuum cleaved single crystals). One method that could be modified and adapted to the existing system is described by Lassabatere et al.[195]

e) Further improvement in the vacuum conditions would be beneficial from the point of view of film cleanliness. The use of a more efficient evacuation system such as a turbo-

molecular pump combined with the titanium-sublimation pump would enable a lower vacuum (1.3×10^{-7} - 1.3×10^{-8} Pa or 10^{-9} - 10^{-10} torr range) to be achieved. Surfaces could also be freed from contaminants, at monolayer level, by bombardment with argon ions. A description of this technique, together with an evaluation of its merits, has been given by Farnsworth.[196] Surface conductivity measurements would also be useful in determining the cleanliness of the prepared surfaces since the conductivity changes are well characterised for adsorption of a number of reactive gases.

f) The surface processes associated with the interaction of ammonia with germanium should be further substantiated with deutrated ammonia. The use of labelled carbon dioxide and oxygen would provide further information for confirming the mode of adsorption of carbon dioxide and be of considerable assistance in further elucidating the nature of the silicon-oxygen species.

REFERENCES

1. R.F. Howe, PhD. Thesis, University of Canterbury, 1971.

2. R.P. Eischens, J. Phys. Chem. Solids, 1960, 14, 56.

3. A. Lubezky and M. Folman, Israel J. Chem., 1971, 9, 469.

4. Z. Calahorra and M. Folman, Japan. J. Appl. Phys. Suppl., 1974, 2(2), 307.

5. R.F. Howe, J.P. Liddy and A. Metcalfe, J.C.S. Faraday 1, 1972, 68, 1595.

6. R.F. Howe and A. Metcalfe, J.C.S. Faraday 1, 1972, 68, 393.

7. R.H. Kingston, "Semiconductor Surface Physics", Philadelphia, (Univ. of Pennsylvannia Press, 1957).

8. S.N. Levine, "Principles of Solid-State Microelectronics", (Holt, Pinehart and Winston, 1963).

9. V.M. Frolov et. al., Doklady. Akad. Nauk. SSSR, 1959, 126, 107 (Chem. Abstr. 53; 21612).

10. G.M. Schwab, Reference 7, page 292.

11. R.D. Iyengar and A.C. Zettlemoyer, J. Colloid Sci., 1965, 20, 85.

12. G. Ertl and T. Giovanelli, Ber. Bunsenges. Physik. Chem., 1968, 72, 74.

13. A.H. Boonstra, Philips Res. Rept. Suppl., 1968, 3, 61.

14. M.J. Sparnaay, Ann. N.Y. Acad. Sci., 1963, 101, 973.

15. S. Sinharoy and M. Henzler, Surface Sci., 1975, 51, 75.

16. M.J.D. Low and K. Matsushita, J. Phy. Chem., 1969, 73, 908.

17. M.J. Bennett and F.C. Tompkins, Trans. Faraday Soc., 1962, 58, 820.

18. F. Meyer and J.J. Vrakking, Surface Sci., 1973, 38, 275.

19. H. Ibach, K. Horn, R. Dorn and H. Luth, ibid., 1973, 38, 433.

20. C.N. Banwell, "Fundamentals of Molecular Spectroscopy", (McGraw-Hill, London, 1966), chp 3.

21. L.H. Little, "Infrared Spectra of Adsorbed Species", (Academic Press, 1966), chp. 15.

22. M. Green and K.H. Maxwell, J. Phys. Chem. Solids, 1959, 11, 195.

23. K. Nakamoto, "Infrared Spectra of Inorganic and Coordination Complexes", (Wiley, New York, 1963).

24. L.J. Bellamy, "Infrared Spectra of Complex Molecules", 2nd Edition, (Methven, 1958).

25. Ministry of Aviation, "An Index of Published Infrared Spectra", (London, 1969) vol.1 and 2.

26. R.A. Nyquist and R.O. Kagel, "Infrared Spectra of Inorganic Compounds", (Academic Press, London, 1971).

27. N. Sheppard and D.J.C. Yates, Proc. Roy. Soc.A (London), 1956, 238, 69.

28. A. Metcalfe and S. Ude Shankar, J.C.S. Faraday 1, 1978, 74, 1945.

29. Reference 21, Chapter 15.

30. G. Blyholder, "Experimental Methods in Catalytic Research", (R.B. Anderson Ed., Academic Press, 1968), Chp. 8.

31. R.P. Eischens and W.A. Pliskin, Adv. in Catalysis, 1958, 10, 1.

32. G. Blyholder, J. Phy. Chem., 1964, 68, 2772.

33. J. Peri and R.B. Hannan, J. Phy. Chem., 1960, 64, 1526.

34. L. Holland, "Vacuum Deposition of Thin Films", (Chapman and Hall, 1956) Chp 2.

35. L. Holland, W. Steckelmacher and J. Yarwood, "Vacuum Manual", (Spon, London, 1974).

36. A. K. Gupta and J.H. Leck, Vacuum, 1975, 25, 362.

37. R.W. Lawson and J.W. Woodward, ibid, 1967, 17, 205.

38. W.J. Potts and A.L. Smith, Appl. Optics, 1967, 6, 257.

39. Perkin-Elmer Instructions Manual (421), 1961.

40. G. Blyholder, Proc. 3rd. Int. Congr. on Catalysis, 1964, July (North-Holland, Amsterdam).

41. Reference 34, page 489.

42. R.W. Roberts and T.A. Vanderslice, "Ultrahigh Vacuum and its Applications", (Prentice-Hall, Englewood Cliffs, 1963).

43. J.W. Swaine and R.C. Plumb, J. Appl. Phys., 1962, 33, 2378.

44. D.K. Pandya, A.C. Rastogi and K.L. Chopra, J. Appl. Phys., 1975, 46, 2966.

45. O.S. Heavens, "Optical Properties of Thin Solid Films", (Butterworths, 1955).

46. Juh Tzeng Lue, J. Phys. E : Sci. Instr., 1977, 10, 161.

47. A.M. Bradshaw and J. Pritchard, Surface Sci., 1970, 19, 198.

48. N.C. Peterson, R.R. Bauman and I.W. Price, Rev. Sci. Instr., 1966, 37, 1316.

49. W. Fuhs, H.J. Hesse and K.H. Langer, Proc. 5th Int. Conf. Amorphous and Liquid Semic., Garmisch-Partenkirchen, Germany, (Taylor and Francis, London, 1974), p.79.

50. A. Barna et.al., ibid., p.109.

51. M.K. Knotek, M. Pollak and T.M. Donovan, ibid., p.225.

52. P.G. LeComber, R.J. Loveland, W.E. Spear and R.A. Vaughan, ibid., p.245.

53. W.E. Spicer, ibid., p.479.

54. G.A.N. Connell, W. Paul and R.J. Temkin, ibid., p.541.

55. T.M. Donovan, M.L. Knotek and J.E. Fischer, ibid., p.549.

56. N.J. Shevchick and W. Paul, J. non-Cryst. Solids, 1972, 8-10, 381.

57. J. Tauc, A. Abraham, R. Zallen and M. Slade, J. non-Cryst. Solids, 1970, 4, 279.

58. M.L. Theye , reference 49, p.483.

59. Idem., Opt. Commun., 1970, 2, 329.

60. H. Goebel, K. Dettmer and F.R. Kessler, Phys. Status Solidi A, 1973, 16, 61.

61. P.S. Walley, Thin Solid Films, 1968, 2, 327.

62. S. Koc, O. Renner, M. Zavetova and J. Zemek, Czech. J. Phys. B, 1972, 22, 1296 (Chem. Abstr. 78: 64088c).

63. A. Barna, P.B. Barna and J.F. Pocza, J. non-Cryst. Solids, 1972, 8-10, 36.

64. R. Bauer and F.L. Galeener, Solid State Commun., 1972, 10, 1171.

65. S.K. Barthwal, P. Nath and K.L. Chopra, ibid., 1975, 16, 723.

66. M.L. Theye, Mater. Res. Bull., 1971, 6, 103.

67. M.J. Bennett and F.C. Tompkins, Proc. Roy. Soc.A, 1960, 259, 28.

68. W. Paul, G.A.N. Connell and R.J. Temkin, Adv. in Phys., 1973, 22, 531.

69. J. Parsons and R. Ballufi, J. Phys. Chem. Solids, 1964, 25, 263.

70. Reference 45, Chp. 3.

71. R.L. Mozzi and B.E. Warren, J. appl. Crystallogr., 1969, 2, 164.

72. J.H. Konnert and J. Karle, Acta. Crystallogr. A, 1972, 29, 702.

73. D.E. Polk, J. non-Cryst. Solids, 1971, 5, 365.

74. Idem., ibid., 1972, 8, 359.

75. P. Chaudhari, J.F. Graczyk and S.R. Herd, Phys. Stat. Solidi B, 1972, 51, 801.

76. J.F. Graczyk and P. Chaudhari, ibid., 1973, 58, 163.

77. P. Chaudhari, J.F. Graczyk, D. Henderson and P. Steinhardt, Phil. Mag., 1975, 31, 727.

78. P. Chaudhari and J.F. Graczyk, reference 49, p.59.

79. D. Henderson and F. Herman, J. non-Cryst. Solids, 1972, 8-10, 359.

80. D.E. Poll and D.S. Bourdeaux, Phy. Rev. Lett., 1973, 31, 92.

81. T.M. Donovan and K. Heinemann, ibid., 1971, 27, 1794.

82. R. Grigorovici, Mater. Res. Bull., 1968, 3, 13.

83. K. Grigorovici and R. Manaila, Nature, 1970, 226, 143.

84. T.B. Light and C.N. Wagner, J. appl. Crystallogr., 1968, 1, 199.

85. A. Howie, O. Krivanek and M.L. Rudee, Phil. Mag., 1973, 27, 235.

86. M.L. Rudee and A. Howie, ibid., 1972, 25, 1001.

87. F.C. Weinstein and E.A. Davis, J. non-Cryst., Solids, 1973/74, 13, 153.

88. M.H. Brodsky and R.S. Title, Phy. Rev. Lett., 1969, 23, 581.

89. M.H. Brodsky, R.S. Title, K. Weisser and G.D. Pettit, Phy. Rev. B, 1970, 1, 2632.

90. P.H. Gaskell, Phil. Mag., 1975, 32, 211.

91. A.H. Clark, Phy. Rev., 1967, 154, 750.

92. O. Renner, Thin Solid Films, 1972, 12, 543.

93. M.L. Theye, reference 49, p.479.

94. R. Grigorovici and A. Vancu, Thin Solid Films, 1968, 2, 105.

95. K.L. Chopra and D.K. Pandya, reference 49, p.1141.

96. K.L. Chpora and S.K. Bahl, Phy. Rev. B, 1970, 1, 2545.

97. T.M. Donovan, W.E. Spicer, J.M. Bennett and E.J. Ashley, Phy. Rev. B, 1970, 2, 397.

98. A.H. Clarke, Phy. Rev., 1967, 154, 750.

99. S.K. Bahl, S.M. Bhagat and R. Glosser, reference 49, p.69.

100. Idem., Solid State Commun., 1973, 13, 1159.

101. J.E. Davey, Solid-State Electron., 1963, 6, 205.

102. G.A. Bootsma and F. Meyer, Surface Sci., 1969, 14, 52.

103. M. Green, Progr. in Semiconductors, 1960, 4, 35.

104. S. Dushman, "Scientific Foundations of Vacuum Technique", (John Wiley, New York, 1949).

105. M. Green and K.H. Maxwell, J. Phys. Chem. Solids, 1959, 11, 195.

106. W. Shockley, Phy. Rev., 1939, 56, 317.

107. J. Bardeen, ibid., 1947, 71, 717.

108. A.C. Zettlemoyer and R.D. Iyengar, "The Solid-Gas Interface", (E.A. Flood, Ed., Dekker, 1967), chp. 26.

109. A. Many, Y. Goldstein and R.B. Grover, "Semiconductor Surfaces", (North-Holland, 1965).

110. J.P. McKelvey, "Solid State and Semiconductor Physics", (Harper Int., 1966), p. 488.

111. M. Lasser et.al., reference 7, p.181.

112. W. Shockley and G.L. Pearson, Phy. Rev., 1948, 74, 223.

113. W.E. Spear, Adv. in Physics, 1977, 26, 811.

114. Idem., reference 49, p.1.

115. M.H. Cohen, Physics Today, 1971, May, 26.

116. J. Tauc, ibid., 1976, October, 23.

117. P.W. Anderson, Phy. Rev. Lett., 1975, 34, 953.

118. N.F. Mott, E.A. Davis and R.A. Street, Phil. Mag., 1975, 32, 961.

119. D. Weaire, Phy. Rev. Lett., 1971, 26, 1541.

120. W.E. Spicer and T.M. Donovan, Proc. 10th Int. Conf. Phys. of Semiconductors, Cambridge-Massachusettes (USAEC div. Tech. Inf.).

121. N.F. Mott, Phil. Mag., 1969, 18, 835.

122. G. Srinivasan, J.J. Chessick and A.C. Zettlemoyer, J. Phys. Chem., 1962, 66, 1819.

123. V. Pravdic, E. McCafferty and A.C. Zettlemoyer, Surface Sci., 1967, 7, 380.

124. J.T. Law, J. Phys. Chem., 1955, 59, 67.

125. M.J. Sparnaay and J. van Ruler, Physica, 1961, 27, 153.

126. A.H. Boonstra and J. van Ruler, Surface Sci., 1966, 4, 141.

127. F. Meyer, ibid., 1971, 27, 107.

128. M.J.D. Low, N. Madison and P. Ramamurthy, ibid., 1969, 13, 238.

129. A.V. Rzhanov and M.P. Sinyukov, (Chemical Abstr. 69: 31653u and 31654u).

130. K.H. Beckmann, Surface Sci., 1966, 5, 187.

131. R. Mathis, M. Barthelat and F. Mathis, Spectrochim. Acta. (Part A), 1970, 26, 1993.

132. R.S. Tobias and S. Hutcheson, J. Organometal. Chem., 1966, 6, 535.

133. G.P. Stavistkaya and Ya I. Ryskin, Optika i Spektro., 1961, 10, 343.

134. E. Borello, A. Zecchina and C. Morterra, J. Phys. Chem., 1967, 71, 2938.

135. K. Tamaru, ibid., 1957, 61, 647.

136. J.H. de Boer, "The Dynamical Character of Adsorption", (Oxford Univ. Press, London, 1953).

137. K.H. Maxwell and M. Green, J. Phys. Chem. Solids, 1960, 14, 94.

138. H. Imai and C. Kemball, Proc. Roy. Soc. A, 1968, 302, 399.

139. R. Surhmann, J.M. Heras, L.V. Heras and G. Wedler, Ber. Bunsenges. Physik. Chem., 1964, 68, 511.

140. Idem., ibid., 1968, 72, 854.

141. Chemical Rubber Co. "Handbook of Chemistry and Physics", 52nd edtn. 1972-73.

142, G. Janos, W. Maria and D. Otto, Acta Chim. (Budapest), 1972, 72, 393.

143. A.J.B. Robertson and E.M.A. Willhoft, Tran. Faraday Soc., 1967, 63, 476.

144. C. Kemball, Adv. in Catalysis, 1959, 11, 223.

145. M. Wahba and C. Kemball, Tran. Faraday Soc., 1953, 49, 1351.

146. J.R. Anderson, "Chemisorption and Reactions on Mettalic Films". Vo. 2 (Academic Press, London, 1971).

147. C.E. Melton and P.H. Emmett, J. Phys. Chem., 1964, 68, 3318.

148. B.Z. Ol'Shanetskii and A.I. Volokitin, Chemical Abstr., 1974, 80: 53172r.

149. M.J. Sparnaay, A.H. Boonstra and J. van Ruler, Surface Sci., 1964, 2, 56.

150. M.J.D. Low, N. Ramasubramanian and V.V. Subba Rao, J. Phys. Chem., 1967, 71, 1726.

151. N.W. Cant and L.H. Little, Can. J. Chem., 1964, 42, 802.

152. G.A. Blomfield and L.H. Little, J. Catalysis, 1971, 21, 149.

153. N.W. Cant and L.H. Little, Can. J. Chem., 1968, 46, 1373.

154. Reference 21, page 185.

155. V.N. Abramov, A.V. Kiselev and V.I. Lygin, Russ. J. Phys. Chem., 1964, 38, 1020.

156. J.J. Lander and J. Morrison, J. Appl. Phys., 1963, 34, 1403.

157. S.N. Kozlov et.al., Chemical Abstr., 72; 136722f.

158. A.H. Boonstra, J. van Ruler and M.J. Sparnaay, Koninkl, Ned. Akad. Wetenschap. Proc. Ser.B, 1963, 66, 64.

159. R.P. Eischens and W.A. Phiskin, Adv. in Catalysis, 1957, 9, 662.

160. Idem., 2nd. Int. Congr. Catalysis, 1960.

161. J.T. Law, J. Phys. Chem., 1955, 59, 543.

162. G. Herzberg, "Infrared and Raman Spectra of Polyatomic Molecules", (Van Nostrand, New York, 1945).

163. Reference 21, page 77.

164. M.P . Brown, R. Okawara and E.G. Rochow, Spectrochim. Acta., 1960, 16, 595.

165. T.N. Srivastava and M. Onyszchuck, Can. J. Chem., 1963, 41, 1244.

166. J.C. Phillips, "Bonds and Bands in Semiconductors", (Academic Press, New York, 1973) Chp.2.

167. B.M.W. Trapnell, Proc.Roy.Soc.A, 1953, 218, 562.

168. M. Green and K.H. Maxwell, J. Phys. Chem. Solids, 1960, 13, 145.

169. J.T. Law, ibid., 1958, 4, 91.

170. M. Green and J.A. Kafalas, Phy. Rev., 1965, 98, 1566.

171. C.A. Carosella and J. Comas, Surface Sci., 1969, 15, 303.

172. R.E. Schlier and H.E. Farnsworth, J. Chem. Phys., 1959, 30, 917.

173. S.P. Wolsky, J. Phys. Chem. Solids, 1959, 8, 114.

174. F. Meyer and J.J. Vrakking, Surface Sci., 1973, 38, 275.

175. G.W. Gobeli and F.G. Allen, J. Phys. Chem. Solids, 1960, 14, 23.

176. D. Brennan, D.O. Hayward and B.M.W. Trapnell, ibid., 1960, 14, 117.

177. M. Green, Ann. N.Y. Acad. Sci., 1963, 101, 1001.

178. M. Green and A. Liberman, J. Phy. Chem. Solids, 1962, 23, 1407.

179. H. Ibach and J.E. Rowe, Phys. Rev. B, 1974, 9, 1951.

180. A. Benninghoven and S. Storp, Appl. Phys. Lett., 1973, 22, 170.

181. R. Dorn, H. Luth and H. Ibach, Surface Sci., 1974, 42, 583.

182. J.R. Ligenza and W.G. Spitzer, J. Phy. Chem. Solids, 1960, 14, 131.

183. N. Cabrera, reference 7, page 327.

184. M.A. Lanyon and B.M.W. Trapnell, Proc. Roy. Soc. (London) A, 1954, 227, 387.

185. H. Ibach, J. Vacuum Sci. Technol., 1972, 9, 713.

186. Idem., Phy. Rev. Lett., 1971, 27, 253.

187. H.J. Hrostowski and R.H. Kaiser, Phy. Rev., 1957, 107, 966.

188, R.E. Richards and H.W. Thompson, J. Chem. Soc., 1949, 124.

189. I. Simon and H.O. McMahon, J. Chem. Phys, 1953, 21, 23.

190. A.V. Rakov, E.V. Potapov and L.P. Mizgireva, Optika i Spektroskopia (Eng), 1968, 25, 59.

191. C. Villemant and F. Kover, Rev. Appl. Phys. (French), 1966, 1, 90 (Chemical Abstr., 66: 6746r)

192. T. Kubota and M. Kamoshida, Japan, J. Appl. Phys., 1972, 11, 15.

193. J.S. Anderson and J.S. Ogden, J. Chem. Phys., 1969, 51, 4189.

194. P.J. Estrup, Physics Today, 1975, April, 33.

195. L. Lassabatere, C. Alibert, J. Bonnet and L. Soonckindt, J. Phys. E : Sci. Instr., 1976, 9, 773.

196. H.E. Farnsworth, "The Solid-Gas Interface", vol.1. (E.A. Flood Ed., Dekker, 1967) chp.13.

APPENDIX 1 Magnetic Tape Code

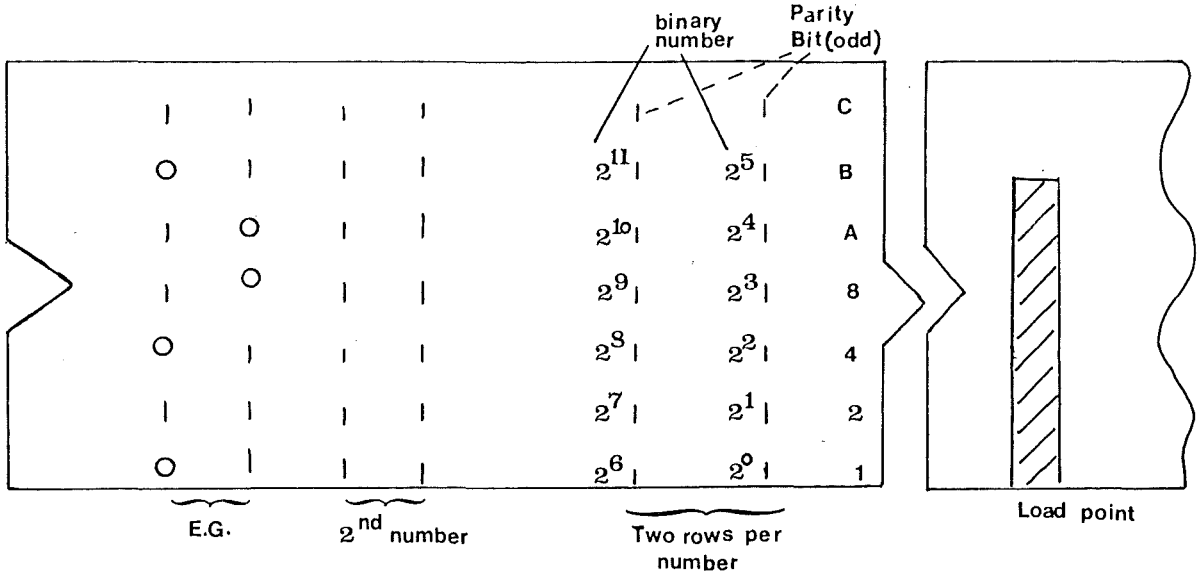

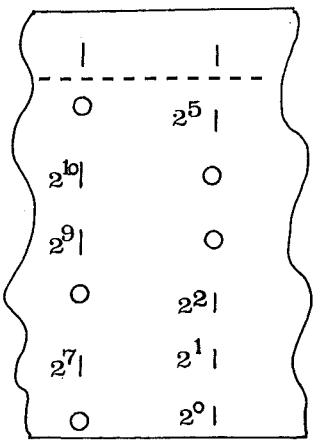

BINARY	DECIMAL
2^0	1
2^1	2
2^2	4
2^5	32
2^7	128
2^9	512
2^{10}	2048
	2727

100% transmittance = 10.00v = 4095 (i.e. $\sum_{n=0}^{11} 2^n$)

$\therefore$ 2727 would correspond to a voltage

of $\frac{2727}{4095} \times 10.00 = 6.66$v

or a transmittance of 66.6%.

APPENDIX 2 Computer Programmes

In the following pages, a full listing of the computer programmes, viz. ALGOLSUBS, MAIN PROGRAM IRSPEC (known as TRIAL) and SUBROUTINE PLOTS, is given.

To process the data on magnetic tape, the tape is handed in with the program deck. Up to 79 spectra may be handled if the background spectrum is the same. The background is usually recorded as the first file on the tape. The data on tape is read in with the aid of program ALGOLSUBS and processed as per instructions given in IRSPEC. The difference spectra are then plotted directly with the aid of SUBROUTINE PLOTS.

The difference spectra are obtained as follows;

1) Background file is read, translated and stored in accumulating array SPECTRUMACCUM.
2) Spectrum file is read and translated. The numbers are subtracted from the corresponding background values and stored in SPECTRUMACCUM.
3) The difference spectrum obtained is then plotted by a Calcomp x-y plotter.
4) If more than 1 spectrum is processed, the difference spectra are all stored automatically before being finally plotted.

CARD DECK :

```
?  USER CHEM 166/
   password

?  CLASS = 6
?  COMPLIE ALGOLSUBS ALGOL LIBRARY
?  DATA
$  LEVEL 3

      (ALGOLSUBS DECK)

?  COMPILE TRIAL FORTRAN LIBRARY GO
?  DATA
$  SET AUTOBIND
$  BIND = FROM ALGOLSUBS
$  BIND STOREY FROM STOREY
$  BIND YVAL FROM YVAL
$  BIND READF FROM READF
$  BIND = PLOTA/-

      (MAIN PROGRAM IRSPEC DECK)
 and (SUBROUTINE PLOTS DECK)

?  DATA FILES

       (DATA DECK)

?  END JOB
```

BURROUGHS B6700 ALGOL COMPILER, VERSION 2.9.190, TUESDAY, 09/12/7

A L G O L S U B S
= = = = = = = = =

```
[DEFINE BUFLENGTH=4500 #;
  DEFINE SCALEF=100000#;
  LONG ARRAY SPECTRUMACCUM[0:2*BUFLENGTH];
    DIRECT FILE TAPEFILE;
  DIRECT ARRAY BUF[0:BUFLENGTH];
COMMENT
      4 * BUFLENGTH    = MAX NUMBER OF  12 BIT  OBSERVATIONS

          LOG(10) OF SCALEF IS THE NUMBER OF SIGNIFICANT DECIMAL
              PLACES WHICH WILL BE STORED IN THE ACCUMULATING ARRAY.
              NOTE THAT  THE ACCUMULATED NUMBER WHEN MULTIPLIED BY THIS
              SCALEF MUST NOT EXCEED 8,000,000 OR IT WILL OVERFLOW
              AND BECOME NEGATIVE.

      FOR AN INDEX X INTO THE STORED ARRAY THE FOLLOWING ACCESS CALLS
      CAN BE MADE FROM FORTRAN:

      CALL STOREY(X,Y)
                          STORES THE VALUE Y INTO THE LOCATION X

      Y=YVAL(X)
                      RETRIEVES THE VALUE FROM THE LOCATION X

    THE PROCEDURE READF  READS A TAPE FILE  AND  ACCUMULATES THE
   INFORMATION INTO THE STORAGE ARRAY AS REQUIRED BY THE FIRST PARAMETER
  AS SHOWN IN THE FOLLOWING EXAMPLES:

      CALL READF(0,NPOINTS,IFLAG)   - SPACES PAST A FILE
      CALL READF(1,NPOINTS,IFLAG)   ADD THIS FILES VALUES TO ACCUM
      CALL READF(2,NPOINTS,IFLAG)   SUBTRACT THIS FILES VALUES FROM ACCUM
      CALL READF(3,NPOINTS,IFLAG) REWINDS TAPE

 END OF COMMENT;]
PROCEDURE STOREY(X,Y);
VALUE X,Y;
REAL X,Y;
  BEGIN

  Y:=INTEGER(Y*SCALEF);
  SPECTRUMACCUM[X DIV 2].[24*(X MOD 2)+23:24]:=Y.[22:23] & Y[23:46:1];
  END;


REAL PROCEDURE YVAL(X);
VALUE X;
REAL X;
BEGIN

  REAL Y;
  Y:=SPECTRUMACCUM[X DIV 2].[24*(X MOD 2)+23:24];
  YVAL:=(Y.[22:23]& Y[46:23:1])/SCALEF;
  END;
```

```
PROCEDURE READF(HOW,NPOINTS,EFLAG);
VALUE HOW;
REAL HOW,NPOINTS,EFLAG;
BEGIN

  OWN BOOLEAN INITIALIZED,EOTAPE;
  REAL LENGTH,XINDEX,VAL,LBIT;
  REAL OLDVAL;
  POINTER PBUF;
  BOOLEAN B;
  LABEL XIT;
  IF NOT INITIALIZED THEN
  BEGIN
        TAPEFILE(KIND=TAPE,LABELTYPE=OMITTEDEOF,DENSITY=1,
      TITLE="ULTAPE.", TRANSLATE=NOTRANS,
      PARITY=0,MAXRECSIZE=4500,MYUSE=IN,EXTMODE=BCL,INTMODE=BCL);

    BUF.IOMASK:=0&25[11:5]; %INHIBIT PARITY RETRY ACTION
    INITIALIZED:=TRUE;
    TAPEFILE.OPEN:=TRUE;
    READ(TAPEFILE,BUFLENGTH,BUF);
  END;
  IF  NOT EOTAPE THEN
  BEGIN
    B:=WAIT(BUF);
    IF BUF.IOEOF THEN EOTAPE:=TRUE;
  END;
   IF HOW EQL 3 THEN
    BEGIN
     REWIND(TAPEFILE);
     REPLACE POINTER (SPECTRUMACCUM) BY 48"00" FOR 2*BUFLENGTH+1 WORDS;
     GO XIT;
    END;
  IF EOTAPE THEN
    BEGIN
      EFLAG:=3;       % END OF TAPE
      GO XIT;
    END;
  IF HOW EQL 0 THEN
  BEGIN       % JUST SPACE PAST THIS FILE
    BUF.IOCW:=0&3[44:2]    %  READ , MEMINHIBIT
            &11[33:4];  %  556 BPI , ODD PARITY
    WHILE NOT BUF.IOEOF DO BEGIN
        READ(TAPEFILE,BUFLENGTH,BUF); WAIT(BUF); END;
    BUF.IOCW:=0;
    GO XIT;
  END;
  DO BEGIN       % READ THE FILE
    LENGTH:=(BUF.IOCHARACTERS)DIV 2;
    LENGTH:=MIN(LENGTH,4*BUFLENGTH-XINDEX);
    IF B THEN EFLAG:=2;       % PARITY ERROR
    PBUF:= POINTER(BUF,6);

    THRU LENGTH DO BEGIN
      IF BOOLEAN(XINDEX) THEN LBIT:=47 ELSE LBIT:=23;
    VAL:=SPECTRUMACCUM[XINDEX,[14:14]].[LBIT:24];
    OLDVAL:=VAL.[22:23]&VAL[46:23:1];
    VAL:=REAL(PBUF,2);
    IF VAL NEQ 0 THEN
    VAL:=INTEGER(LOG(VAL.[11:6]&VAL[11:5:6])*SCALEF);
%     IF HOW EQL 1 THEN VAL:=VAL;      % GOT A BACKGROUND
      IF HOW EQL 2 THEN VAL:=-VAL;    % GOT A SPECTRUM
      VAL:=VAL+OLDVAL;
      SPECTRUMACCUM[XINDEX.[14:14]].[LBIT:24] :=VAL & VAL[23:46:1];
      PBUF:=PBUF + 2;
      XINDEX:= * + 1;
    END OF POINTS IN BLOCK;
    READ(TAPEFILE,BUFLENGTH,BUF);
    B:=WAIT(BUF);
  END UNTIL BUF.IOEOF;
  NPOINTS:= XINDEX;
XIT:
  IF EOTAPE THEN
  BEGIN
    CLOSE(TAPEFILE);
    DEALLOCATE(BUF);
  END ELSE
  BEGIN
    CLOSE(TAPEFILE,*);
    READ(TAPEFILE,BUFLENGTH,BUF);
  END;
   END OF READF.
```

```
B6700  F O R T R A N  C O M P I L A T I O N  M A R K
                                                T R I A L
                                                = = = = =

C                 ************************
C                 * MAIN PROGRAM IRSPEC *
C                 ************************
C
C
C     THIS PROGRAM CALLS SUBROUTINE READF TO READ TAPE AND OBTAIN
C          THE DIFFERENCE BETWEEN BACKGROUND AND SPECTRUM SCANS.
C          RESULTING DIFFERENCE IS THEN PLOTTED BY CALLING SUBROUTINE
C          PLOTS.
C
C
      COMMON INSTR(80),ILABEL(12),JLABEL(12),Y(1100)
C     INPUT DATA
C     CARD 1 : SF=(COLUMN 1-6) SETS THE VALUE OF EACH SCALE DIVISION
C          ON THE Y AXIS(SEE SFACT BELOW), EG. IF SF=715. THEN
C          EACH DIV. IS 0.05 ABSORBANCE UNITS).
C
C     CARD 2 :NSPK= (COLUMN 1) CHOOSES A SPECTRAL RANGE FOR A
C          PARTICULAR PLOT. EG. NSPK=1  RANGE = 4000-3000 CM-1
C                               =2            = 3000-2000 CM-1
C                               =3            = 2000-1000 CM-1
C                               =4            = 1000-600 CM-1
C
C     CARDS 3 AND 4 : DESCRIPTION OF SPECTRUM UP TO 72 ALPHAMERIC
C          CHARACTERS EACH.
C
C     CARD 5 :NFILES =(COLUMNS 1-3) TOTAL NUMBER OF FILES TO BE
C          PROCESSED, I.E. THE MAXIMUM NUMBER OF FILES TO BE
C          SCANNED SEQUENTIALLY ENDING AT THE FILE REQUIRED PLUS
C          ONE (FOR REWINDING PURPOSES). EG. IF BACKGROUND IS ON
C          FILE 1, SPECTRUM REQUIRED ON FILE 7 THEN NFILES=7+1=8.
C               NDIV =(COLUMNS 3-6). IF MULTIPLE SCANNING USED THEN
C          AVERAGE VALUE OBTAINED BY DIVIDING BY THIS INTEGER. IF
C          ONLY ONE SCAN PER SPECTRUM THEN NDIV=1.
C
C     CARD 6 : INSTR= (COLUMNS 1-80) FOR OBTAINING A DIFFERENCE
C          SPECTRUM PUNCH 0 OR BLANK IN COLUMNS CORRESPONDING
C          TO THE FILES NOT REQUIRED, 1 IN THE COLUMN CORRESPONDING TO
C          THE BACKGROUND FILE, 2 IN THE COLUMN CORRESPONDING TO
C          THE FILE REQUIRED AND 3 IN THE COLUMN FOLLOWING THE
C     LAST ONE (TO REWIND TAPE). AN UPPER LIMIT OF 79 IS PLACED
C          ON THE NUMBER OF FILES ON EACH TAPE.
C
C     CARD 7 : ID =(COLUMN 1) FOR PLOTTING SEVERAL SPECTRA ON THE
C          SAME BOX ID=0 FOR THE FIRST PLOT, ID=1 FOR ALL
C          SUCCESSIVE PLOTS AND ID=2 FOR THE LAST PLOT.
C
C     CARD 8 :  INIT= (COLUMNS1-2) FILE NUMBER OF BACKGROUND.
C               IFIN =(COLUMNS2-4) FILE NUMBER OF THE SPECTRUM.
C
C     NOTE : INPUT DATA FOR CARDS 1-8 REQUIRED FOR THE FIRST PLOT,
C          FOR ALL SUCCESSIVE PLOTS ON THE SAME BOX DATA
C          REQUIRED FOR CARDS 4-8 ONLY.
C
   17 READ(5,8,END=900) SF
      SY=0.0
      READ(5,9) NSPK
      READ(5,50) ILABEL
      READ(5,50) JLABEL
    7 READ(5,1) NFILES,NDIV
      READ(5,2) INSTR
      READ(5,6)ID
      READ(5,55) INIT,IFIN
C
C
      NMIN=0
      DO 20 IFILE=1,NFILES
      IF(INSTR(IFILE).EQ.3) GO TO 79
   89 CALL READF(INSTR(IFILE),NP,IFLAG)
      IF(INSTR(IFILE) .EQ. 3) GO TO 20
      IF(NMIN.EQ.0) NMIN=NP
```

```
      IF(NP.LT.NMIN) NMIN=NP
      IF (IFLAG.EQ.3) GO TO 10
      IF(INSTR(IFILE).GT.0) GO TO 70
      IF(INSTR(IFILE).EQ.0) GO TO 20
   70 WRITE(6,60) INIT,IFIN

   20   CONTINUE
   10   CONTINUE
      IF(ID.EQ.2) GO TO 17
      GO TO 7
C
C
   79 L=NMIN/5
      DO 300 J=1,L
      Y(J)=YVAL(5*J)/NDIV
  300 CONTINUE
C
C
  302 CALL PLOTS(Y,L,ILABEL,JLABEL,SF,NSPK,ID,SY)
C
      SY=SY+150.
      SFACT=(SF*0.7)/10000.
      WRITE(6,69)SFACT
      WRITE(6,59)L
      WRITE(6,82)
      GO TO 89
  900 STOP
    1 FORMAT(213)
    2 FORMAT(80I1)
    6 FORMAT(I1)
    8 FORMAT(F6.1)
    9 FORMAT(11)
   50 FORMAT(12A6)
   55 FORMAT(2I2)
   59 FORMAT('0','L=',I4)
   60 FORMAT('0','FILE ',I2,'=FILE ',I2)
   69 FORMAT('0','EACH DIV.= ',F5.2,'ABSORB UNITS')
   82 FORMAT(1X,'*******************************')
      END
```

```
C                    **********************
C                    * SUBROUTINE PLOTS *
C                    **********************
C
      SUBROUTINE PLOTS(X,L,ILABEL,JLABEL,YINC,NSPK,ID,SY)
      DIMENSION X(1),YPLOT(1100),ILABEL(1),JLABEL(1),LABLE(3),ISYMB(4)
C
CC    X= ARRAY CONTAINING POINTS TO BE PLOTTED
CC    L= NO. OF POINTS(1 WVN. INTERVAL)
CC    SCALE Y= VARIABLE, DEPENDS ON SF
CC    SCALE X=1 INCH= 100 CM=1
C
      IF(NSPK .EQ. 1) GO TO 550
      IF(NSPK .EQ. 2) GO TO 551
      IF(NSPK .EQ. 3) GO TO 552
      IF(NSPK .EQ. 4) GO TO 553
  550 ILONG=1500
      ILO=4000
      NX=10
      N=11
      IF(ID.NE.0) GO TO 555
      GO TO 554
  551 ILONG=1500
      ILO=3000
      NX=10
      N=11
      IF(ID.NE.0) GO TO 555
      GO TO 554
  552 ILONG=1500
      ILO=2000
      NX=10
      N=11
      IF(ID.NE.0) GO TO 555
      GO TO 554
  553 ILONG=1200
      ILO=1000
      NX=4
      N=5
C
      IF(ID.NE.0) GO TO 555
  554 CALL AINIT(ILONG)
  555 CALL AORIG(300,200)
      IF(ID.NE.0) GO TO 556
      CALL ALAB(-200,300,ILABEL,15,2,4)
      CALL ALAB(-150,0,JLABEL,72,1,4)
      CALL ABOX(0,0,NX,10,100,70,2)
      DATA ISYMB/'$B  ','CM=1 ','ABSOR ','BANCE '/
      CALL ASCA(-35,-15,100,0,ILO,-100,N,1,2)
      LABLE(1)=ISYMB(1)
      CALL ALAB(150,-20,LABLE(1),4,2,6)
      LABLE(1)=ISYMB(2)
      CALL ALAB(350,-40,LABLE(1),4,2,2)
      LABLE(1)=ISYMB(3)
      CALL ALAB(-50,300,LABLE(1),5,2,4)
      LABLE(1)=ISYMB(4)
      CALL ALAB(-50,400,LABLE(1),5,2,4)
      LABLE(1)=ISYMB(1)
      CALL ALAB(-25,400,LABLE(1),4,2,4)
C
  556 YPLOT(1)=X(1)*10000.
      YMIN=X(1)*10000.
      DO 999 J=2,L
      YPLOT(J)=X(J)*10000.
      IF(YPLOT(J).LE. 0.0) YPLOT(J)=YPLOT(1)
      IF(YPLOT(J) .LT.YMIN) YMIN=YPLOT(J)
  999 CONTINUE
C
      YMIN=YMIN-200.
      YMIN=YMIN-SY
C
      CALL ALINEX(0,1,YPLOT,L,YMIN,YINC)
      IF(ID.NE.2) GO TO 557
      CALL AEND
  557 RETURN
      END
```